CHARACTERIZATION AND REACTIVITY OF NATURAL ORGANIC MATTER IN DRINKING WATER SOURCES

by

Sevinç Aktaş İlgün

BS. in Environmental Eng., Trakya University, 2005

Submitted to the Institute of Environmental Sciences in partial fulfillment of

the requirements for the degree of

Master of Science

in

Environmental Sciences

Boğaziçi University

2010

dedicated to my mother, Mediha Aktaş and father, Fahri Aktaş...

ACKNOWLEDGEMENTS

Master study has a very important role on my occupational background, and I would like to express my sincere gratitude to my thesis supervisor, Prof. Dr. Miray Bekbölet for her guidance, support and encouragement throughout the preparation of this thesis. Without her sympathy, patience and guidance, the accomplishment would be impossible.

I extend my sincere thanks to Assoc. Prof. Dr. Zehra Can and Assist. Prof. Dr. Başak Güven for their kind and supportive attitude to me and showing high interests and valuable advices about this study.

I also have to express my gratefulness to Dr. Ceyda Senem Uyguner who provided generous feedback and support not only in laboratory work but also for guiding me towards the beneficial research. I am very thankful to Sibel Şen Kavurmacı, she has been very supportive and I have benefited her assistance in dealing with the problems that arose during the study.

I owe special thanks to my roommate, Neslihan Er and classmates Esra İlhan, Hülya Ünver, and Musa Rahmanlar without their friendship, social accompany, support and collaboration this whole study would not be enjoying.

The unique friend of mine Ezgi Kösecioğlu, was always by me in good times and in bad. She deserves invaluable thanks than I can ever express for just being there.

I need to express my lovely thanks to my husband Turgay İlgün, who was the reason for me to apply master's degree. His infinite support, encouragements, patience and love has given power to me from the very beginning till the ending. My mother in law, Saadet İlgün and father in law, Kemal İlgün also deserve warm gratitude for their kindness and kindness.

I wish to express the golden thanks to my beloved mother, Mediha Aktaş and father, Fahri Aktaş who have constantly been considering, supportive and lovely as they have always been.

ABSTRACT

Photocatalytic treatment of humic acids as model compounds representing natural organic present in drinking water sources has been studied since 1996. Considering the diverse nature of humic substances, continuous efforts should be directed to the elucidation of the photocatalytic degradation efficiency of humic substances from different origins i.e. terrestrial and aquatic humic acids. The performance of the humic photocatalytic system could be evaluated by selected parameters of UV-vis and fluorescence spectroscopic methods as well as chemical parameters as DOC measurements. The efficiency of photocatalytic treatment was presented by the application of pseudo first order and Langmuir Hinshelwood (L-H) kinetic models. Discussion was presented with reference to the previously studied model humic substances, humic and fulvic acids of various origins.

The shape of UV-vis spectra of FHA and NHA obtained prior to treatment was similar to the photocatalytically oxidized humic acids', as declining with increasing wavelength. While terrestrial humic acid had remarkably higher $Color_{436}$ absorbance than the aquatic humic acid, UV_{254} absorbance was found to be close to each other. While 89 % of $Color_{436}$ removal attained for FHA, 98 % of $Color_{436}$ elimination was achieved for NHA by 60 minutes of irradiation. Additionally, UV_{254} observed to be reduced 73 % for FHA and 75 % for NHA. Correspondingly, DOC content of FHA and NHA were significantly removed by photocatalytic oxidation process. Moreover, fluorescence spectra of raw and oxidized humic acids were beneficial for extensive assessment of photocatalytic oxidation products.

Removal rate of $Color_{436}$ parameter was found to be always faster than UV_{254} removal as well as DOC, estimated by pseudo first order and L-H kinetic models. On the other hand, the increasing trend of the L-H rates was similar to that of first order rates, although L-H rates were approximately half the value of the pseudo first order rates of $Color_{436}$, UV_{365}, UV_{280} and UV_{254}.

ÖZET

İçme suyu kaynaklarında bulunan doğal organic maddeleri (DOM) temsilen kullanılan hümik asitlerin fotokatalitik osidasyon yöntemi le giderimi 1996 yılından beri çeşitli araştırmalara konu olmaktadır. Çok çeşitli yapısı gereği, farklı kaynaklardan elde edilen (su veya toprak) hümik maddelerin fotokatalitik oksidasyon yöntemi ile giderim verimini aydınlatmaya yönelik çalışmalara önem verilmelidir. Hümik – fotokatalitik sisteminin performansı UV-vis ve floresan spektroskopisinden elde edilen parametrelerin yanısıra çözünmüş organic karbon (ÇOK) gibi kimyasal parametrelerin değerlendirilmesi ile belirlenebilir. Fotokatalitik oksidasyonun verimliliği Langmuir Hinshelwood ve birinci dereceden reaksiyon kinetic modelleri üzerinden değerlendirilmiştir. Sonuçlar daha önce yapılan çalışmalarda kullanılan model hümik maddelerden, farklı kaynaklardan olan hümik ve fulvic asitlerden, elde edilen verilere dayanarak verilmiştir.

FHA ve NHA'nın fotokatalitik olarak oksidasyonu sonucu elde edilen UV-vis spektroskopisinde dalga boyu arttıkça logaritmik olarak azalan absorbansı şekilsel olarak ham FHA ve NHA'nın spektroskopisi ile benzerlikler göstermektedir. Toprak kaynaklı hümik asidin su kaynaklı hümik asite göre daha fazla $Renk_{436}$ absorbansı olduğu bulunmuştur, bunula birlikte UV_{254} absorbansları birbirine yakındır. 60 dakikalık fotokatalitik oksidasyon sonucu FHA için % 89, NHA için % 98 $Renk_{436}$ giderimi tespit edilmiştir. UV_{254} giderimleri ise FHA için % 73, NHA için % 75 olarak bulunurken benzer ÇOK giderim oranları elde edilmiştir. Floresan spektroskopisi, hümik asitlerin fotokatalitik olarak oksitlenmesinden meydana gelen bileşiklerin değerlendirilmesinde faydalı sonuçlar sağlamıştır. L-H ve birinci dereceden reaksiyon kinetic modellerine göre hesaplanan $Renk_{436}$ giderim hızlarının UV_{254} giderim hızından daima daha fazla olduğu tespit edilmiştir. $Renk_{436}$, UV_{365}, UV_{280} ve UV_{254} parametreleri için hesaplanan L-H giderim hızı da birinci dereceden reaksiyon giderim hızı gibi artan bir eğilim gösterirken, L-H giderim hızının birinci dereceden reaksiyon giderim hızının yarısı kadar olduğu da önemli bir bulgudur.

TABLE OF CONTENTS

ACKNOWLEDGMENTS iv

ABSTRACT vi

ÖZET vii

TABLE OF CONTENTS viii

LIST OF FIGURES xi

LIST OF TABLES xviii

LIST OF SYMBOLS / ABBREVIATIONS xx

1. INTRODUCTION 1

2. THEORETICAL BACKGROUND 2

2.1. Natural Organic Matter 2

2.2. Humic Substances 3

2.2.1. Characterization of Humic Substances 7

2.2.1.1. Characterization of Humic Substances by UV-vis Spectroscopy 8

2.2.1.2. Characterization of Humic Substances by Fluorescence Spectroscopy 11

2.3. Advanced Oxidation Processes 14

2.3.1. Photocatalytic Oxidation 14

2.3.1.1. Pseudo First Order Kinetic Model 18

2.3.1.2. Langmuir Hinshelwood Kinetic Model 19

3. MATERIALS AND METHODS 20

3.1. Materials 20

3.1.1. Humic Acid Solution 20

3.1.2. Titanium Dioxide Powder 20

3.2. Methods 21

3.2.1. Experimental Set Up 21

3.2.2. Experimental Procedure 21

3.2.2.1. Photocatalytic Oxidation 21

3.2.3. Parameters Studied 22

3.2.4 Analytical Methods 22

3.2.4.1. UV-vis Measurements 22

3.2.4.2. Fluorescence Measurements 23

3.2.4.3. Dissolved Organic Carbon (DOC) Analysis 24

4. RESULTS AND DISCUSSIONS 25

4.1. Material Specification 25

4.1.1. Spectroscopic Analysis of Humic Acids 25

4.1.1.1. UV-vis Spectroscopic Properties of Humic Acids 25

4.1.1.2. Fluorescence Spectroscopic Properties of Humic Acids 30

4.2. Oxidative Treatment of Humic Acids via Photocatalysis 38

4.2.1. Preliminary Experiments 38

4.2.1.1. Experiments Carried Out in the Absence of Light 38

4.2.1.2. Experiments Carried Out in the Absence of Photocatalyst 44

4.2.2. Photocatalytic Degradation of Humic Acid 50

4.2.2.1. Photocatalytic Degradation of FHA 51

4.2.2.2. Photocatalytic Degradation of NHA 54

4.2.2.3. Comparative Evaluation of Photocatalytic Degradation of Humic Acids 58

4.2.3. Effect of Initial Concentration of Humic Acid Photocatalytic Oxidation 63

4.2.3.1. Effect of Initial Concentration of FHA 64

4.2.3.2. Effect of Initial Concentration of NHA 78

4.2.4. Photocatalyst Dosage Effect 91

4.2.4.1. TiO_2 Loading Effect on the Photocatalytic Oxidation of FHA 92

4.2.4.2. TiO_2 Loading Effect on the Photocatalytic Oxidation of NHA 96

4.2.5. Kinetic Model Evaluation 102

4.2.5.1. Pseudo First Order Kinetic Model 102

4.2.5.2. Langmuir Hinshelwood Kinetic Model 110

5. CONCLUSIONS 115

6. REFERENCES 119

LIST OF FIGURES

Figure 2.1.	The hypothetical relationships between humic substances	4
Figure 2.2.	(a) Hypothetical structure of model humic acid (b) Hypothetical Structure of fulvic acid	6
Figure 2.3.	Electronic molecular energy levels	9
Figure 2.4.	Simplified TiO_2 photocatalytic mechanism	15
Figure 4.1.	UV-vis spectra of humic acids (HA: 50 mg L^{-1})	26
Figure 4.2.	UV-vis spectra of (a) FHA and (b) NHA (HA: 10 - 50 mg L^{-1})	27
Figure 4.3.	Effect of excitation wavelength on the emission fluorescence spectra of FHA (HA: 50 mg L^{-1})	31
Figure 4.4.	Effect of excitation wavelength on the emission fluorescence spectra of NHA (HA: 50 mg L^{-1})	32
Figure 4.5.	Synchronous scan fluorescence spectra of FHA and NHA ($\Delta\lambda$ = 18 nm; HA: 50 mg L^{-1})	34
Figure 4.6.	Effect of initial concentration on the emission fluorescence spectra of NHA (Excitation wavelength: 350 nm)	34
Figure 4.7.	DOC normalized emission fluorescence spectra of FHA and NHA (Excitation Wavelength: 350 nm, HA: 50 mg L^{-1})	35
Figure 4.8.	Synchronous scan fluorescence spectra of NHA in various concentrations ($\Delta\lambda$ = 18 nm)	36
Figure 4.9.	DOC normalized synchronous scan fluorescence spectra of FHA and NHA ($\Delta\lambda$ = 18 nm; HA: 50 mg L^{-1})	37

Figure 4.10. UV-vis spectra of (a) FHA and (b) NHA in the absence of light (HA: 20 mg L^{-1}, TiO_2: 0.25 mg mL^{-1}) 39

Figure 4.11. Preliminary experiments conducted in the absence of light (a) FHA and (b) NHA (HA: 20 mg L^{-1}, TiO_2: 0.25 mg mL^{-1}) 40

Figure 4.12. The emission fluorescence spectra of preliminary experiments conducted in the absence of light (a) FHA and (b) NHA (HA: 20 mg L^{-1}, TiO_2: 0.25 mg mL^{-1}, Excitation wavelength: 350 nm) 41

Figure 4.13. The emission fluorescence spectra of preliminary experiments conducted in the absence of light (a) FHA and (b) NHA (HA: 20 mg L^{-1}, TiO_2: 0.25 mg mL^{-1}, Excitation wavelength: 370 nm) 42

Figure 4.14. The synchronous scan fluorescence spectra of preliminary experiments conducted in the absence of light for (a) FHA and (b) NHA (HA: 20 mg L^{-1}, TiO_2: 0.25 mg mL^{-1}, $\Delta\lambda$ = 18 nm) 44

Figure 4.15. UV-vis spectra of (a) FHA and (b) NHA in the absence of TiO_2 (HA: 20 mg L^{-1}, I_0=2.85x10^{16} quanta sec^{-1}) 45

Figure 4.16. Preliminary experiments conducted in the absence of TiO_2 for (a) FHA and (b) NHA (HA: 20 mg L^{-1}, I_0=2.85x10^{16} quanta sec^{-1}) 46

Figure 4.17. The emission fluorescence spectra of preliminary experiments conducted in the absence of TiO_2 (a) FHA and (b) NHA (HA: 20 mg L^{-1}, I_0=2.85x10^{16} quanta sec^{-1}, Excitation wavelength: 350 nm) 47

Figure 4.18. The emission fluorescence spectra of preliminary experiments conducted in the absence of TiO_2 (a) FHA and (b) NHA (HA: 20 mg L^{-1}, I_0=2.85x10^{16} quanta sec^{-1}, Excitation wavelength: 370 nm) 48

Figure 4.19. The synchronous scan fluorescence spectra of preliminary experiments conducted in the absence of TiO_2 (a) FHA and (b) NHA (HA: 20 mg L^{-1}, I_0=2.85x10^{16} quanta sec^{-1}, $\Delta\lambda$ = 18 nm) 49

Figure 4.20. UV-vis spectra of the photocatalytic degradation of FHA (HA: 20 mg L^{-1}, TiO_2: 0.25 mg mL^{-1}; I_0=2.85x10^{16} quanta sec^{-1}) 51

Figure 4.21. Photocatalytic degradation of FHA illustrated by normalized spectroscopic parameters ($Color_{436}$, UV_{365}, UV_{280}, UV_{254}) correlated with DOC removal (HA: 20 mg L^{-1}, TiO_2: 0.25 mg mL^{-1}; I_0=2.85x10^{16} quanta sec^{-1}) 52

Figure 4.22. Effect of excitation wavelength at (a) 350 nm and (b) 370 nm on the emission fluorescence spectra of oxidized FHA (HA: 20 mg L^{-1}, TiO_2: 0.25 mg mL^{-1}; I_0=2.85x10^{16} quanta sec^{-1}) 53

Figure 4.23. The synchronous scan fluorescence spectra of oxidized FHA (HA: 20 mg L^{-1}, TiO_2: 0.25 mg mL^{-1}; I_0=2.85x10^{16} quanta sec^{-1}, $\Delta\lambda$=18 nm) 54

Figure 4.24. UV-vis spectra of the photocatalytic degradation of NHA (HA: 20 mg L^{-1}, TiO_2: 0.25 mg mL^{-1}; I_0=2.85x10^{16} quanta sec^{-1}) 55

Figure 4.25. Photocatalytic degradation of NHA illustrated by normalized spectroscopic parameters ($Color_{436}$, UV_{365}, UV_{280}, UV_{254}) correlated with DOC removal (HA: 20 mg L^{-1}, TiO_2: 0.25 mg mL^{-1}; I_0=2.85x10^{16} quanta sec^{-1}) 56

Figure 4.26. Effect of excitation wavelength at (a) 350 nm and (b) 370 nm on the emission fluorescence spectra of oxidized NHA (HA: 20 mg L^{-1}, TiO_2: 0.25 mg mL^{-1}; I_0=2.85x10^{16} quanta sec^{-1}) 57

Figure 4.27. The synchronous scan fluorescence spectra of oxidized NHA (HA: 20 mg L^{-1}, TiO_2: 0.25 mg mL^{-1}; I_0=2.85x10^{16} quanta sec^{-1}, $\Delta\lambda$=18 nm) 58

Figure 4.28. Initial concentration effect on photocatalytic oxidation of FHA with respect to UV-vis spectra. (a) 10 mg L^{-1} and (b) 20 mg L^{-1} (TiO_2: 0.25 mg mL^{-1}; I_0=2.85x10^{16} quanta sec^{-1}) 64

Figure 4.29. Initial concentration effect on photocatalytic oxidation of FHA with respect to UV-vis spectra. (a) 30 mg L^{-1}, (b) 40 mg L^{-1}, (c) 50 mg L^{-1} (TiO_2: 0.25 mg mL^{-1}; I_0=2.85x10^{16} quanta sec^{-1}) 65

Figure 4.30. Initial concentration effect on photocatalytic oxidation of FHA with respect to normalized (a) $Color_{436}$ and (b) UV_{254} (HA: 10 mg L^{-1}, 20 mg L^{-1}, 30 mg L^{-1}, 40 mg L^{-1} and 50 mg L^{-1}, TiO_2: 0.25 mg mL^{-1}; I_0=2.85x10^{16} quanta sec^{-1}) 66

Figure 4.31. The emission fluorescence spectra at excitation wavelength (a) 350 nm and (b) 370 nm of oxidized FHA (HA: 10 mg L^{-1}, TiO_2: 0.25 mg mL^{-1}; I_0=2.85x10^{16} quanta sec^{-1}) 68

Figure 4.32. The synchronous scan fluorescence spectra of oxidized FHA (HA: 10 mg L^{-1}, TiO_2: 0.25 mg mL^{-1}; I_0=2.85x10^{16} quanta sec^{-1}, $\Delta\lambda$=18 nm) 69

Figure 4.33. The emission fluorescence spectra at excitation wavelength (a) 350 nm and (b) 370 nm of oxidized FHA (HA: 20 mg L^{-1}, TiO_2: 0.25 mg mL^{-1}; I_0=2.85x10^{16} quanta sec^{-1}) 70

Figure 4.34. The synchronous scan fluorescence spectra of oxidized FHA (HA: 20 mg L^{-1}, TiO_2: 0.25 mg mL^{-1}; I_0=2.85x10^{16} quanta sec^{-1}, $\Delta\lambda$=18 nm) 71

Figure 4.35. The emission fluorescence spectra at excitation wavelength (a) 350 nm and (b) 370 nm of oxidized FHA (HA: 30 mg L^{-1}, TiO_2: 0.25 mg mL^{-1}; I_0=2.85x10^{16} quanta sec^{-1}) 72

Figure 4.36. The synchronous scan fluorescence spectra of oxidized FHA (HA: 30 mg L^{-1}, TiO_2: 0.25 mg mL^{-1}; I_0=2.85x10^{16} quanta sec^{-1}, $\Delta\lambda$=18 nm) 73

Figure 4.37. The emission fluorescence spectra at excitation wavelength (a) 350 nm and (b) 370 nm of oxidized FHA (HA: 40 mg L^{-1}, TiO_2: 0.25 mg mL^{-1}; I_0=2.85x10^{16} quanta sec^{-1}) 74

Figure 4.38. The synchronous scan fluorescence spectra of oxidized FHA (HA: 40 mg L^{-1}, TiO_2: 0.25 mg mL^{-1}; I_0=2.85x10^{16} quanta sec^{-1}, $\Delta\lambda$=18 nm) 75

Figure 4.39. The emission fluorescence spectra at excitation wavelength (a) 350 nm and (b) 370 nm of oxidized FHA (HA: 50 mg L^{-1}, TiO_2: 0.25 mg mL^{-1}; I_0=2.85x10^{16} quanta sec^{-1}) 76

Figure 4.40. The synchronous scan fluorescence spectra of oxidized FHA (HA: 50 mg L^{-1}, TiO_2: 0.25 mg mL^{-1}; I_0=2.85x10^{16} quanta sec^{-1}, $\Delta\lambda$=18 nm) 77

Figure 4.41. Initial concentration effect on photocatalytic oxidation of NHA with respect to UV-vis spectra (a) 10 mg L^{-1}, (b) 20 mg L^{-1}, (c) 30 mg L^{-1} (TiO_2: 0.25 mg mL^{-1}; I_0=2.85x10^{16} quanta sec^{-1}) 79

Figure 4.42. Initial concentration effect on photocatalytic oxidation of NHA with respect to UV-vis spectra (HA: 50 mg L^{-1}, TiO_2: 0.25 mg mL^{-1}; I_0=2.85x10^{16} quanta sec^{-1}) 80

Figure 4.43. Initial concentration effect on photocatalytic oxidation of FHA with respect to normalized (a) $Color_{436}$ and (b) UV_{254} (HA: 10 mg L^{-1}, 20 mg L^{-1}, 30 mg L^{-1} and 50 mg L^{-1}, TiO_2: 0.25 mg mL^{-1}; I_0=2.85x10^{16} quanta sec^{-1}) 81

Figure 4.44. The emission fluorescence spectra at excitation wavelength (a) 350 nm and (b) 370 nm of oxidized NHA (HA: 10 mg L^{-1}, TiO_2: 0.25 mg mL^{-1}; I_0=2.85x10^{16} quanta sec^{-1}) 82

Figure 4.45. The synchronous scan fluorescence spectra of oxidized NHA (HA: 10 mg L^{-1}, TiO_2: 0.25 mg mL^{-1}; I_0=2.85x10^{16} quanta sec^{-1}, $\Delta\lambda$=18 nm) 83

Figure 4.46. The emission fluorescence spectra at excitation wavelength (a) 350 nm and (b) 370 nm of oxidized NHA (HA: 20 mg L^{-1}, TiO_2: 0.25 mg mL^{-1}; I_0=2.85x10^{16} quanta sec^{-1}) 84

Figure 4.47. The synchronous scan fluorescence spectra of oxidized NHA (HA: 20 mg L^{-1}, TiO_2: 0.25 mg mL^{-1}; I_0=2.85x10^{16} quanta sec^{-1}, $\Delta\lambda$=18 nm) 85

Figure 4.48. The emission fluorescence spectra at excitation wavelength (a) 350 nm and (b) 370 nm of oxidized NHA (HA: 30 mg L^{-1}, TiO_2: 0.25 mg mL^{-1}; I_0=2.85x10^{16} quanta sec^{-1}) 86

Figure 4.49. The synchronous scan fluorescence spectra of oxidized NHA (HA: 30 mg L^{-1}, TiO_2: 0.25 mg mL^{-1}; I_0=2.85x10^{16} quanta sec^{-1}, $\Delta\lambda$=18 nm) 87

Figure 4.50. The emission fluorescence spectra at excitation wavelength (a) 350 nm and (b) 370 nm of oxidized NHA (HA: 50 mg L^{-1}, TiO_2: 0.25 mg mL^{-1}; I_0=2.85x10^{16} quanta sec^{-1}) 88

Figure 4.51. The synchronous scan fluorescence spectra of oxidized NHA (HA: 50 mg L^{-1}, TiO_2: 0.25 mg mL^{-1}; I_0=2.85x10^{16} quanta sec^{-1}, $\Delta\lambda$=18 nm) 89

Figure 4.52. Effect of TiO_2 loading on the UV-vis spectra of FHA (a) at time zero and (b) upon irradiation period (It) of 30 min (HA: 20 mg L^{-1}, TiO_2: 0.25 mg mL^{-1}; I_0=2.85x10^{16} quanta sec^{-1}) 92

Figure 4.53. Effect of TiO_2 loading on removal efficiency of FHA in terms of (a) $Color_{436}$ and (b) UV_{254} upon irradiation period (It) of 30 min (HA: 20 mg L^{-1}, TiO_2: 0.25 mg mL^{-1}; I_0=2.85x10^{16} quanta sec^{-1}) 93

Figure 4.54. Emission fluorescence spectra of photocatalytically oxidized FHA (a) at time zero and (b) upon irradiation period (It) of 30 min (HA: 20 mg L^{-1}, TiO_2: 0.25 mg mL^{-1};I_0=2.85x10^{16} quanta sec^{-1}, Excitation wavelength: 350 nm) 95

Figure 4.55. Synchronous scan fluorescence spectra of photocatalytically oxidized FHA (a) at time zero and (b) upon irradiation period (It) of 30 min (HA: 20 mg L^{-1}, TiO_2: 0.25 mg mL^{-1}; I_0=2.85x10^{16} quanta sec^{-1}, $\Delta\lambda$=18 nm) 96

Figure 4.56. Effect of TiO_2 loading on the UV-vis spectra of NHA (a) at time zero and (b) upon irradiation period (It) of 30 min 97

Figure 4.57. Effect of TiO_2 loading on removal efficiency of NHA in terms of (a) $Color_{436}$ and (b) UV_{254} upon irradiation period (It) of 30 min (HA: 20 mg L^{-1}, TiO_2: 0.25 mg mL^{-1}; I_0=2.85x10^{16} quanta sec^{-1}) 98

Figure 4.58. Emission fluorescence spectra of photocatalytically oxidized NHA (a) at time zero and (b) upon irradiation period (It) of 30 min (HA: 20 mg L^{-1}, TiO_2: 0.25 mg mL^{-1};I_0=2.85x10^{16} quanta sec^{-1}, Excitation wavelength: 350 nm) 100

Figure 4.59. Synchronous scan fluorescence spectra of photocatalytically oxidized NHA (a) at time zero and (b) upon irradiation period (It) of 30 min (HA: 20 mg L^{-1}, TiO_2: 0.25 mg mL^{-1}; I_0=2.85x10^{16} quanta sec^{-1}, $\Delta\lambda$=18 nm) 101

LIST OF TABLES

Table 2.1.	Elemental contents of commercial humic acids and standard humic substances supplied from IHSS	5
Table 2.2.	UV-vis characterization of aquatic humic substances	10
Table 4.1.	Basic spectroscopic characterization of humic acids (HA: 50 mg L^{-1})	28
Table 4.2.	Specific UV- vis parameters of humic acids	29
Table 4.3	Specific absorbance ratios of humic substances during photocatalytic oxidation	60
Table 4.4.	Pseudo first order kinetic model parameters of different humic acids (HA: 20 mgL^{-1}, TiO_2: 0.25 mg mL^{-1}, I_0=2.85x10^{16} quanta sec^{-1})	103
Table 4.5.	Pseudo first order kinetic model parameters of FHA (HA: 10, 20, 30, 40 and 50 mg L^{-1}, TiO_2: 0.25 mg mL^{-1}, I_0=2.85x10^{16} quanta sec^{-1})	104
Table 4.6.	Pseudo first order kinetic model parameters of NHA (HA: 10 mg L^{-1}, 20 mg L^{-1}, 30 mg $L^{-1}$and 50 mg L^{-1}; TiO_2: 0.25 mg mL^{-1}, I_0=2.85x10^{16} quanta sec^{-1}	106
Table 4.7.	Pseudo first order kinetic parameters of model compounds (HA: 50 mgL^{-1}, TiO_2: 0.25 mg mL^{-1}, I_0=2.85x10^{16} quanta sec^{-1})	109
Table 4.8.	L-H kinetic model parameters of FHA and NHA (HA: 20 mg L^{-1}, TiO_2: 0.25 mg mL^{-1}, I_0=2.85x10^{16} quanta sec^{-1})	111

Table 4.9. L-H kinetic model parameters of IHSS HA, IHSS SHA, AHA and RHA (HA: 50 mg L^{-1}) 112

LIST OF SYMBOLS / ABBREVIATIONS

Symbol	Explanation
Δλ	Bandwidth
A	Related UV-vis parameter (m^{-1}) / DOC content of HS (mg L^{-1})
AHA	Aldrich humic acid
AOP	Advanced oxidation processes
BLF	Black Light Fluorescent Lamp
$Color_{436}$	Absorbance at 436 nm
DBP	Disinfection byproduct
DOC	Dissolved organic carbon
DOM	Dissolved organic matter
F.I.	Fluorescence index
FA	Fulvic acid
FHA	Fluka humic acid
FTIR	Fourier transformation infrared
HA	Humic acid
HOMO	Highest occupied molecular orbital
HPLC	High pressure liquid chromatography
HS	Humic substances
IHSS FA	International humic substance society fulvic acid
IHSS HA	International humic substance society humic acid
IHSS SHA	International humic substance society soil humic acid
It	Irradiation time (min)

k	Pseudo first order reaction rate constant (min^{-1})
K_{LH}	Adsorption coefficient (m)
k_{LH}	Reaction rate constant (m^{-1} min^{-1})
L-H	Langmuir Hinshelwood
LUMO	Lowest unoccupied molecular orbital
NHA	Nordic humic acid
NMR	Nuclear magnetic resonance spectroscopy
NOM	Natural organic matter
Py-GC-MS	Pyrolysis-gas chromatography-mass spectroscopy
QS	Quinone sulfate
R	Pseudo first order rate
RHA	Roth humic acid
R_{LH}	Rate of the reaction (m^{-1} min^{-1})
SCOA	Specific color absorbance
$SCOA_{436}$	Specific color absorbance at 436 nm
SUVA	Specific UV absorbance
$SUVA_{254}$	Specific UV absorbance at 254 nm
$SUVA_{365}$	Specific UV absorbance at 365 nm
$t_{1/2}$	Half life (min)
THM	Trihalomethane
UV_{254}	Absorbance at 254 nm
UV_{280}	Absorbance at 280 nm
UV_{365}	Absorbance at 365 nm

1. INTRODUCTION

The nature and aspects of natural organic matter (NOM) in water are subject matter of significant environmental interest, not only for the reason that it causes aesthetic concerns such as color, taste, and odor; but also leads to the binding and transport of organic and inorganic contaminants; generate redundant disinfection byproducts; provides sources and sinks for carbon; or intervenes photochemical processes. The most significant one of these concerns is the formation of disinfection by-products (DBPs) due to the unavoidable chlorination process applied for disinfection purposes.

In order to overcome the foreseen inconveniences, the removal of NOM is considered as an important process in water treatment field. Conventional physicochemical treatment processes have been applied all over the world including chemical oxidation steps. Numerous studies have also been carried on the removal of NOM by advanced oxidation methods namely photocatalysis (Bekbolet, et al., 2005). On the other hand, extensive research has been performed in order to reveal the reactivities of NOM in terms of precursor model organic compounds such as humic and fulvic acids (Bekbolet 1996 and Uyguner and Bekbolet, 2005b).

By studying different humic acid origins i.e. terrestrial and aquatic HAs, the purpose of this work will be to provide a wider knowledge about the structure and reactivity of NOM in drinking water supplies. The major outcome would be the understanding of the reactivities of DBP precursors' oxidative treatment via photocatalysis. The system will be evaluated by selected parameters of UV-vis and fluorescence spectroscopic methods as well as chemical parameters as DOC measurements. To achieve this goal, photocatalytic treatment of humic acids representing different source dependent properties was performed. The kinetic data were assessed by the application of relevant kinetic models *i.e*. pseudo first order and Langmuir-Hinshelwood (L-H) models. Comparative evaluation of the findings was presented with reference to the results of the previously studied model humic substances, humic and fulvic acids.

2. THEORETICAL BACKGROUND

2.1. Natural Organic Matter

The decay of plant, animal and microbial material in soil and water lead to production of different complex organic molecules, collectively called natural organic matter (NOM). These compounds play numerous important roles in the environment. NOM is ubiquitous in water supply and is consisted of mainly humic and non-humic substances. Thurman (1985) identified approximately 50 percent of dissolved organic carbon (DOC) as humic substances, which is the dominant group of organic compounds in water supplies, and the remainders are non-humic substances. Among the non-humic substances, about 60% of the DOC is contained of hydrophilic acids. In the remaining 40% of the non-humic compounds, 20% are carbohydrates, 14% carboxylic acids, 6% amino acids, and less than 1% is hydrocarbons. The dominant fraction of aquatic NOM is consisted of humic substances.

Maurice et al. (2002) reported NOM is a key component of surface waters, soil pore waters, and shallow ground waters, both in terms of concentration and reactivity. Transportation of trace metals may be controlled by NOM and hydrophobic compounds with the aggregation kinetics of colloidal particles. Furthermore, NOM has significant function in photochemical reactions, and microorganisms use it as organic carbon source. Molecular weight, aromaticity, elemental composition, and functional group content are physicochemical properties of NOM that strongly affect its reactivity. For example, McKnight et al., 1992; Namjesnik et al., 2000 suggested that higher molecular weight, more aromatic components tend to adsorb to mineral surfaces. Other research suggested that an intermediate molecular weight fraction controls adsorption

(Davis and Gloor, 1981; Zhou et al., 2001). The water supply industry encounter many problems due to NOM, however, requiring removal to minimize water color and causing increase to formation of potentially harmful disinfection by-products as a result of chlorination. NOM is also a major reason in decreasing the performance of membrane filtration systems used for water purification and desalination, which is called "bio-fouling". Therefore the removal of NOM draws the major attention in drinking water treatment.

2.2. Humic Substances

As it was described above, humic substances are found in water supplies and comprise a significant portion of NOM. Bekbolet, 2009, summarized the significance of humic substances to water quality in relation to drinking water treatment by contributions to the aesthetic properties of water as color, taste and odor; interference with water treatment by a probable increase in the coagulant demand thereby coagulant residuals, reducing the efficiency of membrane microfiltration and irreparable fouling; precursors of DBPs mainly trihalomethanes (THMs) and haloacetic acids (HAAs) other haloorganic/*other* DBPs that are formed by chlorination of the drinking water for disinfection purposes; their act as corrosion supporters in distribution systems; bacterial regrowth in the distribution system.

Depending on the origin and the age of the material, their size, molecular weight, elemental composition, structure, and the number and position of functional groups differ. Uyguner and Bekbolet (2005c) indicated that, a major fraction of natural organic matter (NOM) present in surface or ground waters is composed of humic substances, which are complex macromolecular products of the chemical and biological degradation of plant and animal residues including lignin, carbohydrates and proteins. Two general conceptual models have been discussed in literature for the formation of humic substances. The first one assumes that they

are formed from the breakdown of plant materials and oxidation due to extracellular enzymes and abiotic processes. A polymerization of simple compounds like quinones that are derived from degraded plant material is stated by the second concept (Suffet and MacCarthy, 1989; Leenheer, 1981; Thurman and Malcolm, 1981). The phrase "humic substances" is used as a general term to express colored material or its fractions attained on the basis of solubility characteristics. The fraction called humic acid (HA) represents the major fraction of humic substances, which is insoluble in water under acidic conditions (pH <2) and soluble at higher pH values. Fulvic acid (FA) is soluble at all pH conditions and humin is the fraction of humic substances that is insoluble in water at all pH values (Aiken et al*.,* 1995).

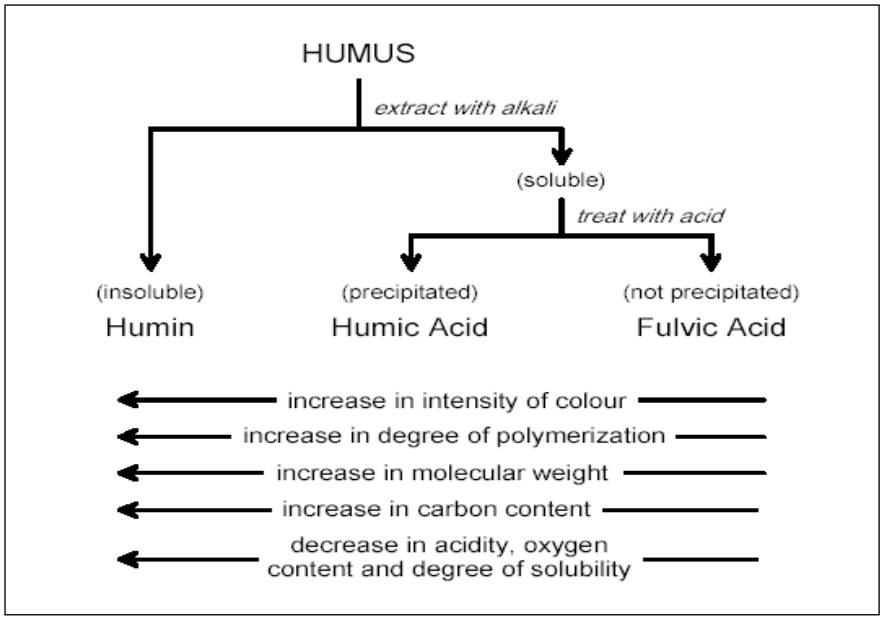

Figure 2.1. The hypothetical relationships between humic substances

Humic and fulvic acids differ from each other by the variations in molecular weight, the number of functional groups (carboxyl and phenolic OH) and the extent of polymerization. The hypothetical relationships are displayed in Figure 2.1, also carbon and oxygen contents can be seen, acidity and degree of polymerization all change systematically with increasing molecular weight. Generally, fulvic acids

have lower molecular weights than humic acids. It is also known that soil derived humic materials are larger than aquatic humic substances (Gaffney et al., 1996).

Humic acids cannot be regarded as single chemical entities described by unique, chemically defined molecular structures. They are considered to be complex aromatic macromolecules with amino acids, amino sugars, peptides, aliphatic compounds involved in linkages between the aromatic groups. However, generic structural models of humic and fulvic acids have been proposed in literature on the basis of available compositional, structural and functional data (Schnitzer and Khan, 1972; Buffle et al., 1977; Stevenson, 1982; Hofrichter and Steinbüchel, 2001). Although the structural analysis is difficult due to the complex polymeric nature and interaction between component chains of humic material; compositional information can be obtained from elemental and functional group analysis as presented in Table 2.1 (C, H, N, S, O were presented as %).

Table 2.1. Elemental contents of commercial humic acids and standard humic substances supplied from IHSS (compiled from Suffet and MacCarthy, 1989)

	Elemental Composition, %				
	C	**H**	**N**	**S**	**O**
IHSS humic acid	52.55	4.40	1.19	0.58	42.53
IHSS soil humic acid	58.13	3.68	4.14	0.44	34.08
Aldrich humic acid	68.98	5.26	0.74	4.24	43.45
Roth humic acid	55.1	4.78	1.34	2.42	27.2
Fluka humic acid	65.79	5.51	0.71	3.16	37.79
IHSS fulvic acid	52.44	4.31	0.72	0.44	42.20

The hypothetical structure for humic acid composed of side aliphatic chains and a hydrophobic aromatic core that is highly substituted with functional groups such as free and bound phenolic OH groups, quinone structures, nitrogen and oxygen as bridge units and COOH groups is shown in Figure 2.2a. Both hydrophilic and hydrophobic sites were considered in the model, a highly polyelectrolytic character and several sites potentially available to bind with metal ions, mineral surfaces and organic compounds. The structure and composition of humic acids are in fact more complex than those of fulvic acids. On the other hand, the model structure of fulvic acid contains both aromatic and aliphatic structures, both extensively substituted with oxygen-containing functional groups (Figure 2.2b).

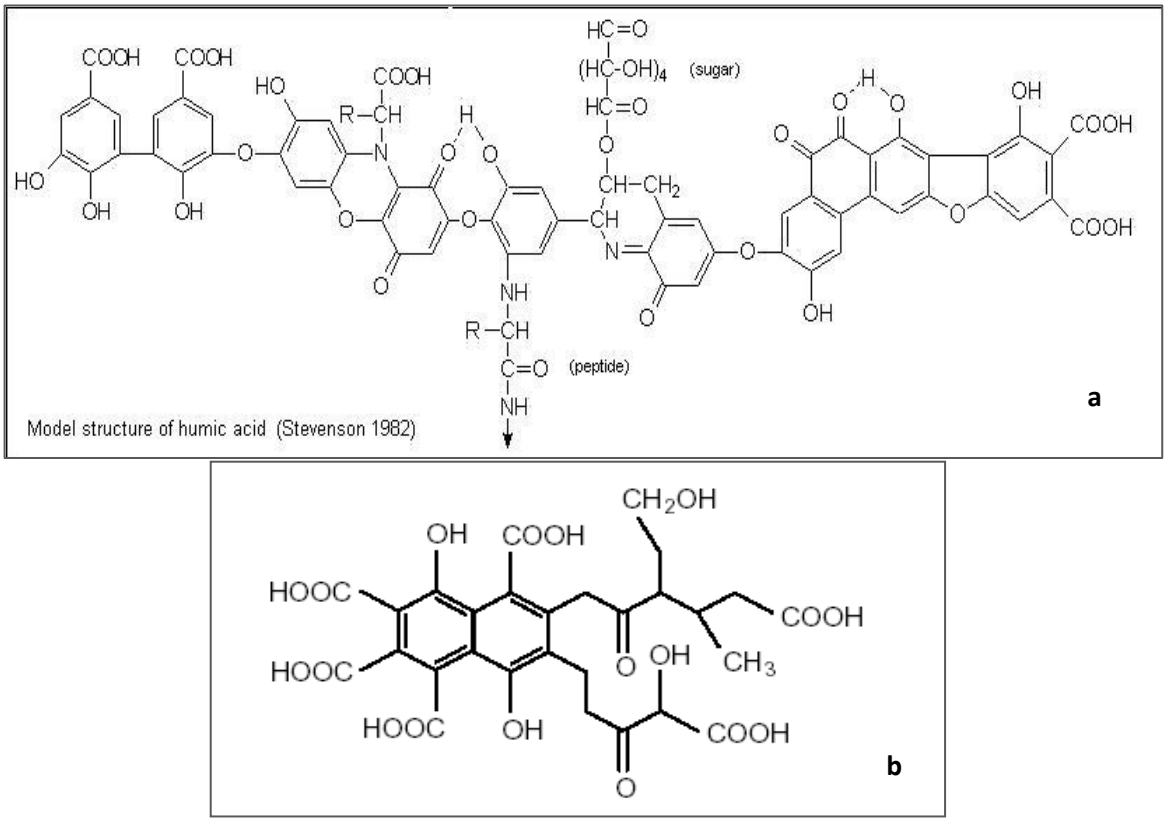

Figure 2.2. (a) Hypothetical structure of model humic acid (Stevenson, 1982), (b) Hypothetical structure of fulvic acid (Buffle, 1977)

Nevertheless, the structures of fulvic acid are more aliphatic and less aromatic than humic acids. As a result of the presence of large amounts of carboxylic acid, phenolic and ketonic groups, their high solubility in water at all pH values is practical. Dissociation and protonation of functional groups in humic molecule depends on the pH of the solution. Dissociated functional groups carry negative charges. Electrostatic repulsions between negatively charged sites with the nearby compounds cause stretching of the molecule.

Moreover, ionic strength of the compounds also effect the electrostatic forces, e.g. the presence of cationic species. (Ghosh and Schnitzer, 1980). Ghosh and Schnitzer, 1980 also reported that at high pH humic molecules show a large, flexible and linear shape, with low ionic strength and low humic concentration; and it can cause a change by reducing the pH to a small, rigid and spherocolloidal conformation, with high ionic strength and high humic concentration. While HSs are reactive components for interactions with many inorganic and organic pollutants, and may decrease toxicities of these pollutants; they are precursors of numerous chlorination by-products that can cause certain cancers. due to the reaction between humic and fulvic acids and chlorine to form trihalomethanes (THMs) in water treatment during the chlorination process, potential harm to humans can happen (Rook, 1977; Reckhow et al., 1990).

2.2.1. Characterization of Humic Substances

In order to explain their impact on the environmental fate, bioavailability and toxicity of organic and metal contaminants in natural water systems, chemical and physical studies of humic substances and their interactions with environmental contaminants are necessary. However, explanation of significance of humic substances is complicated due to their highly heterogeneous character. Hence humic substances cannot be identified by a single chemical characteristic, their concentrations are difficult to quantify. Dissolved organic carbon (DOC) content of water samples is accepted to be the most useful humic related determinant that

provides a useful indication. DOC concentrations in freshwater streams, rivers and lakes which are known to be due to the presence of humic substances vary from less than 0.5 mg L-1 to 100 mg L-1 depending on the nature of the reservoir, including the climate, the trophic status of the water body, and pollutant inputs. Besides DOC content, a number of physical and chemical measurements have been employed to characterize humic substances, including elemental analysis, ultrafiltration, UV-vis spectroscopy, fluorescence spectroscopy Fourier transform infrared (FTIR) spectroscopy, pyrolysis-gas chromatography-mass (Py-GC-MS) spectroscopy, 1H and 13C-NMR spectroscopy (Senesi et al., 1991; Westerhoff et al., 1999; Shin et al., 1999; Schulten and Gleixner, 1999; Kalbitz et al., 2000).

2.2.1.1. Characterization of Humic Substances by UV-vis Spectroscopy. Generally, ultraviolet-visible spectroscopy correspond to electronic excitations between the energy levels that equivalent to the molecular orbitals of the systems (UV = 200 - 400 nm, visible = 400 - 800 nm). For a molecule, this is a process where electrons are promoted from their electronic ground state to an excited electronic state. As a result, energetically favored electron promotion will be from the highest occupied molecular orbital (HOMO) to the lowest unoccupied molecular orbital (LUMO). The electronic structure of a molecule determines its UV light absorbance. Therefore, the UV spectrum indicates the existence of specific bonding arrangements in the molecule. Different electronic excitation that can occur in organic molecules by UV light absobtion was demonstrated in Figure 2.3.

UV-vis spectra of humic substances are featureless with increasing absorption at lower wavelengths. Moreover, they show no separate absorption bands due to the overlapping of the broad absorption bands of the chromophores in the structure of humic acids. The absorption in the UV region is mainly caused by the excitation of electron lone pair, usually oxygen ($n \rightarrow \pi^*$) and by conjugated C=C double bonds ($\pi \rightarrow \pi^*$). The absorption in the visible region is caused by lone pair electrons and charge-transfer systems.

Typically for HS, the absorbance decreases as the wavelength increases (Schnitzer and Khan, 1972; Stevenson, 1982). A slight peak could be identified at approximately 275 nm, which is probably due to quinine structure (Schnitzer and Khan, 1972). Chen et al., (1977) and Langhals et al., (2000) reported correlation between the spectral absorption and pH values; as solution pH decreases absorbance is decreasing too. Depending on the acid-base forms of the chromophores within the molecules; an increase in particle size due to macromolecular associations is expected, as suggested by Chen et al. (1977).

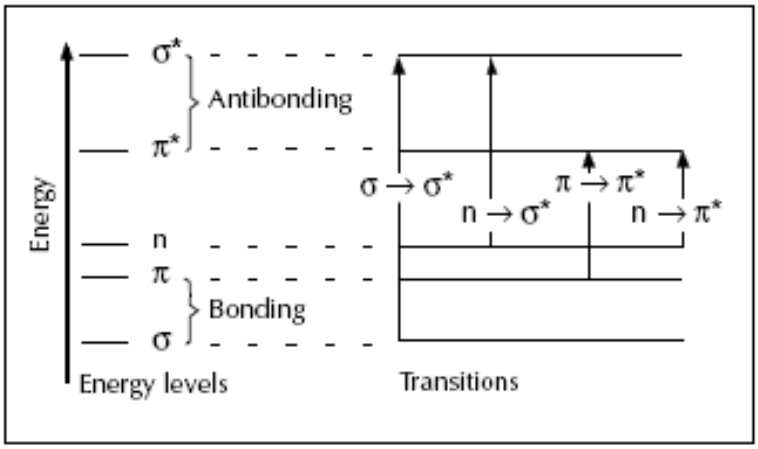

Figure 2.3. Electronic molecular energy levels (Skoog and Leary, 1992)

The wavelength at 254 nm (UV_{254}) and the yellow color representing absorbance at 436 nm ($Color_{436}$) are commonly used for quantification. (Uyguner and Bekbolet, 2005a; Uyguner and Bekbolet, 2006; Uyguner et.al, 2006). UV_{254} is interchangeably measured with total organic carbon (TOC) as a surrogate parameter to represent the natural organic matter (NOM) content in surface waters (Najm et al., 1994). With the similar intention, the changes in the UV-vis properties of humic substances during photocatalytic degradation were also determined at discrete absorption wavelengths (Bekbolet, 1996; Bekbolet et al., 1998; Uyguner and Bekbolet, 2005a, Uyguner and Bekbolet, 2005b) to represent total aromaticity the UV absorptivity at 280 nm was also introduced, because, π-π* electron transition occurs in this UV region (ca. 270-280 nm) for phenolic arenes, benzoic

acids, aniline derivatives, polyenes and polycyclic aromatic hydrocarbons with two or more rings (Chin et al., 1994; Traina et al., 1990). On the other hand, normalization of absorbance to DOC (or TOC) defined as specific absorbance value (SUVA) is very useful to compare different samples (Frimmel et al., 2002). It was reported by Abbt-Braun et al., (2004) that a plot of the specific absorption in the visible range ($Color_{436}$/DOC) against the specific absorption in the UV range (UV_{254}/DOC) exhibit higher values for HA fractions for both the UV and visible range than that of FA fractions. Accordingly, it can be concluded that the double bond density is related to the hydrophobic character.

Various absorption wavelengths have been cited in literature for the spectral differentiation of humic substances (Chen et al., 1977; De Haan et al., 1982; Stevenson, 1982; Buffle et al., 1982; Hayes et al., 1989; Traina et al., 1990; Wang et al., 1990; Chin et al., 1994; Peuravuori and Pihlaja, 1997; Chen et al., 2002; Abbt-Braun and Frimmel, 2002). However, they usually served as additional indexes characterizing humic materials (Choudhry, 1981). Uyguner (2005) compiled related data from literature and summarized as shown in Table 2.2.

Table 2.2. UV-vis characterization of aquatic humic substances (adapted from Hautala et al., 2000)

Wavelength, nm	**Correlative characteristics**	**References**
250, 300, 350	DOC, TOC	De Haan et al., 1982
285	DOC	Buffle et al, 1982
254	DOC, TOC, COD, BOD	Mrkva, 1983; Reynolds and Ahmad, 1997
272, 280	Aromaticity, molecular weight	Triana et al.,1990; Chin et al.,1994; Li et al., 1998
250/365	Aromaticity, molecular weight	Peuravour, and Pihlaja, 1997
465/665	Humification, molecular weight, condensation of aromatic carbon	Bloom and Leenheer, 1989; Stevenson, 1982; Chen et al., 1977

As a consequence of their featureless character, absorption spectra of humic acids in the visible region have been largely disregarded. The featureless absorption spectra were obtained in visible light range due to HAs are naturally expressing brown color. In order to obtain more information from the featureless spectra about the hidden structure of HAs is plausible. Presence of various organic moieties in the structure of humic acids should be reflected in their absorption spectra. Moreover, the data showed that UV absorption is a good indicator of the unsaturated C content of samples and that it can be used as a fast, simple and sensitive method for molecular characterization in general. As a result, the absorption spectra with reference to the chosen wavelengths exhibit structural information as well as DOC content.

2.2.1.2. Characterization of Humic Substances by Fluorescence Spectroscopy. A molecule is excited from a vibrational level in the electronic ground state to one of the many vibrational levels in the electronic excited state by the absorption of UV irradiation. This excited state is usually the first excited singlet state. A molecule in a high vibrational level of the excited state will quickly fall to the lowest vibrational level of this state by losing energy to other molecules through collision. The molecule will also partition the excess energy to other possible modes of vibration and rotation. Fluorescence occurs when the molecule returns to the electronic ground state, from the excited singlet state, by emission of a photon. If a molecule which absorbs UV radiation does not fluoresce it means that it must have lost its energy some other way. These processes are called radiationless transfer of energy. Fluorescence occurs when a molecule absorbs light photons from the UV-visible light spectrum, known as excitation, and then rapidly emits light photons as it returns to its ground state. Fluorescence characterizes the relationship between absorbed and emitted photons at specified wavelengths. This is a precise quantitative analytical technique which is inexpensive and easily mastered.

Excitation, UV absorption, can result in a range of transitions to various vibrational sublevels of excited singlet states. This is the reason that molecular absorption

spectra are often seen to consist of broad peaks. Excitation is then followed by nonradiative relaxation to the lowest sublevel of the S_1 state, via vibrational relaxation and internal conversion. Internal conversion, singlet–triplet intersystem crossing and fluorescence then compete for relaxation to the ground state (S_0). The wavelength of the fluorescence emission is determined by the difference in energy between S_1 and S_0 states. The greater the conjugation in the molecule, the lesser the difference in energy, results in a longer wavelength of fluorescence.

For a transition to take place, the absorbed energy must be equivalent to the difference between the initial electronic state and a high energy state. This value is constant and characteristic of the molecular structure. This is termed the excitation wavelength. All chemical compounds absorb energy which causes excitation of electrons bound in the molecule, such as increased vibrational energy or, under appropriate conditions, transitions between discrete electronic energy states. If conditions permit, an excited molecule will return to ground state by emission of energy through heat and/or emission of energy quanta such as photons. The emission energy or wavelength of these quanta are also equivalent to the difference between two discrete energy states and are characteristic of the molecular structure. Fluorescence occurs when a molecule absorbs photons from the UV-vis light spectrum (200-900 nm), causing transition to a high-energy electronic state and then emits photons as it returns to its initial state, in less than 10-9 sec. Some energy, within the molecule, is lost through heat or vibration so that emitted energy is less than the exciting energy; i.e., the emission wavelength is always longer than the excitation wavelength. The difference between the excitation and emission wavelengths is called the Stokes shift.

Fluorescence techniques have been emphasized in literature to be well suited for studies of natural organic matter because of the sensitivity and nondestructive nature (Senesi et al., 1991). Although the fluorescent structures constitute minor components of the humic macromolecule, their variety and the dependence of their properties on parameters such as molecular weight, concentration and pH

make their investigation particularly useful. Therefore, characterization of humic acids could also be done by fluorescence spectroscopy. Some researchers agree that the basic fluorescence of humic substances contains information relating to structure, functional groups, conformation, and heterogeneity as well as dynamic properties related to their intramolecular and intermolecular interactions (Senesi et al., 1991; Mobed et al., 1996).

Fluorescence spectroscopy is generally acquired in emission, excitation and synchronous scan excitation modes. The emission spectrum is recorded by measuring the relative intensity of radiation emitted as a function of wavelength for a fixed excitation wavelength. The excitation spectrum is recorded by measuring the emission intensity at a fixed wavelength while varying the excitation wavelength. On the other hand, synchronous scan excitation spectra are obtained by measuring the fluorescence intensity while simultaneously scanning over both the excitation and emission wavelengths and keeping a constant between them as $\Delta\lambda = \lambda_{em} - \lambda_{exc}$ (Senesi, 1990). While excitation and emission spectra have provided limited differentiation among various humic fractions, identifying only broad classes of humic and fulvic acids, however, synchronous fluorescence spectroscopy has been used in attempts to resolve the broad, significantly overlapping peaks in the excitation and emission spectra.

While UV absorbance of aromatic rings is less sensitive, both the location and intensity of fluorescence peaks are quite sensitive to functionality. In general, electron donating functional groups (-OH, $-NH_2$) increase the fluorescence intensity while electron accepting functional groups (-COOH) decrease the fluorescence intensity. The presence of carbonyl containing substituent moieties such as hydroxyl, alkoxyl and amino groups causes a shift of fluorescence to longer wavelengths (Senesi, 1990). HAs display a red shift in the fluorescence maxima comparative to FAs from similar sources. This has been ascribed due to the presence of high molecular weight fractions, electron withdrawing substituent moieties and a higher degree of conjugation in the HAs. On the other hand, the

presence of electron withdrawing substituent moieties in FA structure contributes to the relatively short wavelengths of the fluorescence maxima (Mobed et al., 1996). Previous work of Goslan et al. (2004), in the field of fluorescence spectroscopy for characterization of organic matter have established that humic substances typically fluoresce in the excitation range of 300 – 400 nm and the emission range of 400 – 500 nm.

2.3. Advanced Oxidation Processes

Oxidation is defined as the transfer of one or more electrons from an electron donor (reductant) to an electron acceptor (oxidant), which has a higher affinity for electrons. These electron transfers result in the chemical transformation of both the oxidant and the reductant, in some cases producing chemical species with an odd number of valence electrons. These species, known as radicals, tend to be highly unstable and, therefore, highly reactive because one of their electrons is unpaired. Oxidation reactions that produce radicals tend to be followed by additional oxidation reactions between the radical oxidants and other reactants (both organic and inorganic) until thermodynamically stable oxidation products are formed. The ability of an oxidant to initiate chemical reactions is measured in terms of its oxidation potential. In the report published by Dorfman and Adams, 1973 the most powerful oxidants were listed as fluorine, hydroxyl radicals (•OH), ozone, and chlorine with oxidation potentials of 2.85, 2.70, 2.07 and 1.49 electron volts, correspondingly. The end products of complete oxidation (i.e., mineralization) of organic compounds such as benzene are carbon dioxide (CO_2) and water (H_2O).

2.3.1. Photocatalytic Oxidation

In common, photocatalytic processes known as “Advanced Oxidation Processes” can be considered as a set of new technologies collectively that rely on the

generation of very reactive free radicals (e.g. •OH). In recent times the tendency has been to carry out chemical oxidation in the presence of a catalyst that serves as a generator of hydroxyl radicals, and, therefore, the oxidizer in the medium is not necessary. Those reactive radicals are consequently used to degrade the organic pollutants or microorganisms. The principles behind photocatalysis and its environmental applications have been reviewed extensively by Uyguner and Bekbolet, 2006. In order to photoexcite the semiconductor, in the presence of oxygen heterogeneous photocatalytic processes rely on utilizing the near UV radiation. Under these conditions oxidizing species, either bound hydroxyl radical or free holes are generated. These processes are considered heterogeneous in nature because of two active phases; solid and liquid are involved during the reaction sequence. Among many semiconducting oxides as catalysts have been tested; TiO_2 in the anatase form performed the most exciting and efficient features, such as high stability, good performance, ready availability, low toxicity and low cost. The major advantage of the photocatalytic method over UV-C driven AOPs (O_3/UV, H_2O_2/UV) that require light of shorter wavelengths (λ<300 nm) is the optical absorption of TiO_2 in the near UV region. A simplified TiO_2, photocatalytic mechanism is summarized in Figure 2.4.

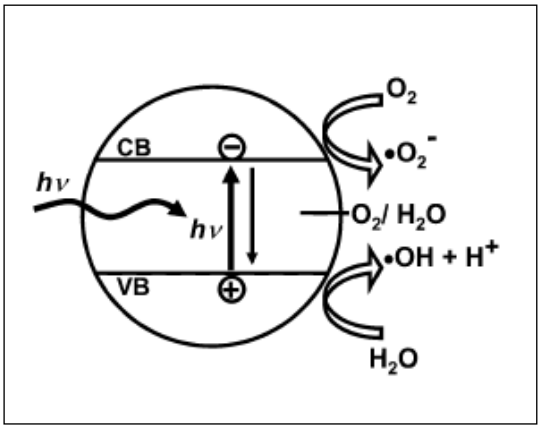

Figure 2.4. Simplified TiO_2 photocatalytic mechanism

Continuous band-gap irradiation (E_{bg} is 3.2 eV (390 nm) in anatase and 3.05 eV (420 nm) in rutile) of an aqueous semiconductor dispersion excites an electron from the valence band (VB) to the conduction band (CB), creating an electron-hole pair. TiO_2 is only active in the ultraviolet region which is less than 10% of the overall solar intensity. Heterogeneous photocatalytic process takes place through a complex sequence of reactions. The relevant reactions at the TiO_2 surface causing the degradation of the organic compounds could be outlined by equations (1)-(13).

The formation of redox pair could either be followed by respective reactions or a recombination reaction resulting in the dissipation of the reactive species (Equations 1-2).

(i) Formation of redox pair through light absorption ($E_{hv} > E_{bg}$):

$$TiO_2 + hv\ (UV) \rightarrow TiO_2\ (e^-_{CB} + h^+_{VB}) \quad (1)$$

(ii) Direct recombination reaction leading to the inactivation of the electron hole pair:

$$TiO_2\ (e^-_{CB} + h^+_{VB}) \rightarrow TiO_2 + heat \quad (2)$$

(iii) Photo-generated holes (h^+_{VB}) may directly oxidize the organic substrate, S anchored to the oxide surface. The principal hole traps are adsorbed H_2O molecules and OH^- forming $HO^\bullet$ radicals. The $HO^\bullet_{(s)}$ radicals adsorbed on the semiconductor surface are the major reactive species due to their high oxidant power (E= +2.80 V) and possible competing reaction leads to the formation of hydrogen peroxide.

$$h^+_{VB} + S \rightarrow S^{\bullet+} \quad (3)$$

$$h^+_{VB} + H_2O \rightarrow HO^\bullet + H^+ \quad (4)$$

$$h^+_{VB} + OH^- \rightarrow HO^\bullet \quad (5)$$

$$HO^\bullet + HO^\bullet \rightarrow H_2O_2 \quad (6)$$

(iv) On the other hand, in the presence of electron hunters (i.e. O_2) reduction reactions may take place leading to the following sequence of the reactions:

$$e^-_{CB} + O_2 \rightarrow O_2^{\bullet -} \quad (7)$$

$$e^-_{CB} + H_2O_2 \rightarrow OH^- + HO^{\bullet} \quad (8)$$

$$O_2^{\bullet -} + H^+ \rightarrow HO_2^{\bullet} \quad (9)$$

$$O_2^{\bullet -} + HO_2^{\bullet} \rightarrow HO_2^- + O_2 \quad (10)$$

$$HO_2^{\bullet} + HO_2^{\bullet} \rightarrow O_2 + H_2O_2 \quad (11)$$

$$H_2O_2 \leftrightarrow HO_2^- + H^+ \qquad pK_a=11.6 \quad (12)$$

$$HO^{\bullet} + HO_2^{\bullet} \rightarrow H_2O + O_2 \quad (13)$$

The degradation of the substrates under investigation is achieved through the reactions of the reactive oxygen species, *i.e.* $HO^{\bullet}$, $HO_2^{\bullet}$, $O_2^{\bullet -}$ .The researchers are mainly concerned about determining the factors that describe the kinetics and physical/chemical pathways of photocatalytic removal of humic acids. In order to explain the limitations of the photocatalytic system; the inhibition and competition effects on the TiO_2/UV system in the presence of humic acid, different TiO_2 brands, various metal ions (Zn, Cu, Cr, Mn, Ca and Mg), some common anions (chloride, nitrate, sulfate and phosphate), oxy-anions (hypochlorite, chlorite, chlorate) and oxidizing species (hydrogen peroxide and bicarbonate) have been studied (Bekbolet and Balcıoğlu, 1996; Gonenc and Bekbolet, 2001; Li et al., 2002; Bekbolet et al., 2002; Wiszniowski et al., 2003; Uyguner and Bekbolet, 2004a). Additionally, Kerc et al., 2003 has also studied the degradation kinetics of a sequential oxidation system that is the combination of preozonation followed by photocatalysis. Furthermore, the properties of photocatalytically oxidized humic acids were investigated focusing on their spectroscopic characterization by UV-vis and fluorescence spectra (Uyguner and Bekbolet, 2005b; Uyguner and Bekbolet, 2005c). However, the photocatalytic oxidation mechanism of humic acids has not been comprehensively elucidated yet. Since insufficient information about the

structural components of humic substances are provided. Changes in the molecular and structural characteristics of humic acid during these processes are not fully illuminated, although certain gross structural characteristics are acknowledged.

2.3.1.1. Pseudo First Order Kinetic Model. Photocatalytic degradation of a variety of organic solutes at low concentrations obeys pseudo first order kinetics as it was extensively explained in literature. The organic compounds (e.g. humic acid, HA) present in the illuminated titania slurry undergo many chain and consecutive reactions. In an ideal case, all intermediate compounds were fully mineralized to carbon dioxide and water.

$$HA \xrightarrow{h\nu/TiO_2} HA_{ox} \rightarrow \rightarrow \rightarrow CO_2 + H_2O + \text{mineral acids} \quad (14)$$

Humic substances is known to obey pseudo first order kinetics and Bekbölet et al., 1998; Bekbölet et al., 2002 expressed the equation of the photocatalytic degradation as;

$$R = - dA / dt = - k A \quad (15)$$

where the terms represented the following meanings;

R: Pseudo first order rate in terms of the specified UV-vis parameters (m^{-1} min^{-1}) or in terms of DOC (mg L^{-1} min^{-1})

A: Specified UV-vis parameters (m^{-1}) or DOC content of HSs (mg L^{-1})

t: Irradiation time (min)

k: Pseudo first order reaction rate constant (min^{-1})

2.3.1.2. Langmuir Hinshelwood Kinetic Model. The photo-degradation kinetics of many organic compounds in TiO_2 suspensions under UV irradiation had often been modeled to the Langmuir-Hinshelwood equation (Eq. (16)) which also covers the adsorption properties of the substrate on the photocatalyst surface (Turchi and Ollis, 1989). With regards to that photocatalysis takes place at the surface, the concentration of substrate adsorbed to the surface directly influences the overall rate of adsorption.

The rate of degradation of humic substances in terms of $Color_{436}$, UV_{254} and other UV-vis parameters was expressed in the following empirical type relationship:

$$R_{LH} = dA / dt = k_{LH} K_{LH} A_0 / (1+K_{LH} A_0) \quad (16)$$

where the terms represented the following meanings;

R_{LH}: Rate of the reaction (m^{-1} min^{-1}),

k_{LH}: Reaction rate constant (m^{-1} min^{-1}),

K_{LH}: Adsorption coefficient of reactant onto TiO_2 under irradiation conditions (m),

A_0: Initial value of the specified UV-vis parameters of humic substances (m^{-1}).

With reference to the previous studies carried out by Bekbolet and co-workers, this study was conducted to fulfill the aim of elucidation of photocatalytic degradation of model humic acids of different origins (Fluka HA and Nordic HA). To achieve this goal investigated against the data obtained from DOC measurement, UV-vis spectra, UV-vis parameters, fluorescence spectra and fluorescence parameters photocatalytically oxidized humic acids were evaluated in the results and discussion section.

3. MATERIALS AND METHODS

3.1. Materials

3.1.1. Humic Acid Solution

Humic substances of terrestrial and aquatic origin were used in bench scale experiments. Commercial humic acid samples were supplied from Fluka humic acid (FHA) and Nordic Humic Acid (NHA) were purchased from the International Humic Substance Society. Brand names were used throughout the text for the purpose of differentiating between humic substances. There is no commercial meaning other than maintaining relevancy to the literature.

A stock solution of 1000 mg L^{-1} was prepared by dissolving the humic acid in distilled deionized water and filtering through filter paper for Nordic humic acid. However, FHA stock solution was prepared according to Urano et al., (1983). Stock solutions of the humic substances were stored in amber glass bottles and were protected from light to prevent decomposition. Appropriate dilutions of humic substances were made weekly from the stock solution using distilled deionized water that had conductivity less than 10 μ S cm^{-1}.

3.1.2. Titanium Dioxide Powder

Degussa P-25 TiO_2 was used as the photocatalyst throughout all photocatalytic oxidation of humic acids performed in this study. Degussa P-25 TiO_2 had 70% anatase and 30% rutile, nonporous crystal structure with the primary particle size of 20 - 30 nm, and BET surface area was 50±15 m^2 g^{-1}.

3.2. Methods

3.2.1. Experimental Set-Up

The photoreactor used was a cylindrical pyrex reaction beaker with a diameter of 7.5 cm, a height of 3.5 cm. A 125 W Black Light Fluorescent Lamp (BLF) with an output spectrum of 320-440 nm was used as the light source. The lamp exhibits emission between 300 nm and 500 nm, and its maximum emission is at 365 nm. The intensity of incident light was measured according to Hatchard and Parker, 1956 as by potassium ferrioxalate actinometer was $2.85x10^{16}$ quanta sec^{-1}. Through all of the experiments, the distance between the lamp and the surface of the suspension in the reactor was kept constant at 16.5 cm (Bekbölet, 1996). In order to focus the light in the center of the photoreactor the photoreactor was enclosed by a mirror covering. The whole system was placed in a container the inner walls of which were coated with Al-foil. Volume of the reaction mixture was 50 mL. An IKAMAG RH magnetic stirrer was employed throughout the duration of the photocatalytic oxidation experiments to provide continuous stirring of the suspension.

3.2.2. Experimental Procedure

Experiments carried out throughout this study were conducted according to the explanation given below.

3.2.2.1. Photocatalytic Oxidation. Appropriate concentrations of humic acid solutions were prepared by dilution from the stock solution. TiO_2 loadings used in the experiments were 0.25 mg mL^{-1}. 50 mL of humic acid solution was poured directly to the reaction vessel containing the required amount of TiO_2. A Black Light Fluorescent Lamp (BLF), 125 W, was located 16.5 cm above the surface of the solution having a light spectrum between 320 – 440 nm (Bekbölet, 1996). In order to ensure a homogeneous mixture of the slurry, it was exposed to sonic

vibration for one minute in Ultrasonic LC30 water bath and then placed on a magnetic stirrer to be irradiated for certain reaction periods ranging from the start of the experiment to 60 minutes. The procedure was repeated with a new sample for each specified irradiation time for all of the runs. Photocatalytic oxidations were conducted in a glass reactor open to the atmosphere, therefore the volume defeat due to the evaporation of water at longer irradiation periods such as 60 minutes was unavoidable. Therefore balance for the evaporation loss after each experiment volume corrections were made with distilled deionized water. Calibrated glassware used in all experiments. For the removal of TiO_2, the suspension filtered through 0.45 μm Millipore Millex-HA cellulose based membrane filter that is attached to a 10 mL syringe. Time dependent changes of filtered samples after photocatalysis were characterized by UV-vis and fluorescence spectroscopy.

3.2.3. Parameters Studied

In this study, in order to describe basic spectroscopic characterization of humic substances UV_{254}, UV_{280}, UV_{365}, $Color_{436}$, Fluorescence intensity and DOC parameters were evaluated. For further evaluations $SUVA_{254}$, $SUVA_{280}$, $SUVA_{365}$, and $SCOA_{436}$ parameters were studied.

3.2.4. Analytical Methods

UV-vis measurements, fluorescence measurements and DOC analysis were done in accordance with the below given explanations.

3.2.4.1. UV-vis Measurements. UV-vis absorption spectra were recorded on a Perkin Elmer Lambda 35 UV/VIS Spectrophotometer employing Hellma quartz cuvettes of 1.0 cm optical path length. Humic and fulvic acids were characterized by UV-vis spectroscopy. Absorbance values at 436 nm ($Color_{436}$) and 254 nm (UV_{254}) were recorded for the evaluation of UV-vis parameters.

Specific UV absorbance ($SUVA_{254}$, cm^{-1} mg^{-1} L) was used to represent DOC normalized aromatic moieties (UV_{254}) whereas specific color absorbance ($SCOA_{436}$, cm^{-1} mg^{-1} L) was defined as $Color_{436}$ / DOC to signify organic carbon normalized color forming moieties.

3.2.4.2. Fluorescence Measurements. Fluoroscence spectra in the emission and synchronous scan modes were recorded on a Perkin Elmer LS 55 Luminescence Spectrometer equipped with a 150W Xenon arc lamp and a red sensitive photomultiplier tube. A 1 cm path length quartz cell was used. The method of measuring fluorescence is that the cuvette holder excites the sample over the entire path length and reads the emitted light at right angles. Both the excitation and the emission slits of the instrument were 10 nm. A scan speed of 400 nm min^{-1} was used with a slit width opening of 10 nm. Opening the slit wider allows more light energy from the xenon light source to excite the molecules in the sample. A larger slit width applies more excitation light energy to a sample, and a less–well defined spectral purity of the excitation and emission bands (e.g., broader emission bands rather than sharper bands) results (Westerhoff et al., 1999). Synchronous scan spectra were recorded in the excitation wavelength range of 300-650 nm excitation wavelength range using the bandwidth of $\Delta\lambda$=18 nm between the excitation and emission monochromators (Senesi, 1990). The scan speed was 400 nm min^{-1}. The emission spectra were scanned over the range of 400-600 nm at a constant excitation wavelength of 350 nm (Senesi, 1990; Hautala et al., 2000). Since all of the spectra were recorded on the same instrument using the same experimental parameters, a comparative discussion of the spectra is acceptable although, no corrections for fluctuation of instrumental factors and for scattering effects (e.g. primary and secondary inner filter effects) were applied to the data (Senesi, 1990; Peuravuori et al., 2002).

Quinone sulfate (QS) solution (1 µg L^{-1} QS in 0.1 N H_2SO_4) was used during the study as a standard solution to monitor the relative energy emitted by the xenon lamp in the fluorimeter (Seitz, 1981; Scully and Lean, 1994). During this study no change in quinone sulfate fluorescence was observed, and consequently the

standard was used as a sensitivity check rather than as an absolute calibration tool.

3.2.4.3. Dissolved Organic Cabon (DOC) Analysis. Dissolved organic carbon content (DOC, mg L^{-1}) measurements of humic substances were performed on a Shimadzu TOC-V WP Total Organic Carbon Analyzer. Calibration of the instrument was done using potassium hydrogen phthalate in the concentration range of 5 - 30 mgL^{-1}.

4. RESULTS AND DISCUSSION

4.1. Material Specification

In this study, in order to characterize natural organic matter in drinking water supplies model compounds of terrestrial and aquatic origin, namely, Fluka humic acid (FHA) and Nordic humic acid (NHA) solutions ranging in concentration from 10 to 50 mg L^{-1} were used. Characterization of the studied humic substances was acquired with respect to their UV-vis spectroscopy and fluorescence spectroscopic parameters, dissolved organic carbon contents and derived parameters.

After the characterization, photocatalytic oxidation of model humic acids was accomplished using TiO_2 Degussa P-25 as the photocatalyst. Based on pseudo first order and Langmuir Hinshelwood kinetic models, the related data were presented in terms of the UV-vis properties of humic substances and the degradation kinetics were comparatively evaluated. Moreover, changes in the molecular and structural characteristics of the humic acid molecule during photocatalytic oxidation were examined by fluorescence spectroscopy (emission and synchronous scan modes).

4.1.1. Spectroscopic Analysis of Humic Acids

In this section, the studied humic substances specifically humic acids representing two different sources (FHA) and NHA) were characterized by UV-vis spectroscopy and fluorescence spectroscopy in emission and synchronous scan modes.

4.1.1.1. UV-vis Spectroscopic Properties of Humic Acids. Characterization of dissolved organic matter in natural waters by means of UV-vis absorption is commonly accepted as conventional and versatile. Normally the UV-vis spectra of humic substances are broad; decrease with increasing wavelength and they do not

exhibit any significant aspects (Schnitzer and Khan, 1972; Traina et al., 1990; Chen et al., 2002; Uyguner and Bekbölet, 2005a). Absorption of light in the UV range by humic substances was caused by π-electrons and reflects aromatic and carboxylic electron systems as well as their conjugates. On the other hand, functional groups with quinoide structures and keto-enol-systems are more responsible for the absorption in the visible range (Frimmel et al., 2002).

UV-vis absorbances with a relative order of absorptivity at 254 nm were measured as follows: FHA > AHA > NHA, ($FHA_{UV254,}$ cm^{-1}: 1.292, AHA_{UV254}, cm^{-1}: 1.278 and $NHA_{UV254,}$ cm^{-1}: 1.229). Persistently, the UV-vis spectra of the humic acids (50 mgL^{-1}) showed a gradually decreasing absorptivity with respect to wavelength in the 200 – 600 nm region (Figure 4.1). The spectra of Nordic humic acid exhibited slightly lower UV absorbance than that of Fluka and Aldrich humic acid. This suggests that FHA and AHA have a relatively high amount of aromatic or polyphenolic organic compounds (Chen et al., 2002). Consistent with literature results, soil derived humic acids have higher absorbance values in the UV-vis region than the aquatic humic acids (Frimmel et al., 2002).

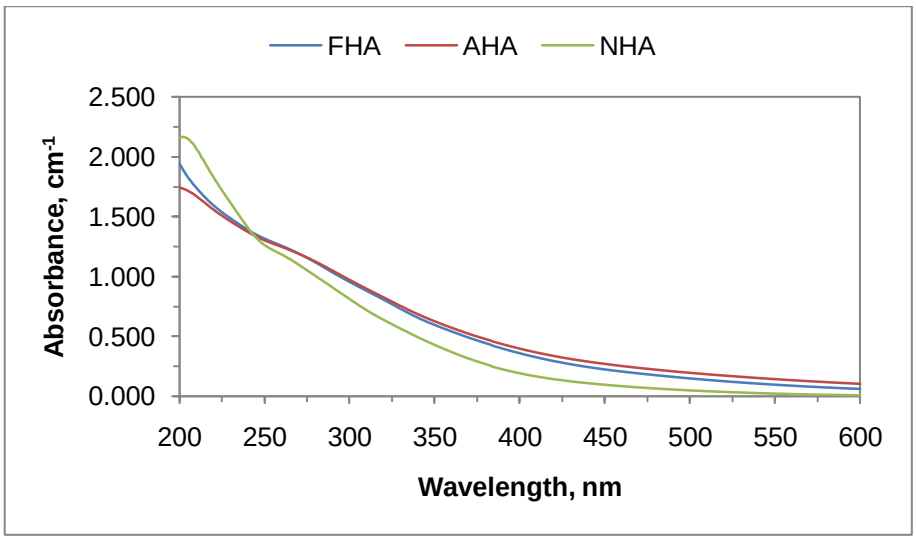

Figure 4.1. UV-vis spectra of humic acids (HA: 50 mg L^{-1})

UV-visible scan spectra of varying concentrations of FHA and NHA ranging from 10 - 50 mg L^{-1} were also displayed in Figure 4.2. All of the spectra displayed the same decreasing profile for both of the humic acids.

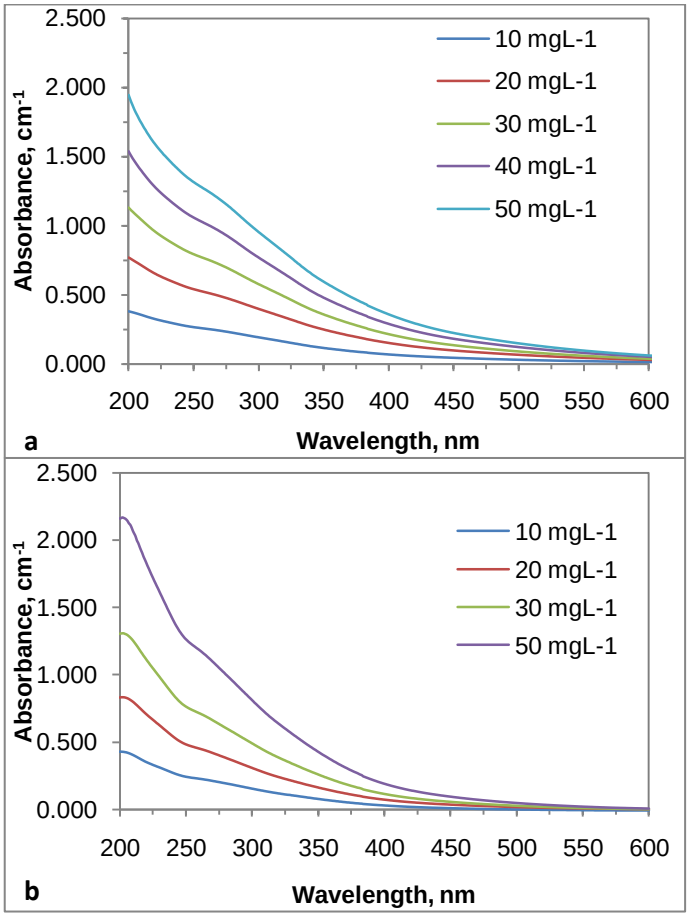

Figure 4.2. UV-vis spectra of (a) FHA and (b) NHA (HA: 10 - 50 mg L^{-1})

DOC values and the specified UV-vis spectroscopic absorbance values i.e. $Color_{436}$, UV_{365}, UV_{280} and UV_{254} were presented in Table 4.1. Depending on the concentration of the working solutions, UV-vis and DOC parameters of the humic substances displayed certain values. The DOC content of FHA (DOC = 20.30 mgL^{-1}) was found to be lower than of NHA (DOC = 26.96 mgL^{-1}) for 50 mgL^{-1} humic acid solutions. DOC contents of the humic acids were found to be in the following order; NHA > FHA > RHA >IHSS HA > AHA > IHSS SHA irrespective to their origin.

Table 4.1. Basic spectroscopic characterization of humic acids (HA: 50 mg L^{-1})

	$Color_{436}$, m^{-1}	**UV_{365}, m^{-1}**	**UV_{280}, m^{-1}**	**UV_{254}, m^{-1}**	**DOC, mg L^{-1}**
FHA	25.4	51.6	111.7	129.2	20.30
NHA	11.4	34.0	100.4	122.9	26.96
AHA*	18.8	39.2	92.1	108.1	15.5
IHSS HA*	15.9	44.3	120.2	148.1	16.16
IHSS soil HA*	28.1	48.4	99.3	114.9	15.48
RHA*	38.0	72.9	159.4	186.3	19.53

* Data collected from Uyguner and Bekbölet, 2005a, where, AHA denotes humic acid supplied from Aldrich, RHA denotes humic acid from Roth and IHSS denotes IHSS, Internatonal Humic Substances Society.

FHA, which is a terrestrial origin humic acid, exhibited 25.4 m^{-1} of $Color_{436}$, whereas NHA illustrated less than half of the value of color forming moieties than FHA as can be seen from Figure 4.1. FHA and NHA had considerably similar UV_{280} and UV_{254} values, emphasizing strong aromatic character. The order of UV_{365}, UV_{280} and UV_{254} absorbing moieties of the samples follows a decreasing trend as; FHA > NHA.

With the purpose of comparison, the data obtained from experimental studies of FHA and NHA were presented in Table 4.1 with reference to the data reported by Uyguner and Bekbölet, 2005a. All humic acids could be expressed by the following decreasing trend in $Color_{436}$ parameter as; RHA > IHSS SHA > FHA > AHA > IHSS HA > NHA. Since both humic acids IHSS HA and NHA are aquatic origin, the lowest $Color_{436}$ values were obtained as expected. Terrestrial humic acids had remarkably higher $Color_{436}$ values than aquatic humic acids.

The UV_{365} parameter displayed as expressed in a decreasing order of RHA > FHA > IHSS SHA > IHSS HA > AHA > NHA irrespective of the source of the samples. Furthermore, RHA was reported to have appreciably high UV_{280} and UV_{254} values as regards the other humic acids emphasizing strong aromatic character. The order of UV_{280} and UV_{254} absorbing moieties of the samples follows a decreasing trend as; RHA > IHSS HA > FHA > NHA > IHSS SHA > AHA, reflecting non-source dependency.

To facilitate the UV-vis absorptivity of different humic acids, derived parameters were assessed using specified UV-vis absorbance values ($Color_{436}$, UV_{365}, UV_{280} and UV_{254}) normalized to the respective DOC contents (m^{-1} mg^{-1} L) such as $SCOA_{436}$, $SUVA_{365}$, $SUVA_{280}$ and $SUVA_{254}$ (Table 4.2). In literature, specific UV absorbance ($SUVA_{254}$, m^{-1} mg^{-1} L) was used to represent DOC normalized aromatic moieties (UV_{254}) whereas specific color absorbance ($SCOA_{436}$, m^{-1} mg^{-1} L) was defined as $Color_{436}$/DOC to signify organic carbon normalized color forming moieties (Uyguner and Bekbölet, 2005a).

Table 4.2. Specific UV- vis parameters of humic acids

	$SCOA_{436}$, m^{-1} mg^{-1} L	**$SUVA_{365}$, m^{-1} mg^{-1} L**	**$SUVA_{280}$, m^{-1} mg^{-1} L**	**$SUVA_{254}$, m^{-1} mg^{-1} L**
FHA	1.3	2.5	5.5	6.4
NHA	0.4	1.3	3.7	4.6
Aldrich HA*	1.2	2.4	6.3	6.7
IHSS HA*	0.9	2.3	6.1	7.8
IHSS soil HA*	1.7	3.0	6.4	7.1
Roth HA*	1.9	3.3	6.5	8.5

* Data collected from Uyguner and Bekbölet, 2005c.

Depending on the explanation that the specific UV absorbance ($SUVA_{254}$) parameter can be used to describe the composition of humic material in terms of hydrophobicity and hydrophilicity, $SUVA_{254} > 4$ indicates mainly hydrophobic and especially aromatic moieties while a $SUVA_{254} < 4$ represents a hydrophilic organic fraction (Edzwald et al. 1985). All specific absorbance values $SCOA_{436}$, $SUVA_{365}$, $SUVA_{280}$, and $SUVA_{254}$ were following increasing trend for both HA species FHA and NHA. Additionally $SCOA_{436}$, $SUVA_{365}$, $SUVA_{280}$, and $SUVA_{254}$ values of NHA were found to be nearly 3.3, 2, 1.5, and 1.4 times lower than FHA.

Considering the data reported by Uyguner & Bekbölet 2005b, $SCOA_{436}$, $SUVA_{365}$, $SUVA_{280}$, and $SUVA_{254}$ values were the highest for RHA sample whereas the lowest values were attained for the NHA (Table 4.2). On the other hand, humic acids originate from aquatic sources IHSS HA and NHA were reported to have the lowest $SCOA_{436}$. Moreover, $SUVA_{365}$, $SUVA_{280}$ and $SUVA_{254}$ values followed a decreasing trend independent from the origin of humic acids.

4.1.1.2. Fluorescence Spectroscopic Properties of Humic Acids. In order to select the appropriate excitation wavelengths for the emission and the synchronous scan spectra preliminary studies were carried out on raw humic acids. Also the effect of concentration of humic acids on the fluorescence spectra was observed. Both aquatic and terrestrial humic acids enclosed inherent fluorescence with the property of parallel variation in the emission maximum when excited at different wavelengths. This by itself indicates the presence of various fluorophores and illustrates the complexity of these materials. Goslan et al., 2004 established that humic substances naturally fluorescence in the excitation range of 300 - 400 nm and the emission range of 400 - 500 nm.

A representative example for the emission scan spectra of FHA at the excitation wavelengths of 350 nm and 370 nm and emission spectra in range of 400 – 600 nm were given in Figure 4.3. The effect of the excitation wavelength on the fluorescence intensity of FHA could be observed most significantly in the region 400-500 nm, whereas the effect could be considered insignificant in the longer wavelength region up to 600 nm. Similar results were obtained for the fluorescence intensity spectra of NHA (Figure 4.4). The decaying profiles of both of the fluorescence spectra displayed an overlaying trend with a slight wavelength shift of 20 nm.

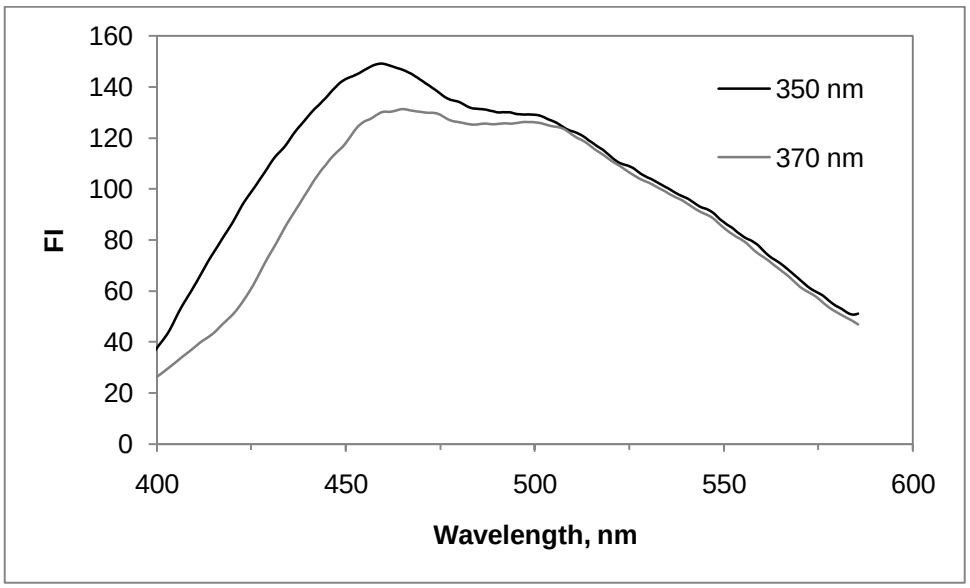

Figure 4.3. Effect of excitation wavelength on the emission fluorescence spectra of FHA (HA: 50 mg L^{-1})

The emission spectra of Fluka humic acid and Nordic humic acid exhibited differing intensity values in the specified range of 400 – 500 nm as illustrated in Figure 4.3 and Figure 4.4. The fluorescence intensities at 450 nm were observed to be differentiated with 18 % and 23 % variation between the lowest and the highest fluorescence intensity. On the other hand, in 500 - 550 nm wavelengths range the intensities

changed with less than 10 % difference. Similar results were reported by Uyguner, 2005 for RHA, IHSS HA, AHA, IHSS SHA. This difference could also be attributed to the diversity in structural composition of the two humic acids.

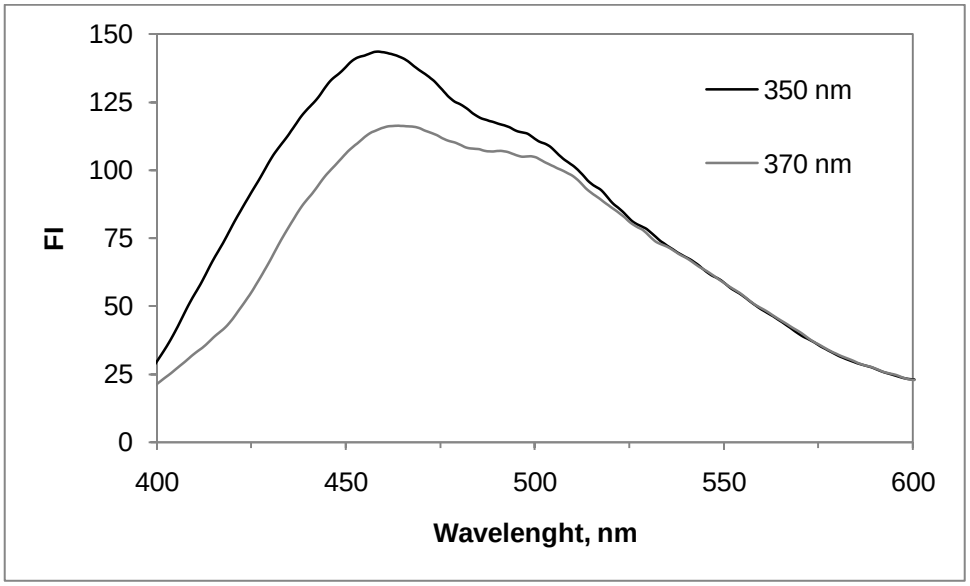

Figure 4.4. Effect of excitation wavelength on the emission fluorescence spectra of NHA (HA: 50 mg L^{-1})

Regarding the highest fluorescence intensity values, excitation wavelengths of 350 nm and 370 were selected for the fluorescence measurements in the emission mode. This selection would be beneficial to follow up the photocatalytic degradation by significant fluorescence measurements. These excitation wavelengths had also been widely used for similar studies in literature (Senesi, 1990; Hautala et al., 2000; Cho and Choi, 2002).

While humic substances exhibit featureless conventional emission spectra, synchronous scan excitation spectra provide a possibility for each fluorescent

component to be identified in a spectral range. Moreover it offers a potential use to reduce overlapping interferences. The synchronous scan fluorescence spectra for FHA and NHA humic acid samples (50 mg L^{-1}) are shown in Figure 4.5. The spectra were plotted as specific fluorescence (fluorescence intensity per unit carbon) vs. excitation wavelength, in order to avoid concentration effects and allow a more precise comparison between the studied samples. $\Delta\lambda$ was chosen as 18 nm throughout this study, to facilitate correspondent results with literature (Senesi, 1990; Rivero et al., 1998; D'Orazio et al., 1999; Peuravuori et al., 2002).

The synchronous scan fluorescence spectra measured proved to be useful for highlighting similarities and differences in the composition of the studied HA. The terrestrial FHA and aquatic NHA have characteristic peaks around 470 nm and 460 nm respectively. Both humic acids displayed a peak with shoulders around 400 nm as represented in Figure 4.5.

The effect of concentration on the fluorescence spectra of humic substances was studied in 10 - 50 mg L^{-1} concentration range for Nordic humic acid. Both the emission and synchronous scan fluorescence spectra of NHA were illustrated in Figure 4.6 and Figure 4.7. Although distinctive fluorescence intensities obtained with emission spectra through different humic acid concentrations, synchronous scan spectra were more informative (Figure 4.6). As expected, the highest fluorescence intensity recorded for the highest humic acid concentration and decreasing trend observed with lower concentrations in the emission spectra.

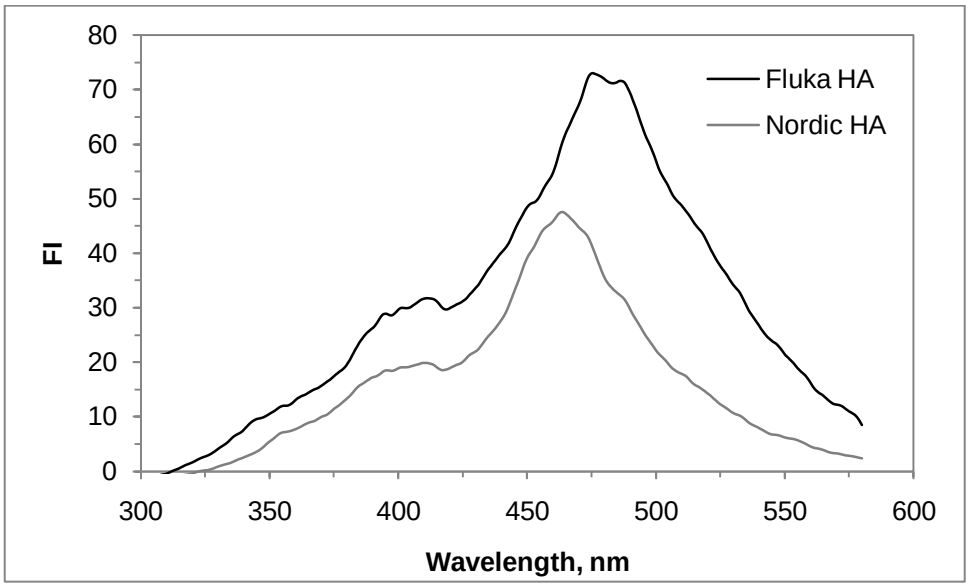

Figure 4.5. Synchronous scan fluorescence spectra of FHA and NHA ($\Delta\lambda$ = 18 nm; HA: 50 mg L^{-1})

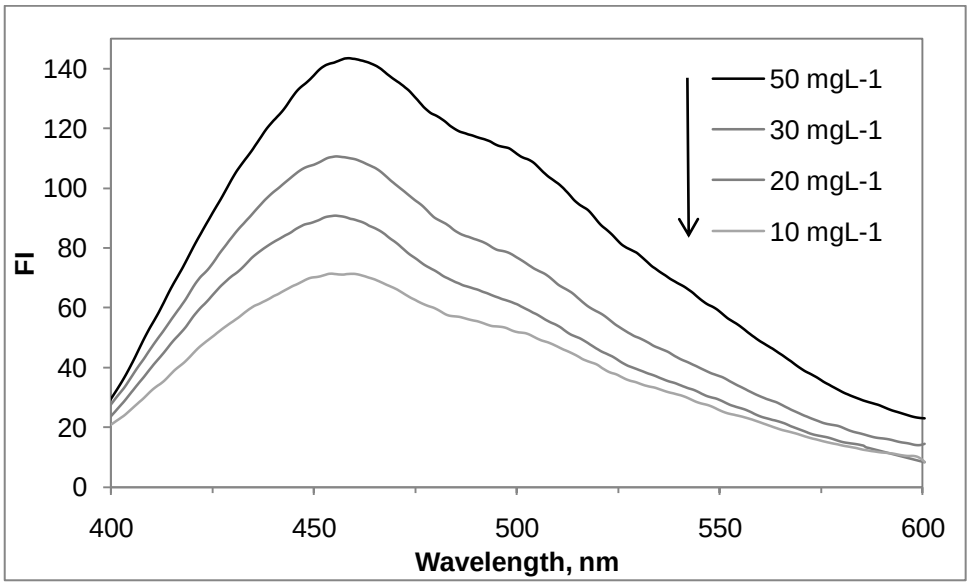

Figure 4.6. Effect of initial concentration on the emission fluorescence spectra of NHA (Excitation wavelength: 350 nm)

Uyguner and Bekbölet, 2005c, reported DOC normalized emission spectra of RHA, IHSS HA, AHA, IHSS SHA in order to avoid concentration effects and allow a more

accurate comparison between the studied samples. However, a plot of the fluorescence intensity per unit dissolved organic carbon of each of the humic substances did not significantly change the shape of the fluorescence spectra; the reason was explained to be due to the DOC contents of humic substances (50 mg L^{-1}) ranging from 15.50 to 20.56 mg L^{-1} as listed in Table 4.1 (Uyguner, 2005; Uyguner and Bekbölet, 2005c). Investigating the fluorescence emission spectra per unit DOC as of FHA and NHA shown in Figure 4.7, the relationship with other humic acids found to be in the following order: AHA > FHA > IHSS HA > IHSS SHA > NHA > RHA. While NHA was reported to have a higher broad peak by Uyguner, 2005, in this study NHA gave a sharp lower peak around ~450 nm. On the other hand IHSS SHA was reported to have a broad peak around ~510 nm, but terrestrial origin FHA did not show similarity in terms of DOC normalized fluorescence emission spectra.

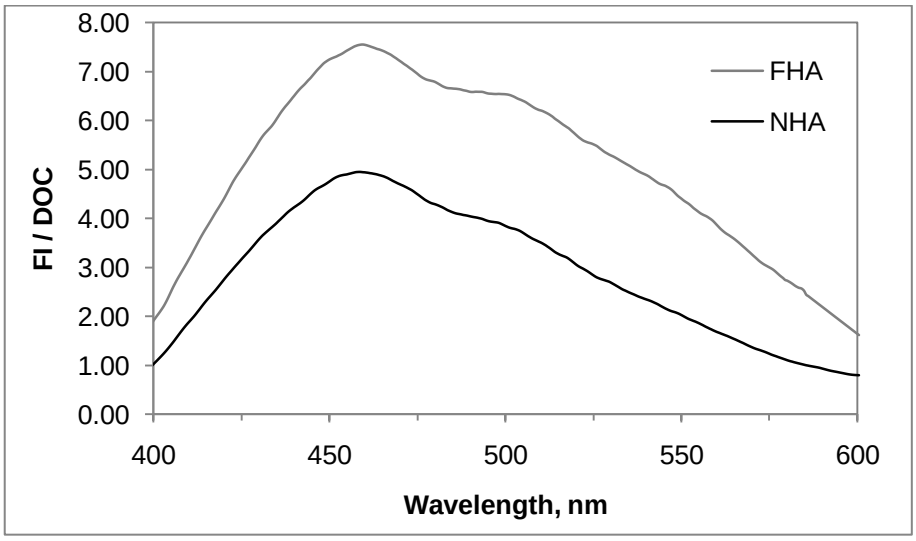

Figure 4.7. DOC normalized emission fluorescence spectra of FHA and NHA (Excitation Wavelength: 350 nm, HA: 50 mg L^{-1})

The synchronous scan spectra of humic acid, changing the concentration attained an inconsequential effect on the position of bands and shoulders but modified their

intensities. The overall fluorescence intensity of humic acid increased up to 50 mg L^{-1} and persisted almost unchanged at higher concentration probably due to intermolecular structure (Figure 4.8). Parallel results were reported for the other humic substances in accordance with the literature (Senesi, 1990).

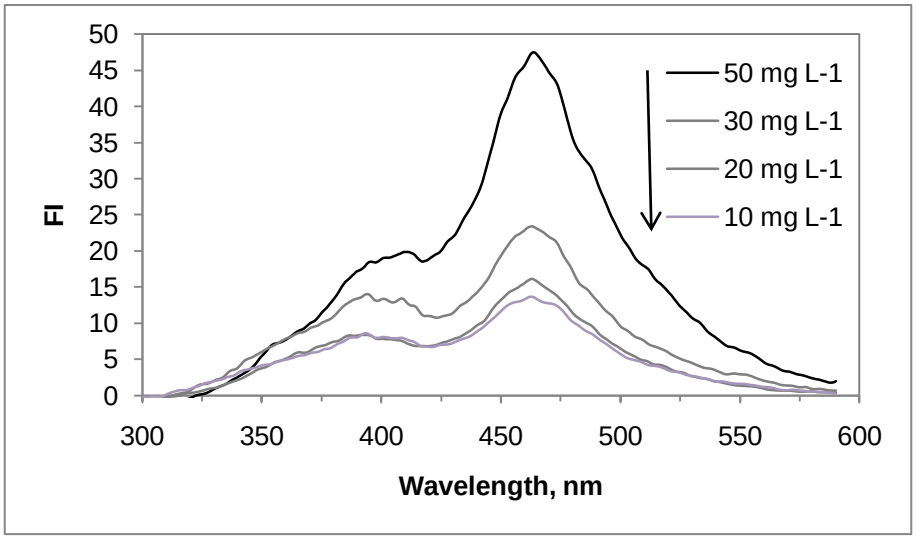

Figure 4.8. Synchronous scan fluorescence spectra of NHA in various concentrations ($\Delta\lambda$ = 18 nm)

DOC normalized synchronous scan fluorescence spectra of FHA and NHA were shown in Figure 4.9. FHA found to have twice the value of fluorescence intensity than NHA. Uyguner and Bekbölet, 2005c, stated consistent data with the results presented in this study: the terrestrial IHSS Soil HA, FHA and AHA had typical peaks around 470 nm with relatively higher intensities than those of Roth and IHSS HA. In addition, a minor peak around 400 nm was reported for IHSS Soil HA as found for FHA and NHA. However, the synchronous scan fluorescence spectra of Roth and IHSS HA were very similar to each other and demonstrated wide bands without any significant feature (Uyguner and Bekbölet, 2005c).

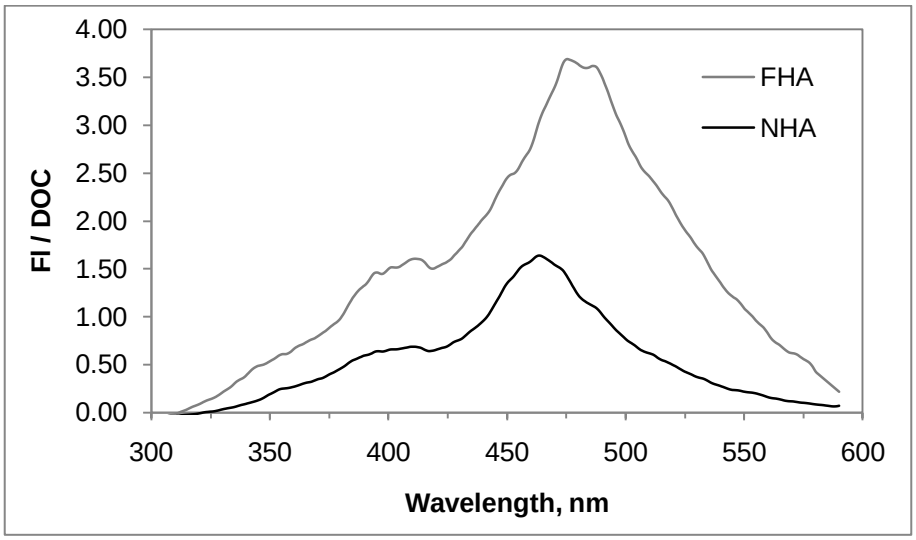

Figure 4.9. DOC normalized synchronous scan fluorescence spectra of FHA and NHA ($\Delta\lambda$ = 18 nm; HA: 50 mg L^{-1})

In view of the fact that the fluorescence spectra reflect the sum of all of the different fluorophores present; distinctive identification of chemical structures responsible for fluorescence is still an open topic for HA, due to the complexity and heterogeneity of humic substances.

4.2. Oxidative Treatment of Humic Acids via Photocatalysis

In this section, humic acids from aquatic and terrestrial origins namely, Fluka humic acid and Nordic humic acid were treated by photocatalytic oxidation using TiO_2 Degussa P-25 as the photocatalyst in the presence of light irradiation. The degradation data were followed by UV-vis and fluorescence spectra, similarly to the changes in DOC content. The related specified UV-vis parameters as $Color_{436}$, UV_{365}, UV_{280} and UV_{254} were evaluated and kinetic modeling of the photocatalytic removal was based on both pseudo first order and Langmuir Hinshelwood models.

4.2.1. Preliminary Experiments

In order to understand interactions between humic acid and TiO_2 preliminary experiments in the absence of UV irradiation and in the absence of the photocatalyst were carried out prior to the characterization of the oxidized humic acids.

4.2.1.1. Experiments Carried Out in the Absence of Light. Through investigation UV-vis spectra of FHA dark experiments, a decrease was observed from time zero to 60 minutes of reaction period with respect to untreated humic acid solution (Figure 4.10a). Similarly to FHA, UV-vis spectra of NHA through dark experiments same decrease was also practical from time zero to 60 minutes of reaction period with respect to untreated humic acid solution (Figure 4.10b).

It was observed that with increasing time period of experiments initial adsorption of humic acid on TiO_2 was increased as well. Moreover, adsorption of aquatic origin NHA on TiO_2 surface was greater than the adsorption of terrestrial FHA as could be visualized by the UV-vis absorption spectra recorded in the 200 to 600 nm wavelength region (Figure 4.10a and Figure 4.10b). Moreover the dark adsorption efficiency of the humic acid onto TiO_2 oxide surface could be evaluated with respect to the specified UV-vis parameters as $Color_{436}$ and UV_{254}.

Studied UV-vis parameters revealed that; experiments conducted from 10 to 50 minutes with FHA revealed an average of 60% and 70% $Color_{436}$ and UV_{254} removal respectively. In extended reaction time i.e. 60 minutes, a slight decline was observed.

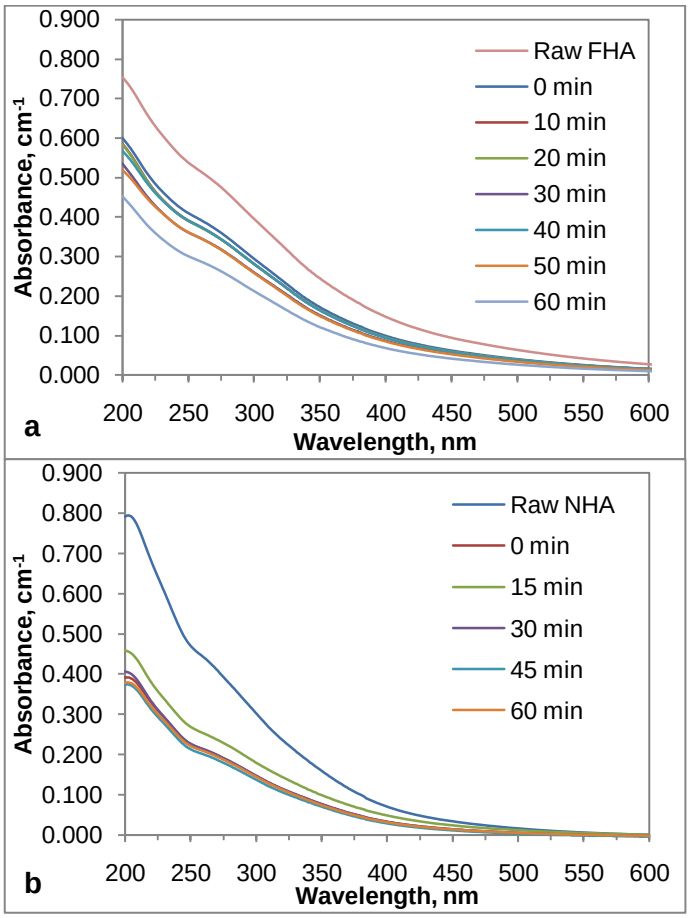

Figure 4.10. UV-vis spectra of (a) FHA and (b) NHA in the absence of light (HA: 20 mg L^{-1}, TiO_2: 0.25 mg mL^{-1})

This decrease could be explained by the adsorption feature of TiO_2 (Figure 4.11a). Uv-vis parameters acquired from the preliminary experiments of FHA (20 mgL^{-1}) were shown in Figure 4.11a. Unlike FHA, after 15 minutes of NHA and TiO_2 reaction in the absence of light an increase was observed. 30% of $Color_{436}$ and 33% of UV_{254} removal attained. When we compare initial adsorption of HA on TiO_2, it can be concluded that this early stage of the reaction adsorbed HA on TiO_2 surface could be desorbed. On the other hand average $Color_{436}$ and UV_{254} removals were 53% and 50% (Figure 4.11b).

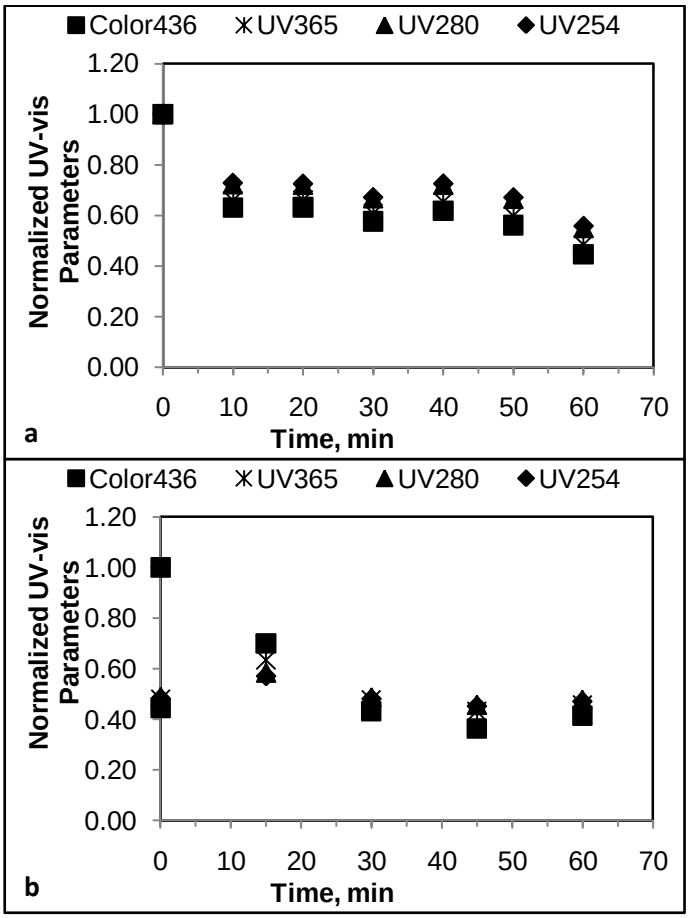

Figure 4.11. Preliminary experiments conducted in the absence of light (a) FHA and (b) NHA (HA: 20 mg L^{-1}, TiO_2: 0.25 mg mL^{-1})

FHA and NHA samples which were subjected to the preliminary experiments in the absence of light were excited at 350 nm and 370 nm and the fluorescence emission spectra were drawn against fluorescence intensity (FI) (Figure 4.12 and Figure 4.13). Examining the emission spectra of the samples excited at 350 nm, a peak with 136 FI was recorded around ~455 nm. The emission spectra of FHA displayed that fluorescence intensity of the samples did not change significantly after the time periods from 10 minutes to 60 minutes (Figure 4.12a), the lowest fluorescence intensity was 121 for time zero while after 50 - 60 minutes it was 135.

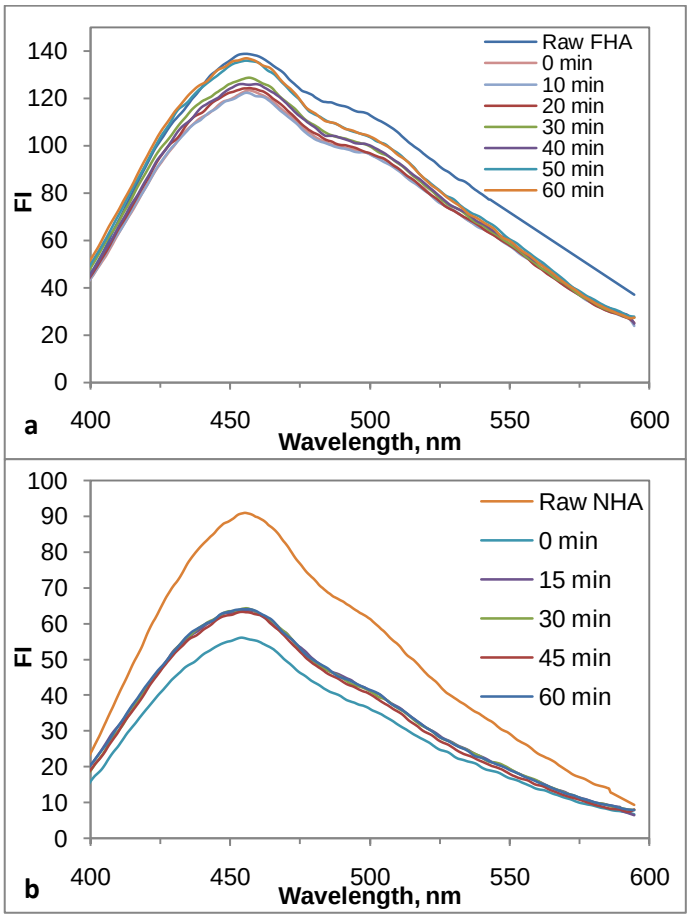

Figure 4.12. The emission fluorescence spectra of preliminary experiments conducted in the absence of light (a) FHA and (b) NHA (HA: 20 mg L^{-1}, TiO_2: 0.25 mg mL^{-1}, Excitation wavelength: 350 nm)

The fluorescence emission spectra of NHA was also drawn (Figure 4.12b). It was observed that initial adsorption of fluorescent moieties was achieved by the decrease in fluorescence intensity in the major peak around ~450 nm. It was measured 90 for raw NHA and 55 at time zero. After longer time from 15 minutes to 60 minutes, higher fluorescence intensity was assessed as 60. This result was found to be consistent with the increase reported for Uv-visible parameters i.e. $Color_{436}$ and UV_{254}.

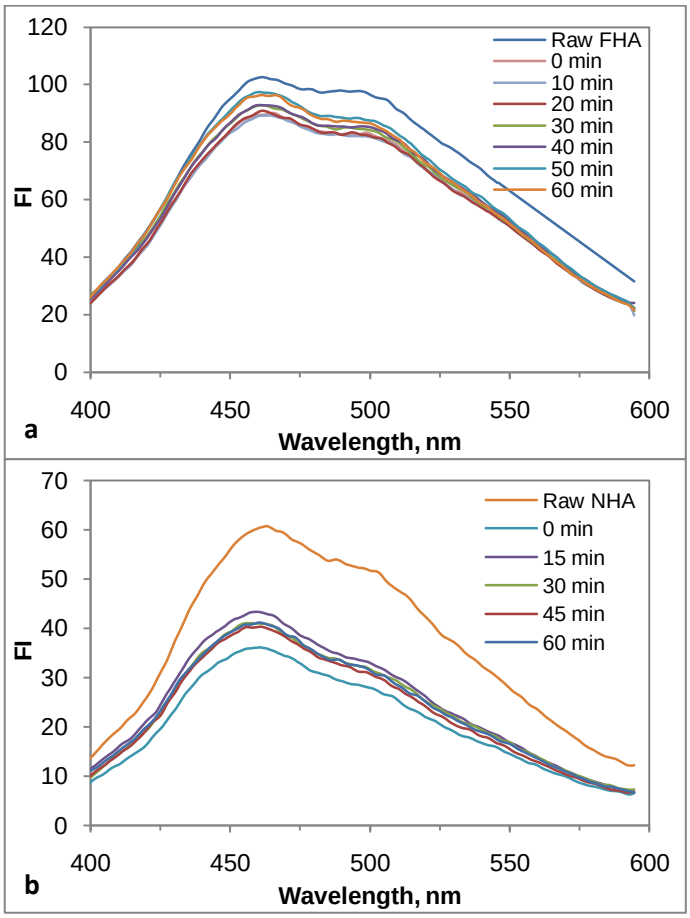

Figure 4.13. The emission fluorescence spectra of preliminary experiments conducted in the absence of light (a) FHA and (b) NHA (HA: 20 mg L^{-1}, TiO_2: 0.25 mg mL^{-1}, Excitation wavelength: 370 nm)

Exciting the samples at 370 nm; fluorescence emission spectra (Figure 4.13) revealed a different shape than the excitation at 350 nm of both humic acids (FHA and NHA). While the samples excited at 350 nm gave only one peak around ~450 nm; exciting at 370 nm caused one major peak around ~455 nm and a shoulder around ~500 nm. Through the experiment sequence of FHA from 10 minutes to 60 minutes not more than 10 units of fluorescence intensity decrease was detected in the fluorescence intensity of the main peak. Similarly the shoulder around ~500 nm was declined less than 10 % in the fluorescence intensity (Figure 4.13a). On the other

hand NHA displayed greater drop off in the major peak's fluorescence intensity at initial adsorption point from 59 to 35, while the shoulder around ~500 nm was disappeared. The adsorbed fluorescent substances could have been desorbed through longer time periods, since the fluorescence intensity was found to be increased from 35 to 40 respectively from time zero to 60 minutes.

Synchronous scan spectra of preliminary experiments conducted in the absence of light for FHA and NHA were shown in Figure 4.14. The spectra obtained through experiments were evaluated against the raw humic acids' spectra, and both humic acids' spectra were displaying different patterns. Noticeably, the major peak for FHA and NHA were recorded near to 470 nm and 460 nm respectively. Not only the locations but also the measured fluorescence intensities of the peaks were different. Synchronous scan spectra of FHA, illustrated by Figure 4.14a, gave a major peak around ~470 nm and a minor peak around ~400 nm with 40 and 25 fluorescence intensities respectively.

After 30 minutes of reaction time period, another minor peak reached its maximum fluorescence intensity around ~350 nm, while it was not applicable for the raw FHA. This peak was not observed for longer experimental periods e.g. 60 minutes. Similar to FHA, the characteristic peak of NHA around ~460 nm and a minor peak around ~400 were obtained from the synchronous spectra with the fluorescence intensities of 18 and 9 respectively. Noticeable changes in the shape of synchronous scan fluorescence spectra of NHA were seen in Figure 4.14b. The peaks which were emerged after 15 minutes and 60 minutes of reaction time in the region of 350 nm were not observed for 30 minutes and 45 minutes of reaction periods.

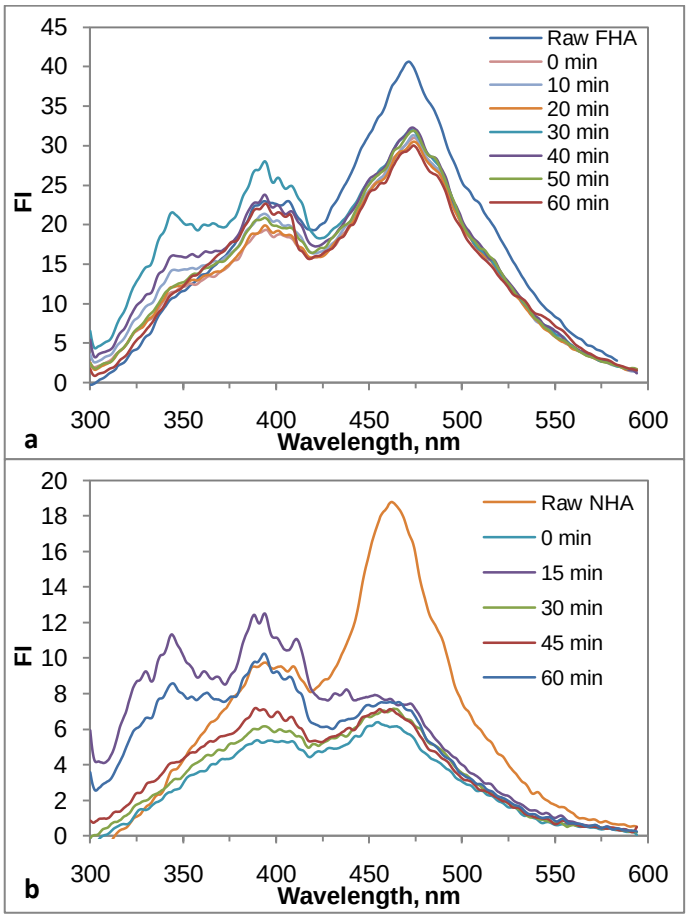

Figure 4.14. The synchronous scan fluorescence spectra of preliminary experiments conducted in the absence of light for (a) FHA and (b) NHA (HA: 20 mg L^{-1}, TiO_2: 0.25 mg mL^{-1}, $\Delta\lambda$ = 18 nm)

4.2.1.2. Experiments Carried Out in the Absence of Photocatalyst. Due to its composition and attached structural compounds, yellow-brown colored NOM absorbs light. Frimmel (1998), investigated the effect of visible light ($\lambda >$ 400 nm), UV-A (defined as the range between 320 nm $< \lambda <$400 nm) region and UV-B (defined as the range between 280 nm $\leq \lambda <$ 320 nm) range on NOM. It was reported that, irradiation of the diluted aqueous NOM samples did not lead to a significant decrease in the overall organic carbon content. Since DOC content of the samples after irradiation expressed less than 10 % and it was not systematic. Although the spectral

absorbance was sensitive enough to prove the bleaching effect in the samples irradiated for 6 - 12 hours in both the "UVA" and the "UVB" experiment, maximum effect was on conjugated n-bonds and $n \rightarrow \pi^*$ transitions absorbing around 320 nm with less than 15 % change after 12 hours of irradiation.

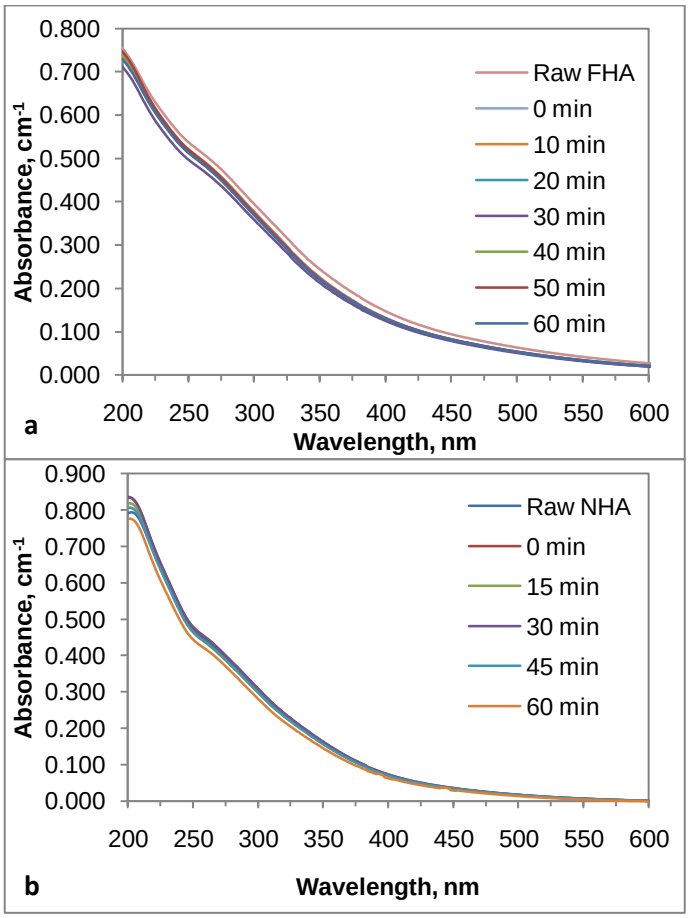

Figure 4.15. UV-vis spectra of (a) FHA and (b) NHA in the absence of TiO_2 (HA: 20 mg L^{-1}, I_0=2.85x10^{16} quanta sec^{-1})

FHA and NHA were treated in the absence of the photocatalyst with similar intention to the experiments carried out in the absence of light (Figure 4.15a and Figure 4.15b). Keeping the experimental conditions constant, only TiO_2 was not included in these experiments. However, it did not display a significant decreasing trend on the spectra for any time period of reactions as expected.

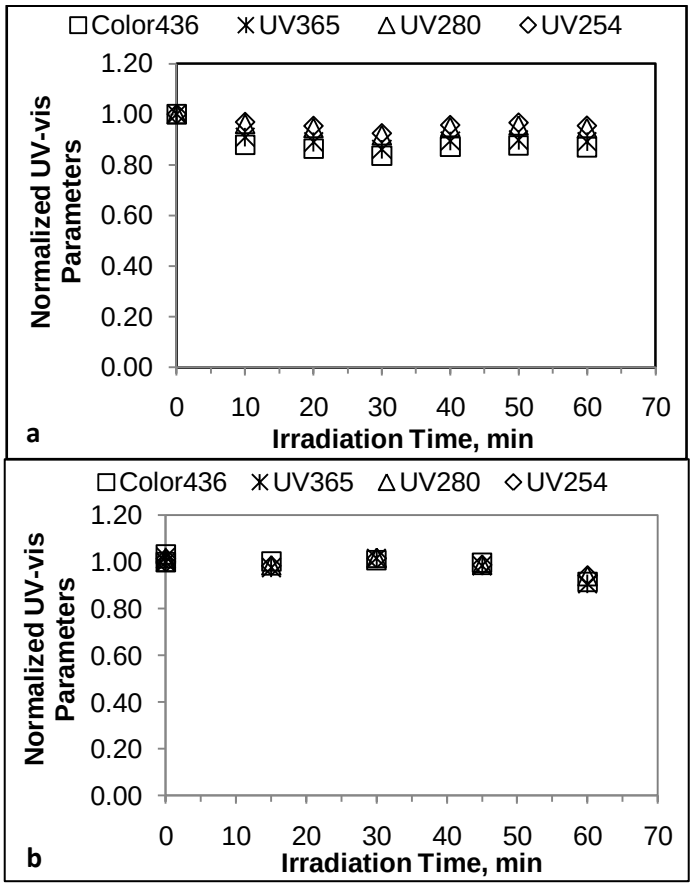

Figure 4.16. Preliminary experiments conducted in the absence of TiO_2 for (a) FHA and (b) NHA (HA: 20 mg L^{-1}, I_0=2.85x10^{16} quanta sec^{-1})

Furthermore, considerable time dependant changes neither for FHA nor for NHA were recorded in the selected UV-vis parameters (i.e. $Color_{436}$ and UV_{254}) as well. After 60 minutes of irradiation period, detected $Color_{436}$ and UV_{254} in the solutions were 87 % and 95 % for FHA and 91 % and 94 % for NHA. This suggested that in the absence of the photocatalyst, humic acids did not exhibit any remarkable decrease in UV-vis parameters. Furthermore, initial adsorption was not achieved because TiO_2 was not present in the solution (Figure 4.15 and Figure 4.16).

Similarly to the preliminary experiments carried out in dark; FHA and NHA which were subjected to the preliminary experiments in the absence of TiO_2 were excited at 350

nm and 370 nm and the fluorescence emission spectra were illustrated against fluorescence intensity by Figure 4.17 and Figure 4.18. The emission spectra of FHA (excitation wavelength: 350 nm) treated in the absence of the photocatalyst was different from the dark reactions in shape (Figure 4.17a).

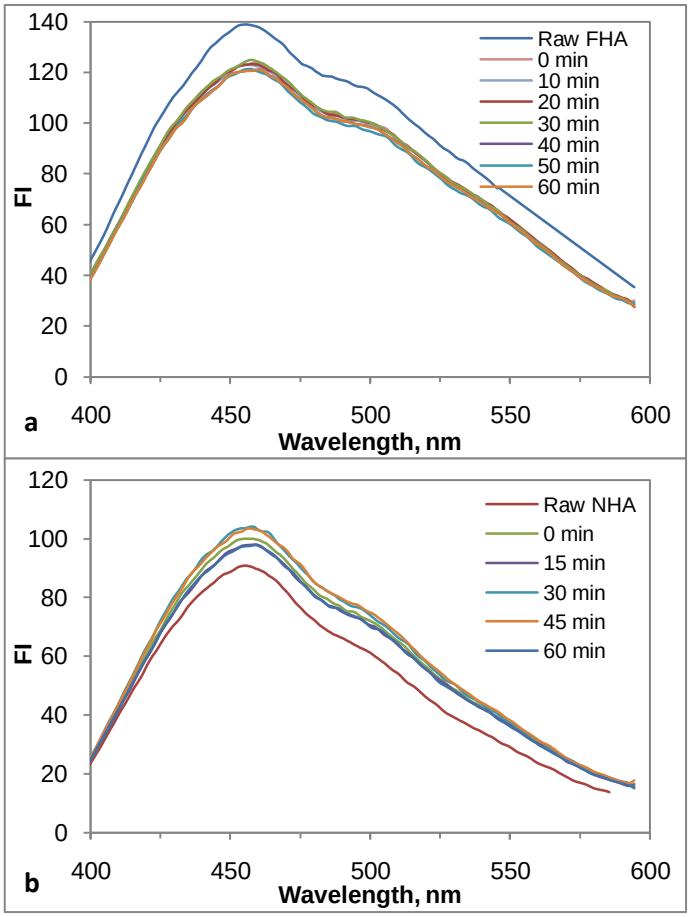

Figure 4.17. The emission fluorescence spectra of preliminary experiments conducted in the absence of TiO_2 (a) FHA and (b) NHA (HA: 20 mg L^{-1}, I_0=2.85x10^{16} quanta sec^{-1}, Excitation wavelength: 350 nm)

Raw FHA had a major peak in the region of 450 nm and a shoulder ~500 nm when excited at 350 nm by means of fluorescence intensity 140 and 100 correspondingly.

Starting from time zero to 60 minutes of experimental sequence fluorescence intensities slightly declined and remained unchanged. Conversely to FHA, NHA fluorescence intensity observed to be in increasing trend through emission spectra (Figure 4.17b). Excitation at 370 nm emission spectra of both FHA and NHA (Figure 4.18a and Figure 4.18b) were observed to be in the same trend of excitation at 350 nm but with lower fluorescence intensities respectively.

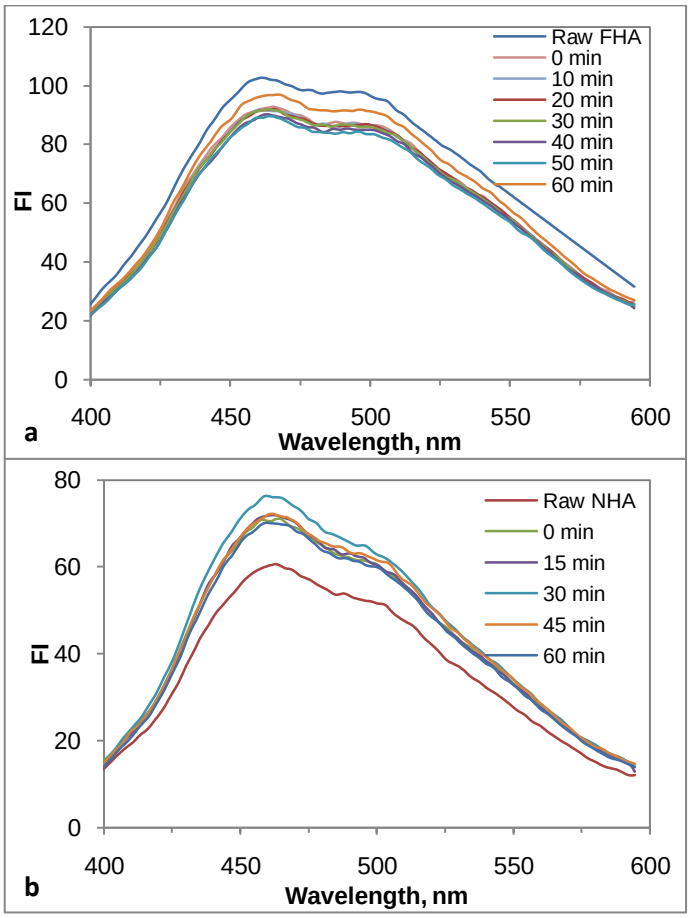

Figure 4.18. The emission fluorescence spectra of preliminary experiments conducted in the absence of TiO_2 (a) FHA and (b) NHA (HA: 20 mg L^{-1}, I_0=2.85x10^{16} quanta sec^{-1}, Excitation wavelength: 370 nm)

The synchronous spectra were also changing in the same way as emission spectra shown in Figure 4.19. Experiments carried out with FHA were decreased and remained unchanged from time zero to longer stages. Only a slight increase was observed after 60 minutes of reaction in the major peak's fluorescence intensity compared to shorter reaction time periods of the experiments.

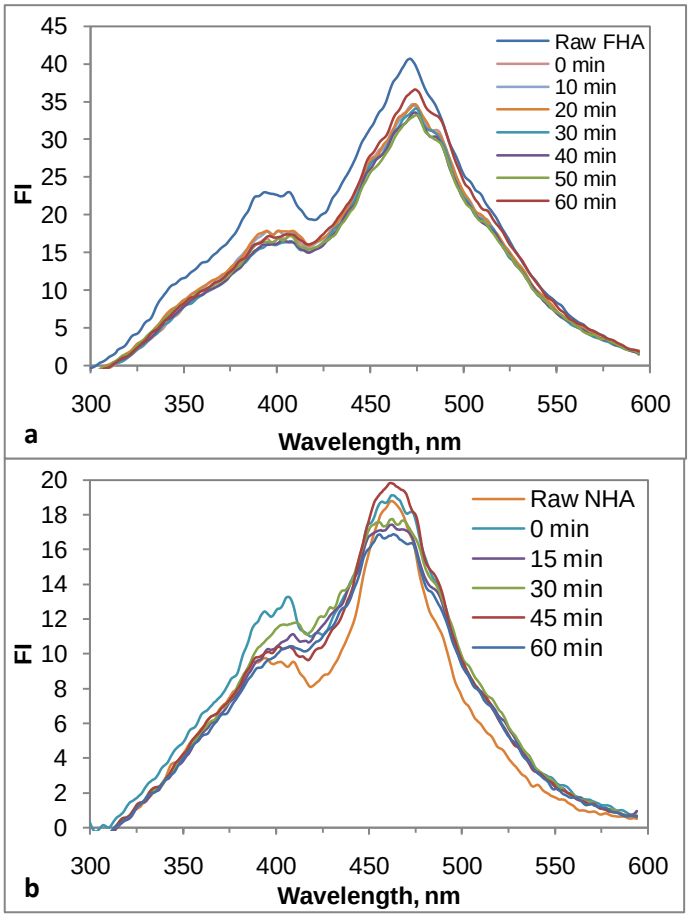

Figure 4.19. The synchronous scan fluorescence spectra of preliminary experiments conducted in the absence of TiO_2 (a) FHA and (b) NHA (HA: 20 mg L^{-1}, I_0=2.85x10^{16} quanta sec^{-1}, $\Delta\lambda$ = 18 nm)

Reactions conducted using NHA followed different pattern from the oxidized FHA. At time zero and 45 minutes of reaction period the synchronous spectra were observed to be increasing. However 15 minutes, 30 minutes and 60 minutes of reaction time period caused a slight increase in the fluorescence intensity of the minor peak, but the major peak was reduced. Obviously depicted in Figure 4.19b, above mentioned changes were not systematic and therefore would not be considered as meaningful.

After the preliminary experiments carried out without TiO_2, the characteristic sharp peak in the region of 470 nm of raw FHA and the moderate peak around 400 nm decayed in intensity (Figure 4.19a). However, the typical sharp peak in the region of 460 nm of raw NHA was observed to be increasing in fluorescence intensity at time zero and after 45 minutes of reaction and reducing after 15 minutes, 30 minutes and 60 minutes of reaction time period. But the moderate peak around 400 nm rose in intensity after all reaction sequences; the maximum intensity caused by time zero was nearly 13 FI while raw NHA had 10 FI at the same wavelength region (Figure 4.19b).

4.2.2. Photocatalytic Degradation of Humic Acid

Throughout photocatalytic oxidation, humic acids of different origin (terrestrial and aquatic) were used in bench-scale experiments. While commercial FHA was purchased from Fluka, Nordic Humic Acid (NHA) was purchased from the International Humic Substance Society. Although a wide range of humic acid solutions between 10 mg L^{-1} - 50 mg L^{-1} were studied, in order to discuss relative results a representative humic acid concentration of 20 mg L^{-1} was selected for FHA and NHA. TiO_2 loadings were kept constant as 0.25 mg mL^{-1}, while the solution was still clear enough to allow light penetration into the solution.

4.2.2.1. Photocatalytic Degradation of FHA. The soil origin humic acid FHA was prepared in 20 mg L^{-1} concentration, furthermore oxidized humic acid was inspected by UV-visible spectra, fluorescence spectra, UV-visible parameters, fluorescence parameters and DOC as well as raw humic acid. TiO_2 dose in the solutions were maintained as 0.25 mg mL^{-1}.

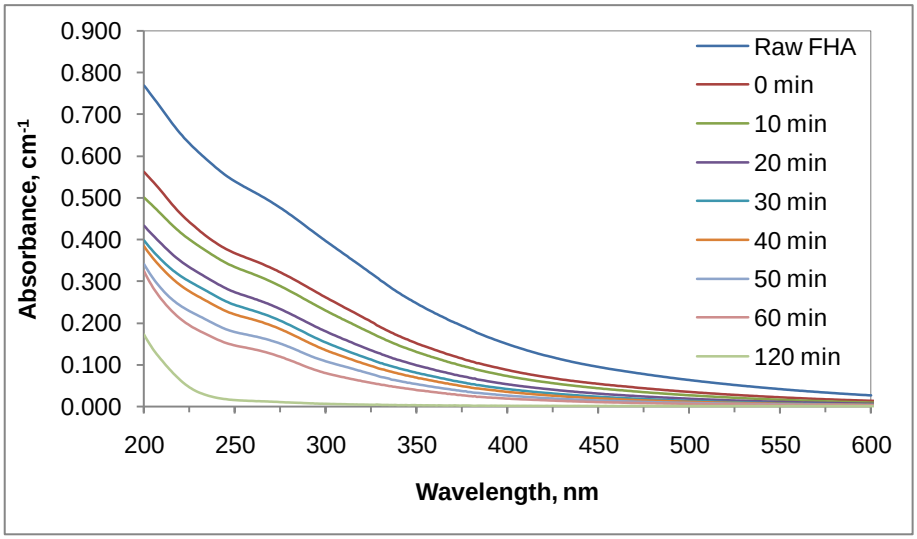

Figure 4.20. UV-vis spectra of the photocatalytic degradation of FHA (HA: 20 mg L^{-1}, TiO_2: 0.25 mg mL^{-1}; I_0=2.85x10^{16} quanta sec^{-1})

As already mentioned previously, the UV-visible spectra of humic acids are broad, featureless and monotonously decrease with increasing wavelength. A representative example of the time dependent UV-visible spectra was given for the photocatalytic oxidation of FHA (Figure 4.20). The oxidized humic acid samples also followed the same decreasing trend as presented in Figure 4.20. The effect of prolonged irradiation time was displayed by the spectra recorded for 120 min irradiation time displaying no distinctive absorbance recordings for the indicated spectroscopic parameters, $Color_{436}$ and UV_{254} as well as the others (Figure 4.21).

While 52 % of $Color_{436}$ removed in 10 minutes of irradiation, 89 % removal achieved after 60 minutes. In extended irradiation times i.e. 120 min, $Color_{436}$ was thoroughly

removed from the suspension, only 0.02 % $Color_{436}$ was detected for FHA. Similar to $Color_{436}$, UV_{254} changes demonstrated declining pattern with 73 % and 97 % of UV_{254} reduction after 60 minutes and 120 minutes of irradiation with FHA respectively. Moreover, DOC removal data were also determined to display the expected declining profile with respect to UV-vis parameters. 63 % of DOC removal was achieved after 60 minutes of irradiation as demonstrated in Figure 4.21.

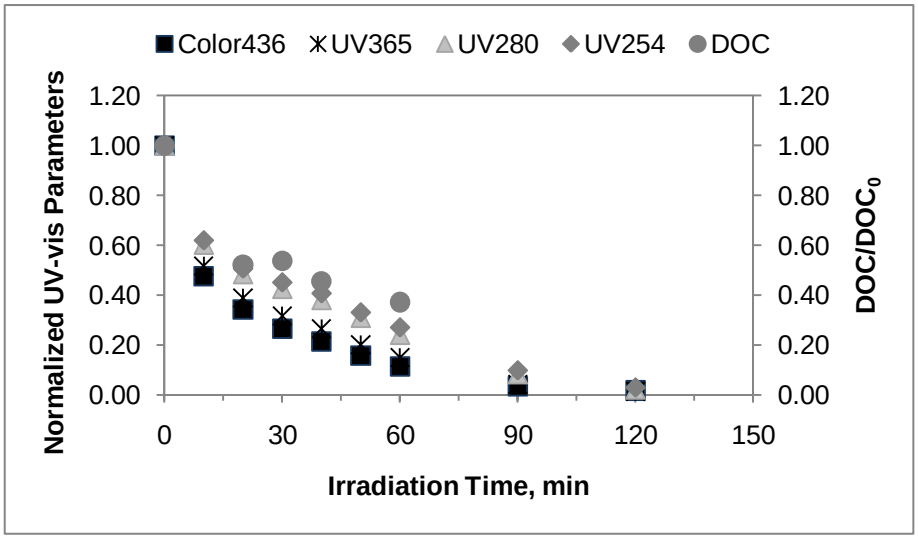

Figure 4.21. Photocatalytic degradation of FHA illustrated by normalized spectroscopic parameters ($Color_{436}$, UV_{365}, UV_{280}, UV_{254}) correlated with DOC removal (HA: 20 mg L^{-1}, TiO_2: 0.25 mg mL^{-1}; I_0=2.85x10^{16} quanta sec^{-1})

The emission fluorescence spectra of FHA samples were displayed in Figure 4.22. While Figure 4.22a shows the spectra of the samples excited at 350 nm, Figure 4.22b shows the excitation at 370 nm. It was obtained that both excitation wavelength caused a major peak in the region of 450 nm, but with differentiating in the fluorescence intensities. Both of the excitation wavelength caused similar change in the emission spectra after photocatalytic oxidation of FHA. While at the emission spectra of time zero was nearly unchanged, maximum fluorescence intensities were obtained after 30 minutes of reaction intervals; almost 220 FI when excited at 350 nm and nearly 135 FI at 370 nm excitation wavelength. Conversely, after prolonged irradiation time periods i.e. 60 minutes fluorescence intensity of the major peaks were

decreased; 153 FI and 95FI were recorded with respect to excitation wavelength of 350 nm and 370 nm.

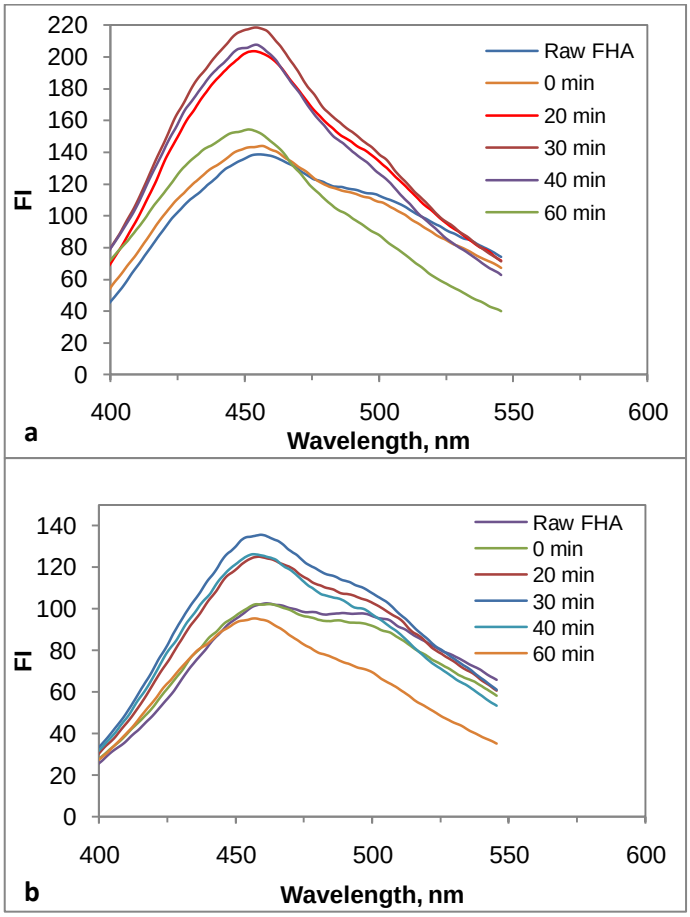

Figure 4.22. Effect of excitation wavelength at (a) 350 nm and (b) 370 nm on the emission fluorescence spectra of oxidized FHA (HA: 20 mg L^{-1}, TiO_2: 0.25 mg mL^{-1}; I_0=2.85x10^{16} quanta sec^{-1})

The synchronous scan fluorescence spectra for oxidized FHA were shown in Figure 4.23. Raw FHA has a sharp peak around 472 nm with a relative fluorescence intensity of 40.6 and a moderate peak around 400 nm. It was remarkable that the characteristic peak of FHA was significantly reduced even with the sole action of TiO_2

prior to irradiation; moreover the importance of initial adsorption of the humic acid onto TiO_2 was proved.

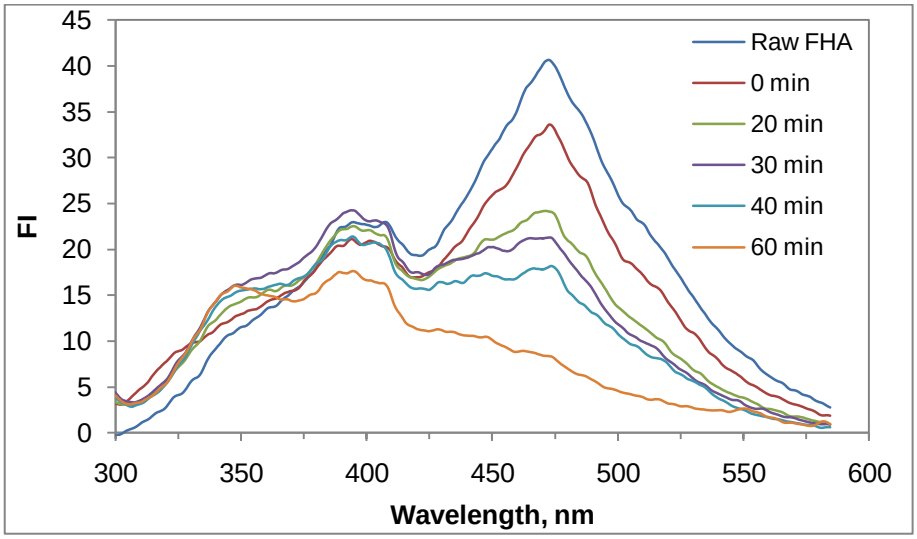

Figure 4.23. The synchronous scan fluorescence spectra of oxidized FHA (HA: 20 mg L^{-1}, TiO_2: 0.25 mg mL^{-1}; I_0=2.85x10^{16} quanta sec^{-1}, $\Delta\lambda$=18 nm)

After 60 min of irradiation, the characteristic sharp peak of raw FHA completely disappeared; the moderate peak around 400 nm decayed in intensity and another peak of low intensity in the region of 350 nm came out. While the moderate peak (in the region of 400 nm) was decreased in fluorescence intensity of a $\Delta FI = 7$, the new peak was recorded to have nearly 15 FI. These results were also found to be corresponding with the results reported by Uyguner and Bekbölet, 2005a.

4.2.2.2. Photocatalytic Degradation of NHA. Likewise FHA, raw NHA was prepared in 20 mg L^{-1} concentration and it was subjected to photocatalytic degradation in the presence of 0.25 mg mL^{-1} TiO_2. UV-vis spectra, fluorescence spectra, UV-vis

parameters, fluorescence parameters and removal of DOC content of NHA were evaluated.

As it was discovered for FHA a parallel declining logarithmic decay profile in UV-vis absorbance spectra were also attained for NHA predictably (Figure 4.24). Irradiation time dependent changes were observed in spectroscopic properties during each stage of humic acid photocatalytic degradation starting with t = 0 min which was the initial titanium dioxide introduction to humic acid solution in the absence of irradiation. After 60 minutes of photocatalytic oxidation, $Color_{436}$ was nearly expired while UV_{254} absorbance was still be red around ~0.10 cm^{-1}.

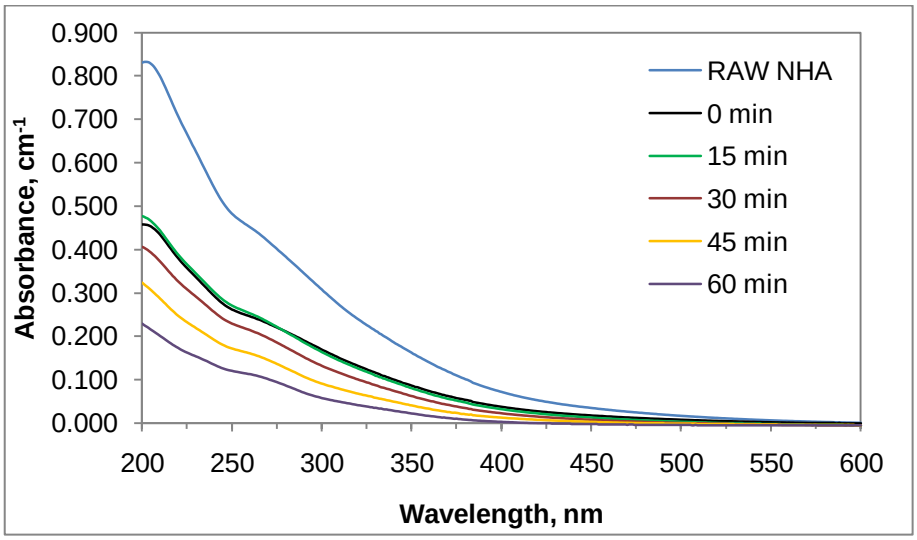

Figure 4.24. UV-vis spectra of the photocatalytic degradation of NHA (HA: 20 mg L^{-1}, TiO_2: 0.25 mg mL^{-1}; I_0=2.85x10^{16} quanta sec^{-1})

On the other hand considering selected UV-visible parameters while 60 % of $Color_{436}$ and 44 % UV_{254} removal was recorded at the end of short period experiments i.e. 15 minutes; 98 % of $Color_{436}$ elimination achieved by 60 minutes of irradiation with NHA. Furthermore only 25 % UV_{254} ascertained after 60 minutes (Figure 4.25). In addition to Uv-vis spectroscopic parameters, DOC content was also decreasing with

increasing reaction time periods. 60 minutes of photocatalytic oxidation caused 51 % of DOC removal from the initial NHA solution.

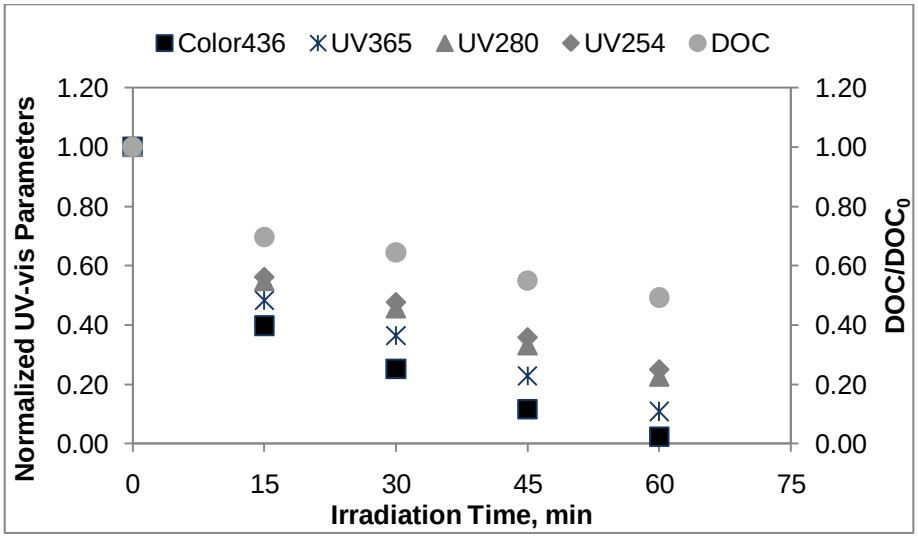

Figure 4.25. Photocatalytic degradation of NHA illustrated by normalized spectroscopic parameters ($Color_{436}$, UV_{365}, UV_{280}, UV_{254}) correlated with DOC removal (HA: 20 mg L^{-1}, TiO_2: 0.25 mg mL^{-1}; I_0=2.85x10^{16} quanta sec^{-1})

The emission spectra of NHA samples were displayed in Figure 4.26. While Figure 4.26a shows the spectra of the samples excited at 350 nm, Figure 4.26b shows the excitation at 370 nm. It was obtained that both excitation wavelength caused a major peak in the region of 450 nm, but with dissimilar fluorescence intensities. While time zero had the lowest fluorescence intensity, the spectrum of 20 minutes of reaction period crossed with the raw humic acids' emission spectrum. On the contrary, the greatest fluorescence intensities were obtained after 30 minutes, 40 minutes and 60 minutes of reaction intervals; almost 110 FI when excited at 350 nm and nearly 70 FI at 370 nm excitation wavelength.

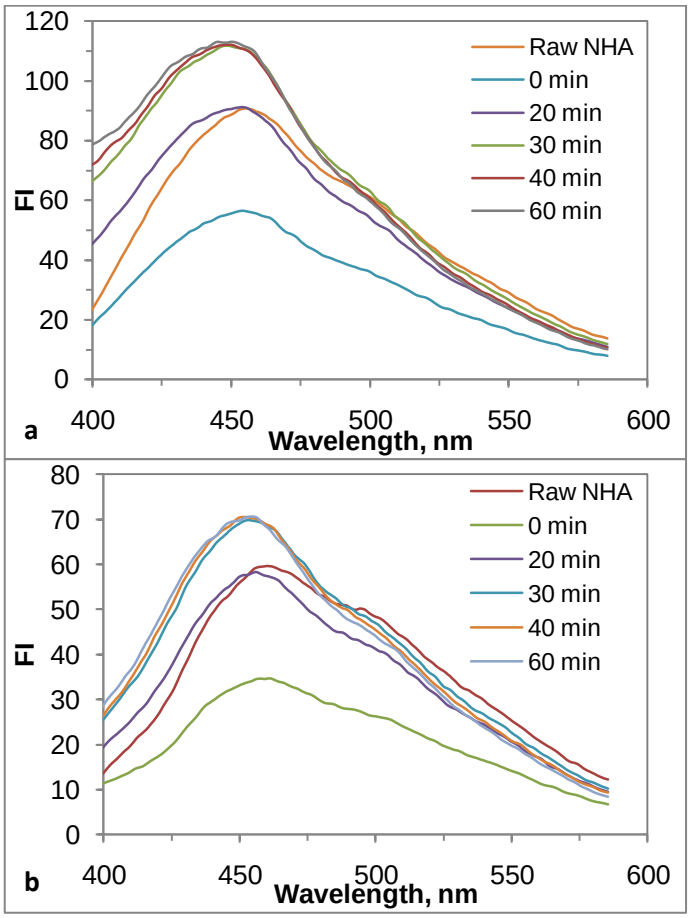

Figure 4.26. Effect of excitation wavelength at (a) 350 nm and (b) 370 nm on the emission fluorescence spectra of oxidized NHA (HA: 20 mg L^{-1},TiO_2: 0.25 mg mL^{-1}; I_0=2.85x10^{16} quanta sec^{-1})

Figure 4.27 shows the synchronous scan fluorescence spectra of oxidized NHA. Raw NHA had a sharp peak around 462 nm with a relative fluorescence intensity of 16 and an insignificant peak around 400 nm. Different from FHA, synchronous fluorescence scan exhibited an individual shape after photocatalytic oxidation of NHA. While the characteristic peak of NHA was eliminated through photocatalytic oxidation process, the emergence of two new peaks around 340 and 390 nm was recorded (Figure 4.27). Furthermore, systematically increasing in fluorescence intensity with increasing reaction time periods of those two peaks was noted.

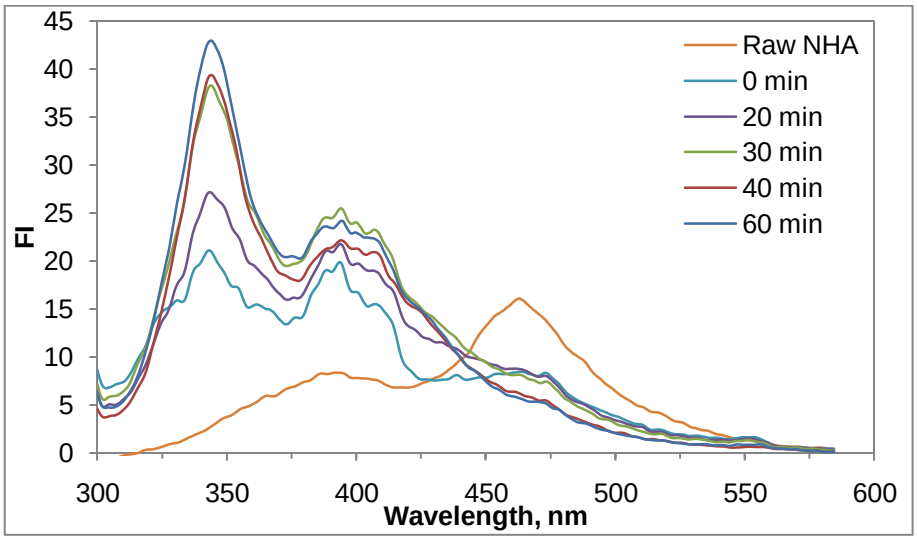

Figure 4.27. The synchronous scan fluorescence spectra of oxidized NHA (HA: 20 mg L^{-1}, TiO_2: 0.25 mg mL^{-1}; I_0=2.85x10^{16} quanta sec^{-1}, $\Delta\lambda$=18 nm)

It can be concluded from Figure 4.23 and Figure 4.27, oxidation of FHA and NHA followed different patterns for both humic acids. While more fluorescent species were removed through photocatalytic oxidation of FHA, new fluorescent compounds were in increasing trend around 350 nm and 400 nm with longer oxidation periods for NHA. Since the peaks obtained in the synchronous spectra of raw NHA were shifted by the photocatalytic oxidation, changes in the fluorescence parameters cannot be argued more. However new peaks were acquired around 340 nm and 400 nm, with further investigation of fluorescent fractions in the structure of humic acids can be achievable.

4.2.2.3. Comparative Evaluation of Photocatalytic Degradation of Humic Acids. In order to deliver a comprehensive evaluation, the spectroscopic data (UV-vis spectra, UV-vis parameters, SCOA and SUVA, fluorescence spectra and parameters) obtained through photocatalytic oxidation of FHA and NHA in this study were compared to other humic acids which were studied in literature namely RHA, IHSS

SHA, AHA, and IHSS HA by Uyguner and Bekbölet 2005a, Uyguner and Bekbölet 2005b, Uyguner and Bekbölet 2005c and Uyguner 2005.

UV-vis spectra of oxidized FHA and NHA were following similar decreasing trend with respect to increasing wavelength by increasing oxidation periods, correspondingly Uyguner and Bekbölet (2005b) and Uyguner (2005) reported similar changes in the UV-vis spectra of photocatalytically treated RHA, IHSS SHA, AHA, and IHSS HA. On the other hand, when selected UV-vis parameters were evaluated; at time zero (t=0) initial adsorption of NHA on TiO_2 was higher than of the FHA, 53% and 43% respectively in means of $Color_{436}$ since the samples were not UV light irradiated oxidation of HA was not attained. It was noticeable that approximately 50% of NHA was removed by initial adsorption while 40% of FHA was adsorbed by TiO_2 prior to photocatalytic oxidation. NHA showed a higher removal of $Color_{436}$, 98% of $Color_{436}$ elimination achieved by 60 minutes of irradiation. However, this higher removal was possible with 2 hours of irradiation process for FHA. Furthermore only 25 % UV_{254} ascertained after 60 minutes of photocatalytic oxidation for NHA, while 60 minutes of photocatalytic oxidation of FHA demonstrated a decrease of 73 % UV_{254}. Figure 4.21 and Figure 4.25 also shows similarities between DOC removal and photocatalytic degradation of FHA and NHA as expressed by the specified UV-vis spectroscopic parameters. After 60 minutes of photocatalytic treatment only 37% and 49% of DOC remained in the solution respectively.

Because photocatalytic oxidation of humic acids were resulted in decreasing UV-vis intensities indicated the removal of organic carbon content, the interpretation of the specific absorbance parameters such as $SUVA_{254}$, $SUVA_{280}$, $SUVA_{365}$ and $SCOA_{436}$ were presented in Table 4.3 for FHA and NHA as well as for RHA, IHSS SHA, AHA, and IHSS HA.

Table 4.3 Specific absorbance ratios of humic substances during photocatalytic oxidation

	$SCOA_{436}$ m^{-1} mg^{-1} L			**$SUVA_{365}$ m^{-1} mg^{-1} L**			**$SUVA_{280}$ m^{-1} mg^{-1} L**			**$SUVA_{254}$ m^{-1} mg^{-1} L**		
	Initial	30 min	60 min	Initial	30 min	60 min	Initial	30 min	60 min	Initial	30 min	60 min
FHA	1.4	0.7	0.4	2.7	1.6	1.1	5.8	4.6	3.8	6.7	5.6	4.9
NHA	0.4	0.2	0.02	1.3	0.8	0.3	4.0	2.8	1.8	4.9	3.6	2.5
AHA*	1.3	0.7	0.5	2.7	1.8	1.1	-	-	-	7.5	5.9	47
RHA**	1.9	2.1	2.0	3.7	4.0	3.9	-	-	-	9.5	10.8	10.4
IHSS SHA**	1.7	2.2	2.5	3.9	4.7	1.7	-	-	-	7.1	10.1	12.4
IHSS HA**	0.8	0.8	0.6	2.3	2.1	2.0	-	-	-	7.8	7.3	7.0

*Uyguner and Bekbölet, (2005b) **Uyguner, (2005).

While insignificant decrease (≤5 %) was observed for $SUVA_{280}$ and $SUVA_{254}$ after the introduction of TiO_2, $SCOA_{436}$ and $SUVA_{365}$ values were found to be change 20 % and 15 % respectively. However, after 30 minutes of irradiation and in the presence of organic carbon in the reaction medium, considerable decreases as 50 % $SCOA_{436}$, 40 % $SUVA_{365}$ and 21 % $SUVA_{280}$ and 16 % $SUVA_{254}$ were achieved. After 60 minutes of reaction time approximately 20 % higher removal of $SCOA_{436}$ and $SUVA_{365}$, with approximately 10 % higher removal of $SUVA_{280}$ and $SUVA_{254}$ were attained.

Considering SCOA/SUVA values; all of the specific absorbance values of oxidized Nordic humic acid at time zero were found to be less than 7 %. After 30 minutes of irradiation and in the presence of organic carbon in the reaction medium,

considerable decreases as 50 % $SCOA_{436}$, 39 % $SUVA_{365}$ and 30 % $SUVA_{280}$ and 26 % $SUVA_{254}$ were achieved. Furthermore, after 60 minutes of reaction period approximately 95 % $SCOA_{436}$, 77 % $SUVA_{365}$, 55 % $SUVA_{280}$ and 49 % $SUVA_{254}$ removal were attained (Table 4.3). Compare to that of raw humic acid approximately 95 % $SCOA_{436}$, 77 % $SUVA_{365}$, 55 % $SUVA_{280}$ and 49 % $SUVA_{254}$ removal were achieved for NHA after 60 minutes of photocatalytic degradation revealing lessened degree of aromaticity in relation to the removal of organic carbon. At this stage the reaction medium was composed of non reacted humic acids and the degradation products expressing almost 49 % removal of DOC. The decreasing trend of DOC and the relevant parameters also indicate the mineralization of humic acid to carbon dioxide and water.

Similar and contrary results were acknowledged in the literature for IHSS FA, RHA, AHA, IHSS SHA, IHSS HA (Uyguner and Bekbölet, 2005b; Uyguner, 2005). In consideration of the differences in the chemical and physical aspects of humic substances from various origins, each humic acid was expected to pursue different photocatalytic degradation pattern depending on the spectroscopic data available throughout pseudo first order kinetic model parameters. Consequently, in order to ascertain divergent trends for the SCOA / SUVA values calculated for the different photocatalytic irradiation times was reliable. Uyguner and Bekbölet, 2005b, reported that the initial $SUVA_{254}$ and $SCOA_{436}$ values for AHA were found to be slightly decreasing (≤10 %) after the introduction of TiO_2. On the other hand, after 30 minutes of irradiation and in the presence of rich organic carbon content in the reaction medium, substantial decreases as 21 % $SUVA_{254}$ and 46 % $SCOA_{436}$ were achieved. Compared to that of raw humic acid approximately 37 % decrease of $SUVA_{254}$ was achieved for AHA after 60 minutes of photocatalytic degradation, resulted in lessened degree of aromaticity with respect to the removal of organic carbon. Bearing in mind that relatively higher $Color_{436}$ removal compared to the removal of UV_{254} were also reported.

The alterations observed in $SCOA_{436}$ would be restricted by the irradiation time, since relatively higher removal rate of $Color_{436}$ with reference to the removal rates of UV_{365}, UV_{280} and UV_{254} was observed. As a result, $SCOA_{436}$ parameter possibly would not exhibit a distinctive consequence attributable to the lower $Color_{436}$ detected during extended periods of photocatalytic oxidation process. Humic acids were degraded to a smaller amount UV-vis absorbing compounds in the course of the formation of a chain of intermediates and their subsequent reactions, as could be verified by the decrease in the SCOA/SUVA values. Edzwald et al., 1985 reported $SUVA_{254}$ was to be proportional to both the apparent molecular weight and the aromaticity of humic substances.

Moreover the photocatalytic degradation profiles of humic acid were also assessed through fluorescence spectral evaluation. When the emission fluorescence spectra of photocatalytically oxidized FHA and NHA were examined, the major difference noticed was related to the shape of the spectra. Exciting the samples at 370 nm; fluorescence emission spectra, as demonstrated in Figure 4.22 and Figure 4.26, revealed a different shape than the excitation at 350 nm of the both humic acids (FHA and NHA). While the samples excited at 350 nm gave only one peak around ~450 nm; exciting at 370 nm caused one major peak around ~455 nm and a shoulder around ~500 nm. Photocatalytic oxidation caused a decrease in the peak heights for FHA; on the contrary photocatalytic treatment of NHA resulted in an increase in the peak heights obtained in the emission spectra.

Synchronous scan fluorescence spectra of oxidized FHA and NHA were also investigated in the same manner. Raw FHA had a sharp peak around 472 nm with a relative fluorescence intensity of 40.6 and a moderate peak around 400 nm while raw NHA had reached its maxima around 462 nm with a relative fluorescence intensity of 16 and an insignificant peak around 400 nm. Peuravuori et al., 2002 ascribe the

maximum around 460 nm to polycyclic aromatics consisting of seven fused benzene rings.

Extensive studies using IHSS FA, RHA, AHA, IHSS SHA, IHSS HA were conducted by Uyguner, 2005 and Uyguner and Bekbölet, 2005a. After 60 min of irradiation, the characteristic sharp peak of raw FHA completely disappeared as could be seen from Figure 4.23; the moderate peak around 400 nm decayed in intensity and another peak of low intensity in the region of 350 nm came out. Different from FHA, synchronous fluorescence scan exhibited an individual shape after photocatalytic oxidation of NHA. While the characteristic peak of NHA was eliminated through photocatalytic oxidation process, the emergence of two new peaks around 340 and 390 nm was recorded (Figure 4.27). The two new peak was in a manner of increasing with increasing irradiation time (It, min) of photocatalysis. The synchronous scan fluorescence spectra for oxidized AHA and for IHSS SHA published by Uyguner, 2005, were displaying similarities with the synchronous scan fluorescence spectra for oxidized NHA. On the other hand, IHSS HA and RHA reported to have individual synchronous scan fluorescence spectra by Uyguner, 2005.

4.2.3. Effect of Initial Concentration of Humic Acid Photocatalytic Oxidation

Different concentrations of FHA and NHA (10 mg L^{-1}, 20 mg L^{-1}, 30 mg L^{-1}, 40 mg L^{-1} and 50 mg L^{-1}) solutions were treated, in order to relate with natural water supplies' humic acid content. The photocatalyst content was kept constant as 0.25 mg mL^{-1}. The UV-vis spectra were in logarithmic decaying shape for all concentrations; maximum absorbance value reached at 200 nm and absorbance spectra displayed a decreasing trend with respect to increasing wavelength, for both photocatalytically treated FHA and NHA. Moreover the photocatalytic degradation profiles of humic acid were also assessed through fluorescence spectral evaluation.

4.2.3.1. Effect of Initial Concentration of FHA. FHA in 10 mg L^{-1}, 20 mg L^{-1}, 30 mg L^{-1}, 40 mg L^{-1} and 50 mg L^{-1} concentrations were subjected to photocatalytic oxidation. Figure 4.28, Figure 4.29 and Figure 4.30 show the change in means of the UV-visible spectra and $Color_{436}$ and UV_{254} parameters respectively, which is corresponding to the results given in material specification section. As it was displayed on the charts below (Figure 4.28 and Figure 4.29), increasing the initial concentration of FHA did not change the effect of photocatalytic oxidation on either spectrum.

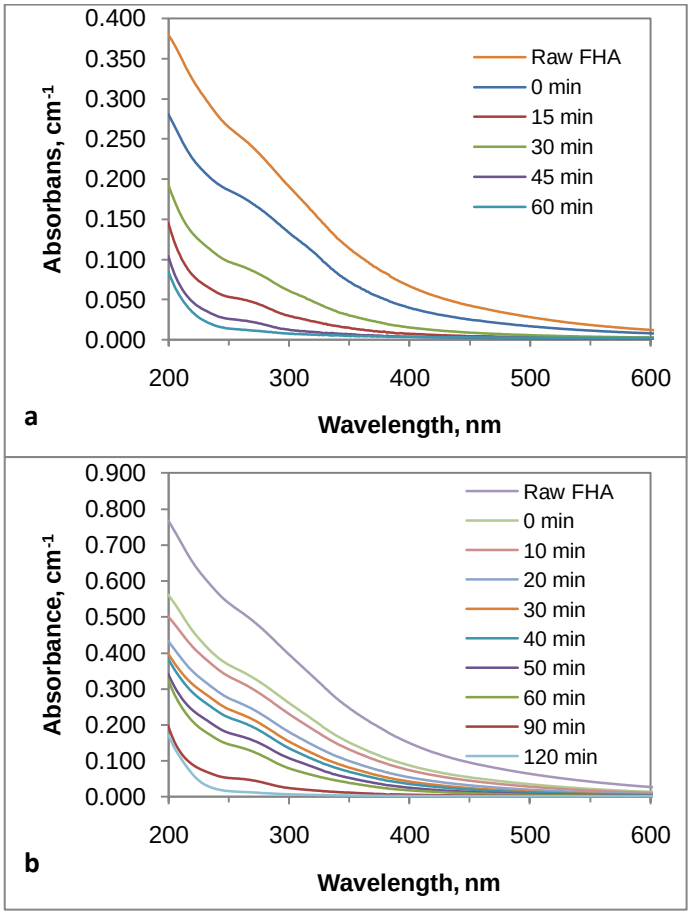

Figure 4.28. Initial concentration effect on photocatalytic oxidation of FHA with respect to UV-vis spectra (a) 10 mg L^{-1} and (b) 20 mg L^{-1} (TiO_2: 0.25 mg mL^{-1}; I_0=2.85x10^{16} quanta sec^{-1})

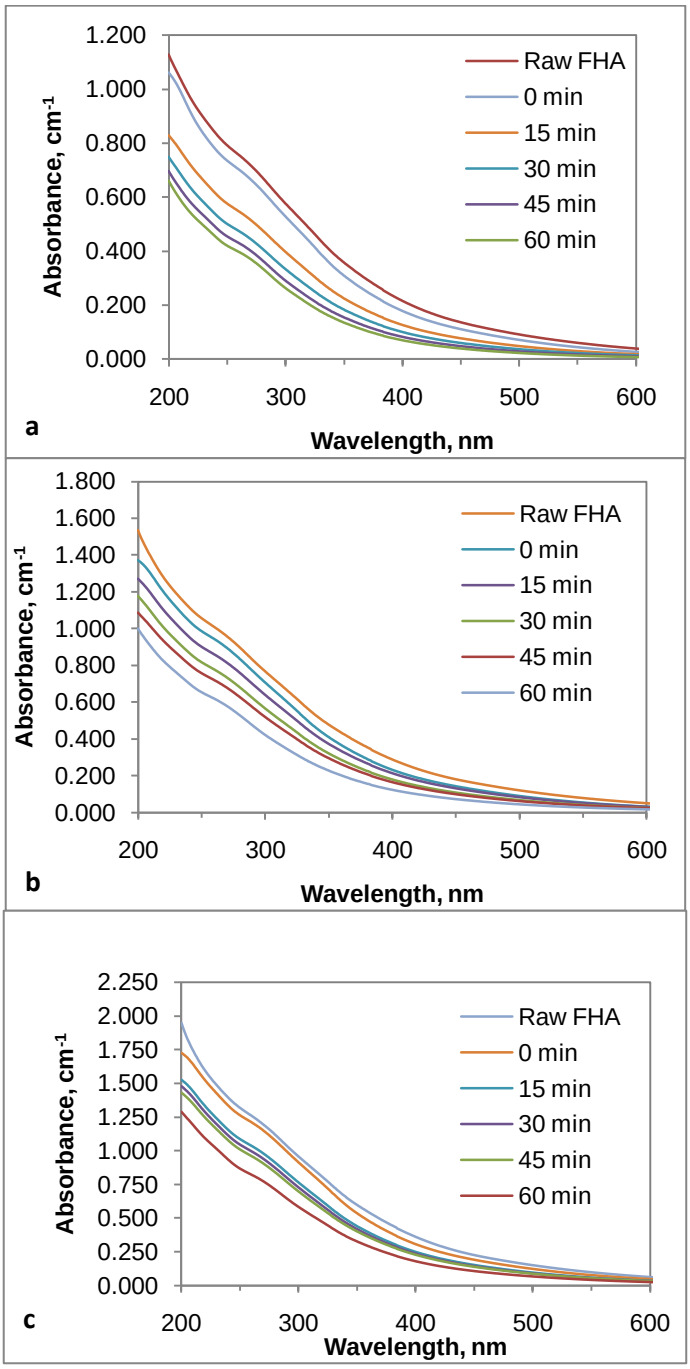

Figure 4.29. Initial concentration effect on photocatalytic oxidation of FHA with respect to UV-vis spectra (a) 30 mg L^{-1}, (b) 40 mg L^{-1}, (c) 50 mg L^{-1} (TiO_2: 0.25 mg mL^{-1}; I_0=2.85x10^{16} quanta sec^{-1})

All of the UV-visible spectra were in lessening trend with increasing irradiation time periods, from time zero to 60 minutes. There was a parallel relationship between the FHA concentration and measured light absorbance per cm. The absorbance per cm of raw FHA was increasing with increasing concentration of FHA as seen by Figure 4.28 and Figure 4.29. Also the UV-vis spectra were in logarithmic decaying shape for all concentrations; maximum absorbance value reached at 200 nm and absorbance spectra displayed a decreasing trend with respect to increasing wavelength. Moreover, the shape of UV-vis spectra did not change significantly with respect to increasing irradiation time.

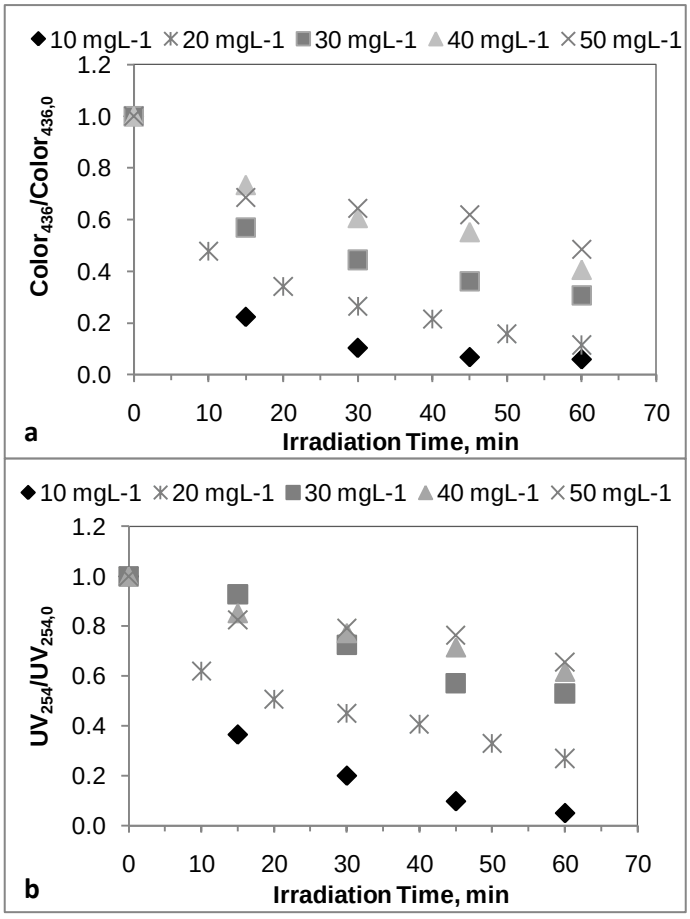

Figure 4.30. Initial concentration effect on photocatalytic oxidation of FHA with respect to normalized (a) $Color_{436}$ and (b) UV_{254} (HA: 10 mg L^{-1}, 20 mg L^{-1}, 30 mg L^{-1}, 40 mg L^{-1} and 50 mg L^{-1}, TiO_2: 0.25 mg mL^{-1}; I_0=2.85x10^{16} quanta sec^{-1})

In relation to the UV-vis spectra evaluation, selected UV-visible parameters were also investigated. After 60 minutes of treatment, $Color_{436}$ removal was 94 %, 89 %, 69 %, 59 % and 52 % for FHA 10 mg L^{-1}, 20 mg L^{-1}, 30 mg L^{-1}, 40 mg L^{-1} and 50 mg L^{-1} respectively. As the concentration of FHA decreases, the success of photocatalytic oxidation in means of $Color_{436}$ removal was increasing.

Similar trend was obtained for UV_{254} parameter too; UV_{254} removal was found to be 95 %, 73 %, 47 %, 38 % and 35 % with respect to the initial concentration of FHA as 10 mg L^{-1}, 20 mg L^{-1}, 30 mg L^{-1}, 40 mg L^{-1} and 50 mg L^{-1} correspondingly. This suggested as the concentration of FHA decreased, the UV_{254} removal achievement of photocatalytic oxidation was found to be increasing. Considering the selected parameters, it was disclosed that removal efficiency of the photocatalytic oxidation followed the same trend irrespective of the initial humic acid concentration.

Moreover the photocatalytic degradation profiles of humic acid were also assessed through fluorescence spectral evaluation. In a similar manner as presented for photocatalytic degradation of humic acid (20 mg L^{-1}), fluorescence spectra were recorded for 350 nm and 370 nm excitation wavelengths in emission mode as well as synchronous mode. Examining the initial concentration effect starting from 10 mg L^{-1} to 50 mg L^{-1} of FHA on fluorescence spectra, following results were disclosed as presented in Figure 4.31 and Figure 4.32.

Exciting the photocatalytically oxidized 10 mg L^{-1} FHA samples at 350 nm and 370 nm caused a peak around ~450 nm from time zero until 30 minutes of irradiation in addition to the raw FHA, while the same peak was removed after prolonged time periods of experiments e.g. 45 minutes and 60 minutes. Furthermore, the shape of peak was destructed with extended photocatalytic oxidation process (Figure 4.31).

However, the peaks observed on the synchronous scan fluorescence spectra (Figure 4.32) were changing in a different trend than the peaks observed in emission spectra by excitation at 350 nm and 370 nm. Raw FHA revealed a sharp peak at 470 nm and a broad peak in the region of 400 nm with relative fluorescence intensities of 21 and 12.

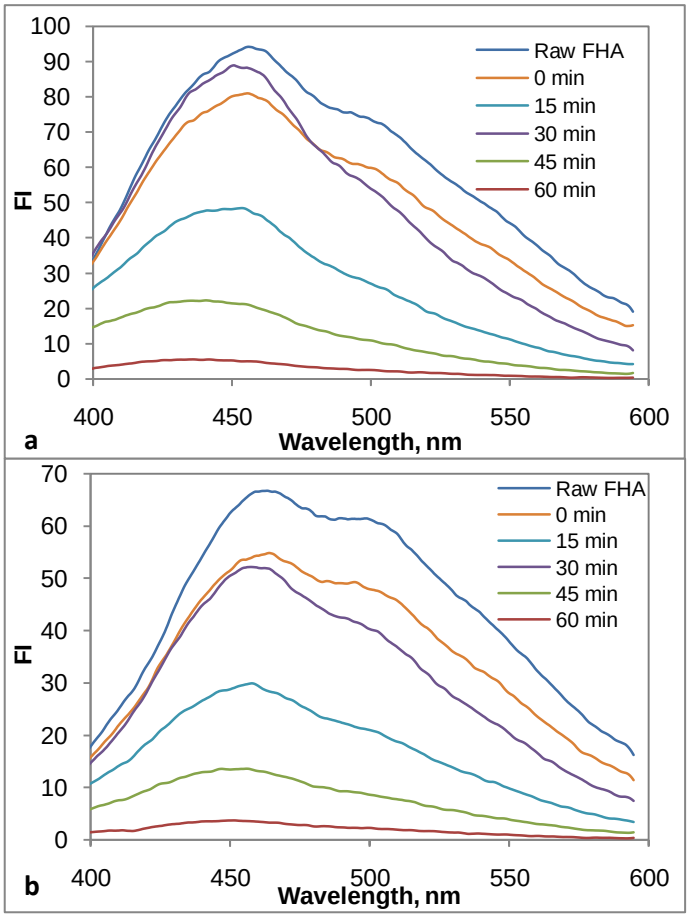

Figure 4.31. The emission fluorescence spectra at excitation wavelength (a) 350 nm and (b) 370 nm of oxidized FHA (HA: 10 mg L^{-1}, TiO_2: 0.25 mg mL^{-1}; I_0=2.85x10^{16} quanta sec^{-1})

While a modest fall was observed in fluorescence intensities for the both characteristic peaks of FHA at time zero, after 15 minutes of reaction time period the major peak was not present any more and the moderate peak was reduced from 12 to 7 as a new peak was emerged about ~350 nm with an approximate fluorescence intensity of 8.5. Increasing the reaction time to 30 minutes caused a significant increase in the fluorescence intensities of the peaks observed around ~350 nm and 400 nm. Nevertheless, after 45 minutes of experimental time scale all of the peaks were absent (Figure 4.32).

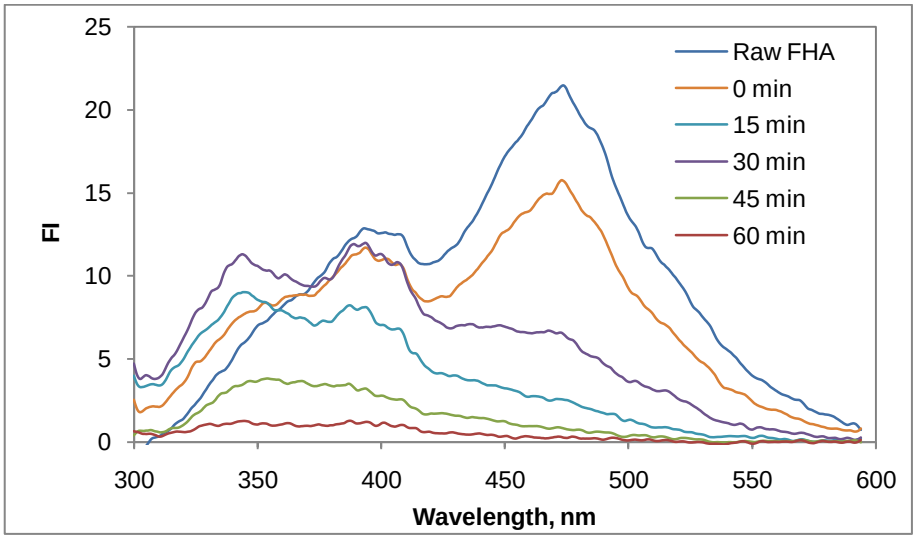

Figure 4.32. The synchronous scan fluorescence spectra of oxidized FHA (HA: 10 mg L^{-1}, TiO_2: 0.25 mg mL^{-1}; I_0=2.85x10^{16} quanta sec^{-1}, $\Delta\lambda$=18 nm)

Figure 4.33 shows the alteration in emission fluorescence spectra of the oxidized 20 mg L^{-1} FHA samples at 350 nm and 370 nm. The raw FHA revealed a peak around ~450 nm with 143 FI which was excited at 350 nm. Compared to the raw FHA at time zero the shape and intensity of the spectra showed an insignificant change, nearly the same. But longer irradiation periods caused a dramatic increase in the intensity of the peak from 143 to nearly 220 after 30 minutes. On the other hand, after 60 minutes of

reaction time fragment it was reduced to 153 FI. Since the fluorescent compounds formed in early stages of photocatalytic oxidation process, these compounds could have been reduced to smaller molecules which were not fluorescent with the extended reaction time periods. Similarly to the excitation at 350 nm, the samples excited at 370 nm were following the same trend on the spectra. A slight difference can be noted that after 60 minutes of photocatalytic oxidation, the fluorescence intensity of the peak was lessened more than it was for 350 nm excitation. Since the peak remained below the raw FHA's fluorescence intensity.

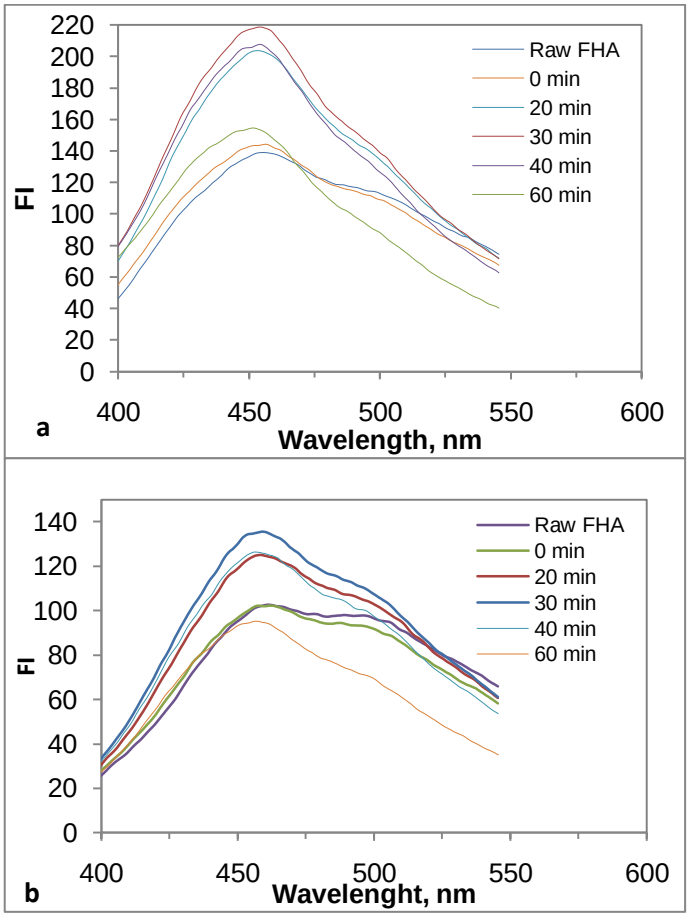

Figure 4.33. The emission fluorescence spectra at excitation wavelength (a) 350 nm and (b) 370 nm of oxidized FHA (HA: 20 mg L^{-1}, TiO_2: 0.25 mg mL^{-1}; I_0=2.85x10^{16} quanta sec^{-1})

Increasing reaction time periods caused a reduction tendency in the major peak (observed in the region of ~472 nm), displayed on synchronous fluorescence scan spectra (Figure 4.34). This peak was still present after 45 minutes of treatment, but 60 minutes of reaction period caused complete elimination. A moderate peak was present for all of the oxidized FHA as well as raw FHA. On the other hand, in the region of ~350 nm a new peak appeared (15 FI) after extended reaction time period of 60 minutes as it was observed after 30 minutes for 10 mgL^{-1} FHA.

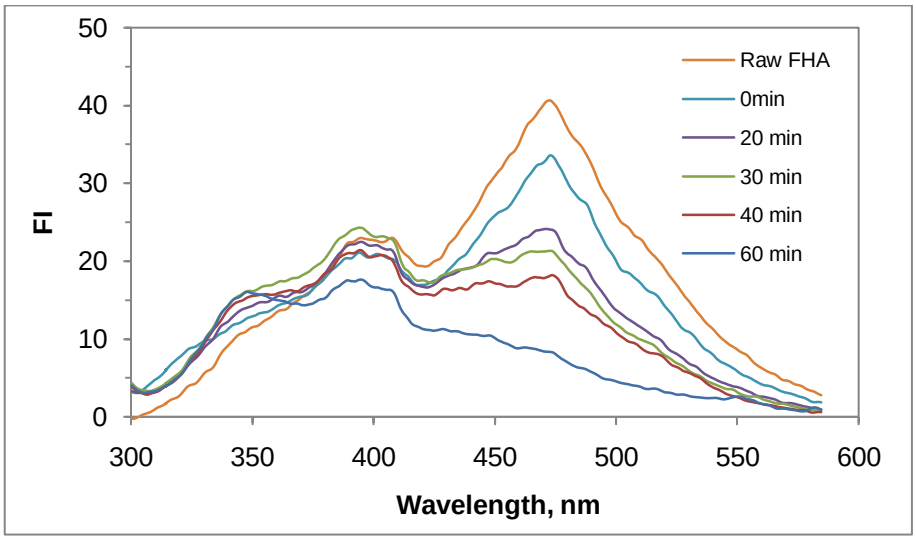

Figure 4.34. The synchronous scan fluorescence spectra of oxidized FHA (HA: 20 mg L^{-1}, TiO_2: 0.25 mg mL^{-1}; I_0=2.85x10^{16} quanta sec^{-1}, $\Delta\lambda$=18 nm)

Since FHA concentration increased to 30 mgL^{-1}, oxidized FHA showed dissimilar alterations in the peaks observed than the lower FHA concentrations (e.g. 10 mgL^{-1} and 20 mgL^{-1}) through emission and synchronous fluorescence spectra (Figure 4.34 and Figure 4.36).

Upon excitation of the photocatalytically oxidized 30 mg L^{-1} FHA samples at 350 nm and 370 nm, emergence of peaks around 450 nm in emission fluorescence spectra were noticed. Although these peaks were not distorted at the initial state of the pre-adsorption phase prior to initiation of photocatalysis (It= 0 min) a raising trend in peak height was observed from 15 minutes to 60 minutes of oxidation time periods. While 160 FI was measured for raw FHA, after 60 minutes of treatment it was found to be 275 FI for excitation at 350 nm. The raw FHA excited at 370 nm had a broad peak with approximately 125 FI, while oxidized FHA had about 175 FI after 60 minutes of reaction period displayed a 45 FI difference.

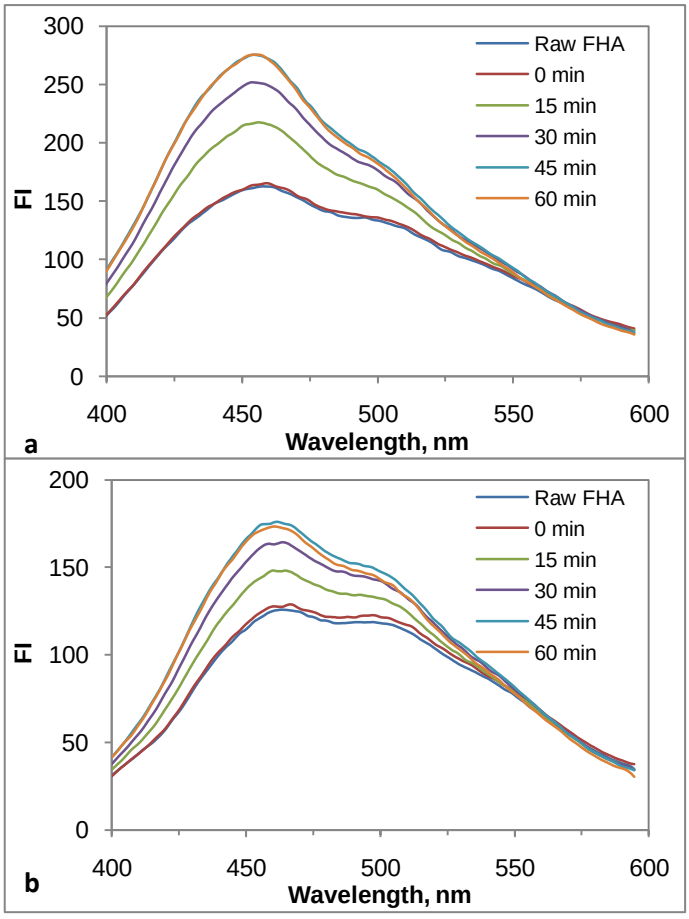

Figure 4.35. The emission fluorescence spectra at excitation wavelength (a) 350 nm and (b) 370 nm of oxidized FHA (HA: 30 mg L^{-1}, TiO_2: 0.25 mg mL^{-1}; I_0=2.85x10^{16} quanta sec^{-1})

Conversely, the peaks monitored in the synchronous spectra were reduced in fluorescence intensity with increasing oxidation periods. While raw FHA displayed a major peak at 472 nm with a fluorescence intensity of 55, after 60 minutes of irradiation period it was reduced to 30. However the moderate peaks in the region of 400 nm were tend to be mounting with increasing oxidation stages. At time zero, this peak measured to have 23 FI, while after 60 minutes of reaction period it was 29 raised up nearly to the raw FHA's peak.

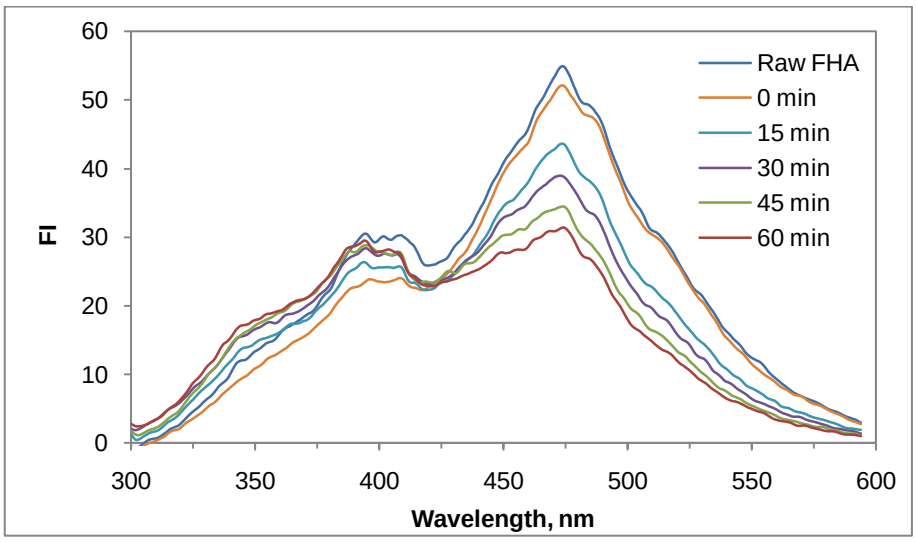

Figure 4.36. The synchronous scan fluorescence spectra of oxidized FHA (HA: 30 mg L^{-1}, TiO_2: 0.25 mg mL^{-1}; I_0=2.85x10^{16} quanta sec^{-1}, $\Delta\lambda$=18 nm)

Further increase in humic acid concentration was also examined in a consistent manner. FHA (40 mg L^{-1}) was subjected to photocatalytic oxidation and the emission spectra were recorded both for excitation wavelength at 350 nm and 370 nm (Figure 4.37). It was observed that extended irradiation periods caused a dramatic increase in the fluorescence intensity of the peaks representing a requirement for longer irradiation period to achieve comparative removal efficiencies. Raw FHA had 175 FI, while the oxidized FHA revealed 310 FI after 60 minutes of treatment in the emission

fluorescence spectra at excitation wavelength 350 nm. While the broad peak of raw FHA had an approximate fluorescence intensity of 130, after 60 minutes of oxidation process nearly 210 FI was recorded from Figure 4.37b. On the contrary, further increasing the initial concentration of FHA to 40 mg L^{-1}, the decreasing effect of photocatalysis on the fluorescence intensity of the peaks in both emission and synchronous scan spectra were reversed, but 38 % UV_{254} removal was evaluated indicating destruction in the aromatic core of humic acid structure.

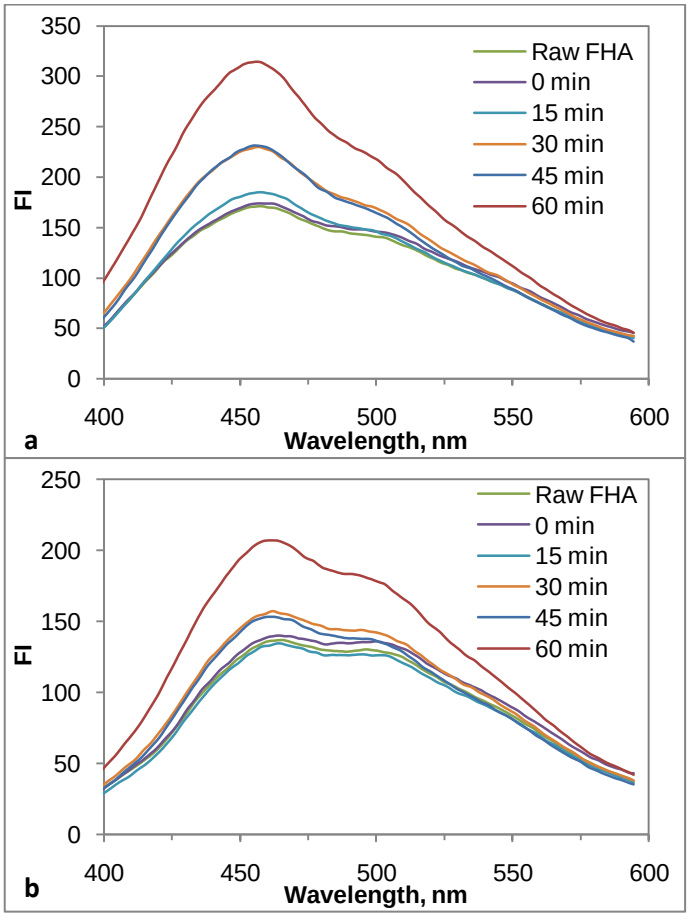

Figure 4.37. The emission fluorescence spectra at excitation wavelength (a) 350 nm and (b) 370 nm of oxidized FHA (HA: 40 mg L^{-1}, TiO_2: 0.25 mg mL^{-1}; I_0=2.85x10^{16} quanta sec^{-1})

Examining the synchronous fluorescence spectra of oxidized FHA (40 mg L^{-1}) the major peak at 472 nm was in decreasing trend with the increasing reaction time periods, despite the fact that the moderate peak in the region of 400 nm was mounting in fluorescence intensity. Since it was measured to be nearly 30 FI for raw FHA, after 60 minutes of oxidation 39 FI was recorded as seen by Figure 4.38.

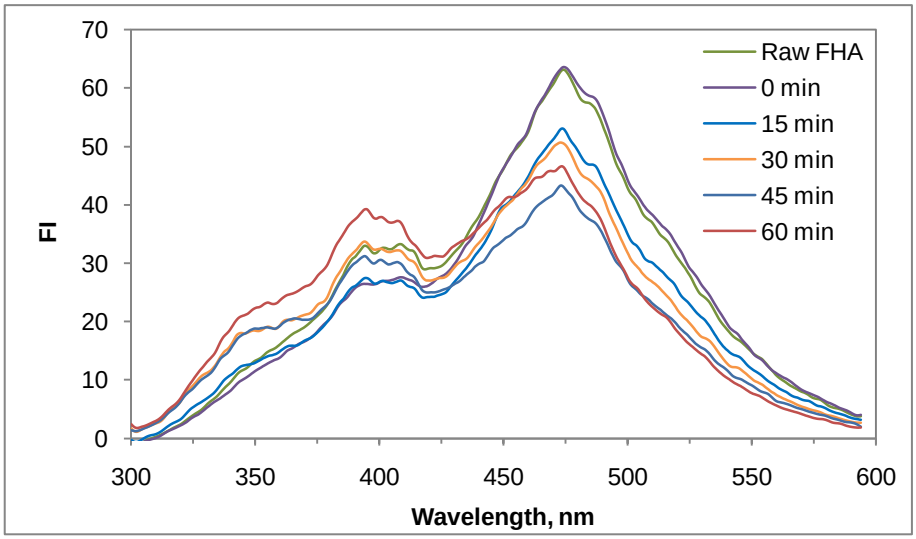

Figure 4.38. The synchronous scan fluorescence spectra of oxidized FHA (HA: 40 mg L^{-1}, TiO_2: 0.25 mg mL^{-1}; I_0=2.85x10^{16} quanta sec^{-1}, $\Delta\lambda$=18 nm)

The highest initial FHA concentration studied was 50 mg L^{-1}, and the fluorescence emission spectra were evaluated together with the synchronous fluorescence spectra as it was done for lower FHA dilutions (Figure 4.39a, Figure 4.39b and Figure 4.40).

In the both emission spectra Figure..A and Figure..B, parallel results were obtained to the oxidized 40 mg L^{-1} FHA. Excitation at 350 nm revealed sharp peaks about 450 nm, while at 370 nm excitation broad peaks were applicable in the same region of emission fluorescence spectra. It was disclosed that after 60 minutes of irradiation

period caused a remarkable increase in the fluorescence intensity of the peaks, while gradually increasing trend was practical with increasing experimental time periods between time zero and 45 minutes. 145 FI of raw FHA was raised to 290 FI after 60 minutes of photocatalytic oxidation in the emission spectra at excitation wavelength 350 nm. Also the same trend was noticeable in Figure 4.39b; since 130 FI verified for raw FHA, approximately 190 FI was measured after 60 minutes of oxidation process.

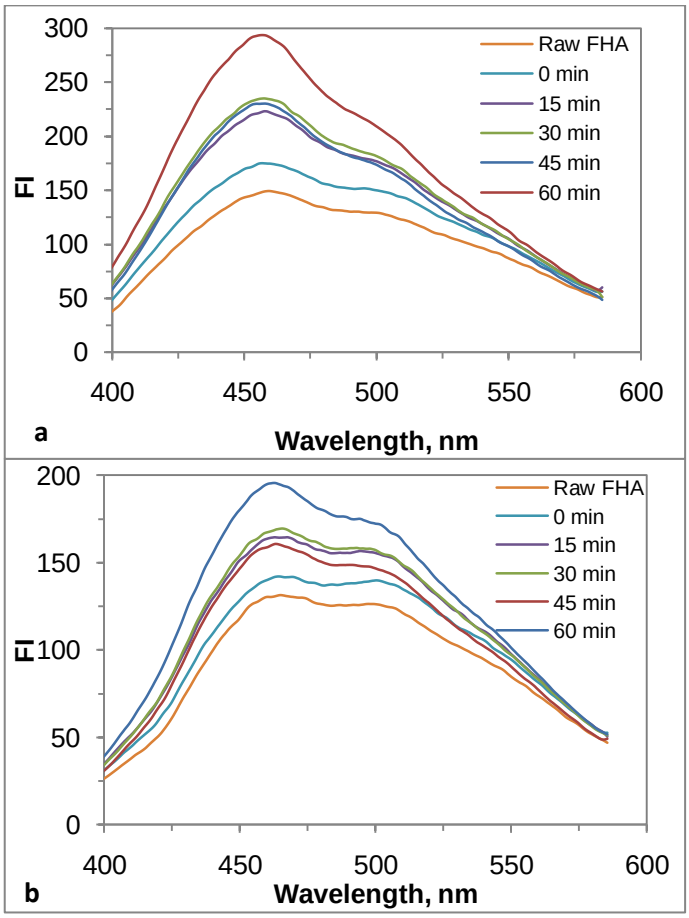

Figure 4.39. The emission fluorescence spectra at excitation wavelength (a) 350 nm and (b) 370 nm of oxidized FHA (HA: 50 mg L^{-1}, TiO_2: 0.25 mg mL^{-1}, I_0=2.85x10^{16} quanta sec^{-1})

The major peak at 472 nm was in declining with the increasing reaction time periods in the synchronous fluorescence spectra of oxidized FHA (50 mg L^{-1}); parallel to the major peak the moderate peak in the region of 400 nm was also lessened in fluorescence intensity. Since the major peak was measured to have nearly 70 FI for raw FHA, after 60 minutes of oxidation 50 FI was recorded as showed by Figure 4.40. Furthermore the moderate peak was also reduced from 30 FI to 25 FI after 45 minutes of treatment, however after 60 minutes of reaction time period a slight increase was observed in the fluorescence intensity (nearly 29 FI).

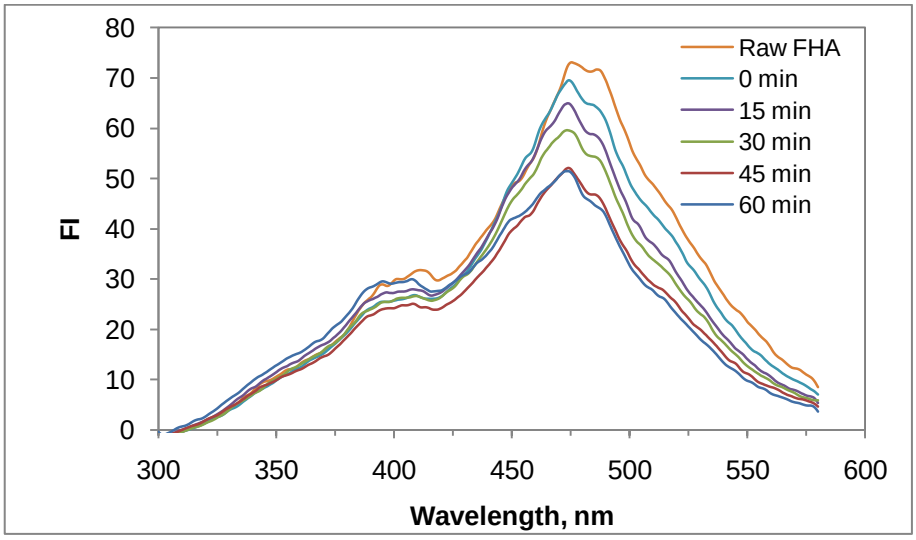

Figure 4.40. The synchronous scan fluorescence spectra of oxidized FHA (HA: 50 mg L^{-1}, TiO_2: 0.25 mg mL^{-1}; I_0=2.85x10^{16} quanta sec^{-1}, $\Delta\lambda$=18 nm)

Compared to the lower concentrations of FHA e.g. 10 mg L^{-1} and 20 mg L^{-1}, comparatively higher concentrations of FHA (30, 40 and 50 mg L^{-1}) did not demonstrate any peaks in the region of 350 nm by the synchronous fluorescence scan after photocatalytic oxidation. However, it was applicable after 15 minutes of irradiation for 10 mg L^{-1} FHA and after 60 minutes of irradiation for 20 mg L^{-1} FHA. Although UV_{254} removal success of photocatalysis was decreasing with increasing

concentrations of FHA, it was still effective as 95 %, 73 %, 47 %, 38 % and 35 % removals with respect to the initial FHA concentrations of 10 mg L^{-1}, 20 mg L^{-1}, 30 mg L^{-1}, 40 mg L^{-1} and 50 mg L^{-1}. Additionally, 60 minutes of photocatalytic oxidation period resulted in 58 %, 63 %, 33 %, 31 % and 8 % DOC removal with respect to initial FHA concentrations of 10 mg L^{-1}, 20 mg L^{-1}, 30 mg L^{-1}, 40 mg L^{-1} and 50 mg L^{-1}.

4.2.3.2. Effect of Initial Concentration of NHA. With similar approach to FHA, NHA in 10 mg L^{-1}, 20 mg L^{-1}, 30 mg L^{-1} and 50 mg L^{-1} concentrations were subjected to photocatalytic oxidation too. UV-visible spectra and selected parameters of $Color_{436}$ and UV_{254} showed reducing trend with respect to increasing irradiation time periods (Figure 4.41, Figure 4.42 and Figure 4.43), which is corresponding to the results given in material specification section.

As it was discussed previously for FHA, also increasing the initial concentration of NHA did not change the effect of photocatalytic oxidation on either spectrum. Considering UV-visible spectra, a decreasing trend with increasing irradiation time periods, from time zero to 60 minutes was detected. UV-vis spectrum was plotted absorbance value per cm against the excitation wavelength (nm). There was an analogous relationship between the concentration of NHA and measured light absorbance value per cm; they were changing with direct proportion. This was illustrated by Figure 4.41 and Figure 4.42. The absorbance per cm of raw NHA was increasing with increasing concentration of NHA. Moreover the shape of UV-vis spectra displayed logarithmic decaying shape for all concentrations; absorbance spectra displayed a decreasing trend with respect to increasing wavelength from 200 nm to 600 nm. The shape of UV-vis spectra did not change, but reduced in the absorbance value by the oxidation of NHA.

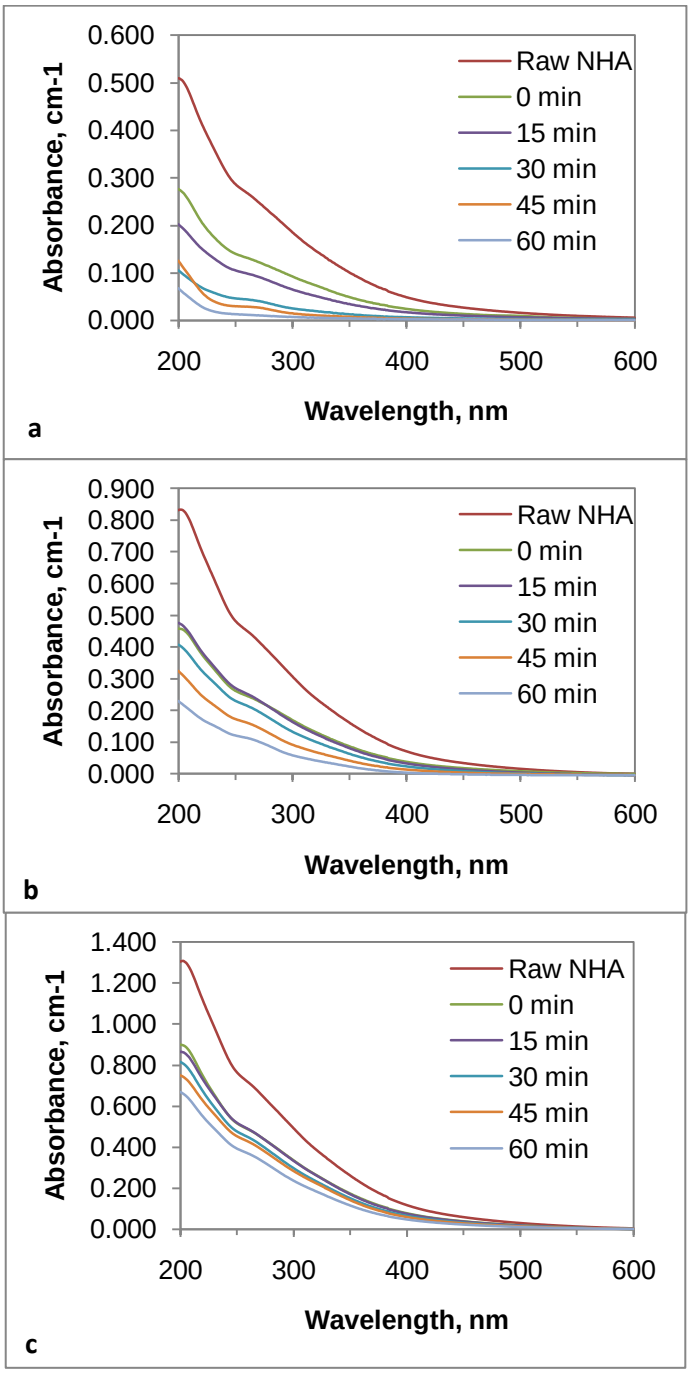

Figure 4.41. Initial concentration effect on photocatalytic oxidation of NHA with respect to UV-vis spectra (a) 10 mg L^{-1}, (b) 20 mg L^{-1}, (c) 30 mg L^{-1} (TiO_2: 0.25 mg mL^{-1}; I_0=2.85x10^{16} quanta sec^{-1})

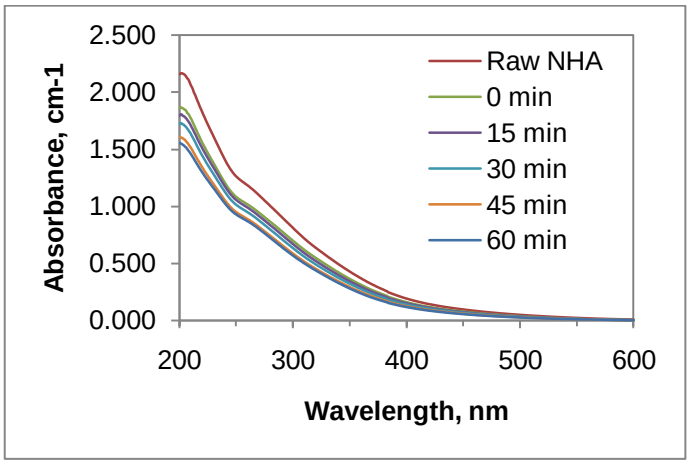

Figure 4.42. Initial concentration effect on photocatalytic oxidation of NHA with respect to UV-vis spectra (HA: 50 mg L^{-1},TiO_2: 0.25 mg mL^{-1}; I_0=2.85x10^{16} quanta sec^{-1})

On the other hand the effect of initial NHA concentration on the photocatalytic oxidation was also studied examining the selected UV-vis parameters ($Color_{436}$ and UV_{254}).$Color_{436}$ removal 98 %, 90 %, 62 % and 41 % was assessed with respect to concentration of NHA 10 mg L^{-1}, 20 mg L^{-1}, 30 mg L^{-1} and 50 mg L^{-1} after 60 minutes of irradiation. With reducing concentration of NHA, the impact of photocatalytic oxidation in means of $Color_{436}$ removal was increasing.

UV_{254} was following similar trend with $Color_{436}$, UV_{254} elimination was 95 %, 75 %, 49 % and 26 % with respect to concentration of NHA 10 mg L^{-1}, 20 mg L^{-1}, 30 mg L^{-1} and 50 mg L^{-1}. It was noticeable in Figure 4.43 that the oxidation of 50 mg L^{-1} NHA did not display any further UV_{254} removal efficiency more than 20% after 30 minutes irradiation time. Maximum UV_{254} exclusion was reached after 60 minutes of irradiation. Similar results were applicable for the oxidized samples of 30 mg L^{-1} NHA. On the other hand, more dramatic UV_{254} exclusions were achieved after oxidation of 10 mg L^{-1} and 20 mg L^{-1} NHA. This proposed as the concentration of NHA decreasing, UV_{254} removal was increasing.

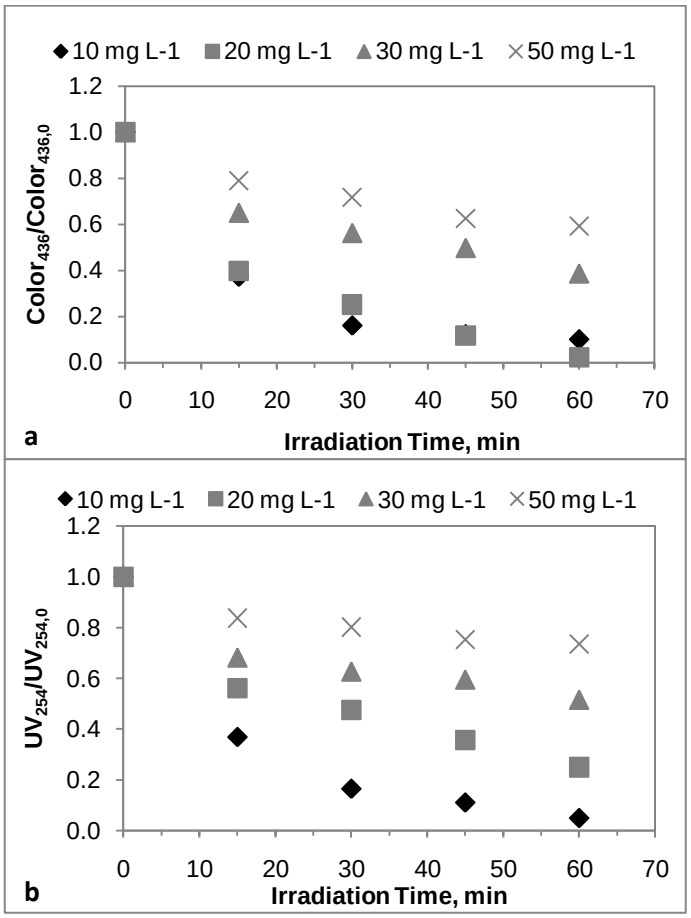

Figure 4.43. Initial concentration effect on photocatalytic oxidation of FHA with respect to normalized (a) $Color_{436}$ and (b) UV_{254} (HA: 10 mg L^{-1}, 20 mg L^{-1}, 30 mg L^{-1} and 50 mg L^{-1}, TiO_2: 0.25 mg mL^{-1}; I_0=2.85x10^{16} quanta sec^{-1})

Furthermore the photocatalytic degradation profiles of humic acid were also assessed through fluorescence spectral evaluation. In a similar manner as presented for photocatalytic degradation of humic acid (20 mg L^{-1}), fluorescence spectra were recorded for 350 nm and 370 nm excitation wavelengths in emission mode in addition to synchronous mode. In order to investigate the initial concentration effect on the photocatalytic oxidation starting from 10 mg L^{-1} to 50 mg L^{-1} of NHA on fluorescence spectra, following results were disclosed as presented.

Firstly, emission fluorescence spectra of oxidized 10 mg L^{-1} of NHA were demonstrated in Figure 4.44 with respect to excitation wavelengths of 350 nm and 370 nm. When the samples were excited at 350 nm, emission spectra observed to be in reducing trend with increasing reaction time periods. The difference of fluorescence intensity (ΔFI) between the main peak at 460 nm of raw NHA and after 60 minutes of irradiation was calculated to be 67. Furthermore a minor peak could still be assessed after 45 minutes of treatment; but it was vanished after 60 minutes of irradiation.

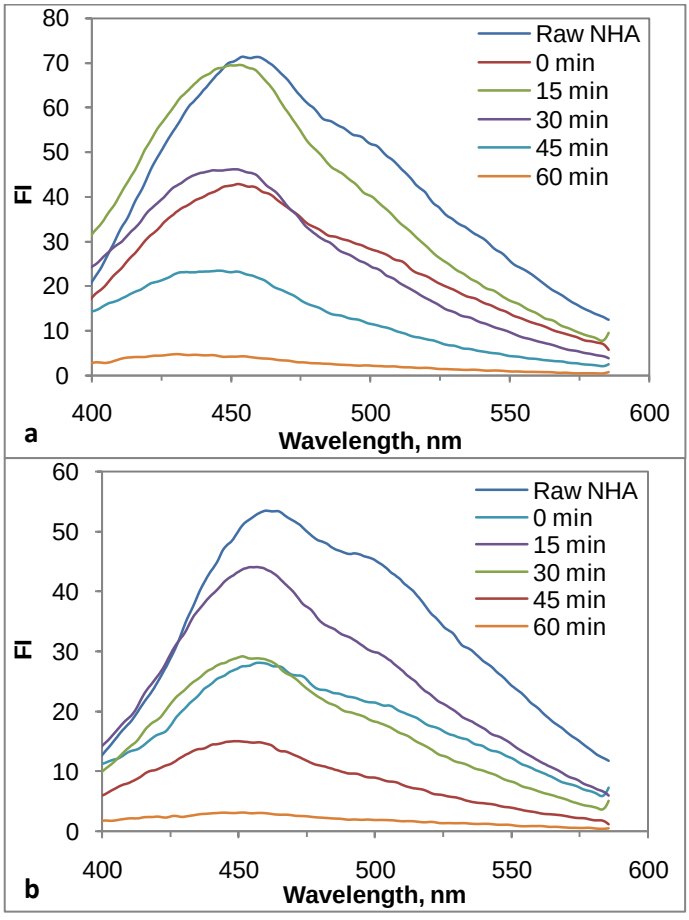

Figure 4.44. The emission fluorescence spectra at excitation wavelength (a) 350 nm and (b) 370 nm of oxidized NHA (HA: 10 mg L^{-1}, TiO_2: 0.25 mg mL^{-1}; I_0=2.85x10^{16} quanta sec^{-1})

It can be concluded that fluorescent compounds found in the structure of raw NHA were degraded by the photocatalytic oxidation, and it was successful to achieve nearly 96 percent of removal in fluorescence intensity of the peak. Parallel results were obtained in the emission spectra at 370 nm excitation wavelength as well. Different from the emission spectra, the shape of synchronous fluorescence spectra of NHA showed impressive modifications after photocatalytic oxidation process. Two main peaks were present in the synchronous fluorescence scan of raw NHA. The major peak at 460 nm with ~15 FI, and the moderate peak at 400 nm ~12 FI were recorded. At time zero, not only the major peak became extinct, but also a new peak rose in the region of 350 nm with 31 FI. Additionally, the moderate peak at 400 nm was increased in fluorescence intensity from 15 to 22. When the samples were subjected to photocatalytic irradiation, those two peaks were lessened in fluorescence intensity with increasing reaction time periods. Different from shorter reaction periods, at 550 nm, a minor peak was identified in the synchronous scan fluorescence spectra of 45 minutes treated sample (Figure 4.45).

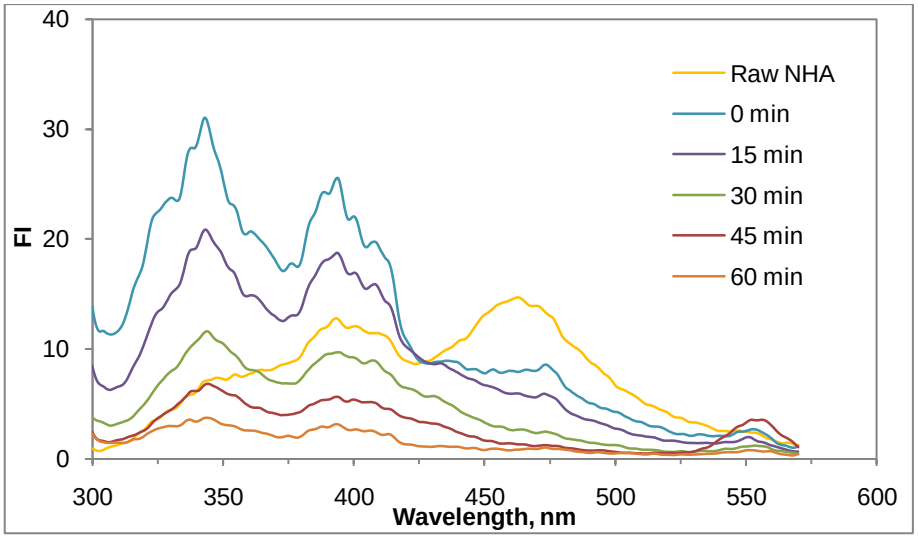

Figure 4.45. The synchronous scan fluorescence spectra of oxidized NHA (HA: 10 mg L^{-1}, TiO_2: 0.25 mg mL^{-1}; I_0=2.85x10^{16} quanta sec^{-1}, $\Delta\lambda$=18 nm)

20 mg L^{-1} NHA was subjected to photocatalytic oxidation as well, and the emission spectra were recorded both for excitation wavelength at 350 nm and 370 nm. Not only raw NHA but also oxidized samples revealed peaks at around 450 nm in the emission fluorescence spectra as presented in Figure 4.46 for both excitation wavelengths. Exciting the raw NHA at 350 nm a peak height with 90 FI was noticed in the emission fluorescence spectrum; whereas the same raw NHA solute was excited at 370 nm lower fluorescence intensity (60 FI) was recorded for the peak in the emission spectrum.

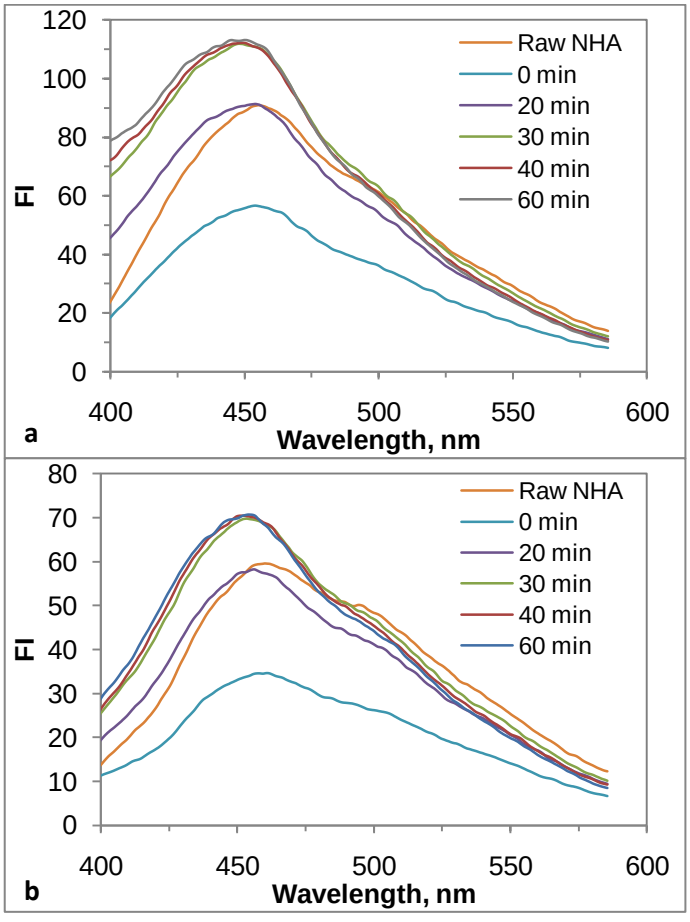

Figure 4.46. The emission fluorescence spectra at excitation wavelength (a) 350 nm and (b) 370 nm of oxidized NHA (HA: 20 mg L^{-1}, TiO_2: 0.25 mg mL^{-1}; I_0=2.85x10^{16} quanta sec^{-1})

Exciting the samples at 350 nm; the peak was reduced 33 units in fluorescence intensity at the initial adsorption point (It = 0) compared to raw NHA. ΔFI was found 25 between the peaks of raw NHA and the sample treated for 60 minutes. Parallel relationship was noticeable when the samples were excited at 370 nm. The peak was reduced 24 units in fluorescence intensity at the initial adsorption point (It=0) compared to raw NHA. ΔFI was found 9 between the peaks of raw NHA and the sample treated for 60 minutes.

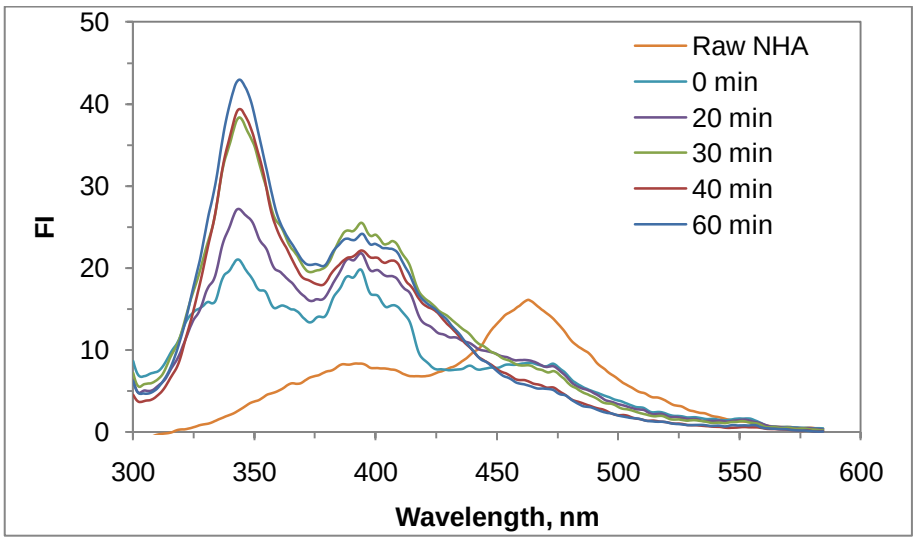

Figure 4.47. The synchronous scan fluorescence spectra of oxidized NHA (HA: 20 mg L^{-1}, TiO_2: 0.25 mg mL^{-1}; I_0=2.85x10^{16} quanta sec^{-1}, Δλ=18 nm)

Modifications in the shape of synchronous fluorescence spectra of oxidized 20 mg L^{-1} NHA were similar to the photocatalytic oxidation of 10 mg L^{-1} NHA (Figure 4.47). Two main peaks were present in the synchronous fluorescence scan of raw NHA. While the major peak was mounted at 460 nm with nearly 16 FI, the moderate peak recorded at 400 nm which had 8 FI for raw NHA. When TiO_2 was introduced to the solution not only the major peak became extinct, but also a new peak rose in the region of 350 nm with 21 FI. Additionally, the moderate peak at 400 nm was also

increased in fluorescence intensity from 8 to 19. On the other hand when the samples were subjected to photocatalytic irradiation, those two peaks were lessened in fluorescence intensity with increasing reaction time periods from 20 – 60 minutes. After 60 minutes of treatment; ΔFI at 350 nm was 22, at 400 nm was 6 between time zero and 60 minutes.

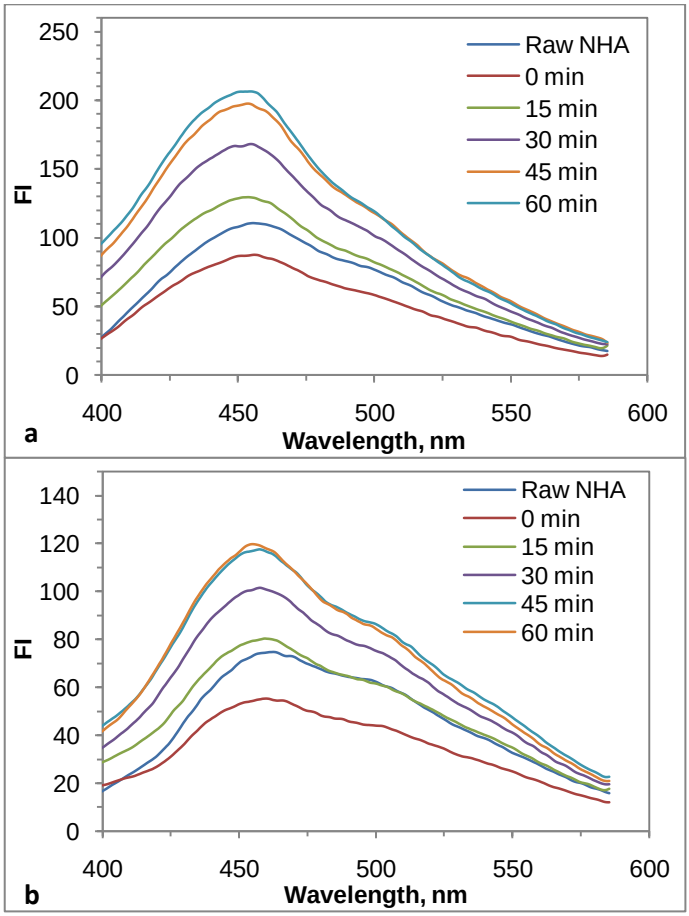

Figure 4.48. The emission fluorescence spectra at excitation wavelength (a) 350 nm and (b) 370 nm of oxidized NHA (HA: 30 mg L^{-1}, TiO_2: 0.25 mg mL^{-1}; I_0=2.85x10^{16} quanta sec^{-1})

Since NHA concentration was increased to 30 mg L^{-1}, oxidized NHA expressed resembling alterations in the peaks observed for the lower NHA concentrations (e.g.

10 mg L^{-1} and 20 mg L^{-1}) through emission and synchronous fluorescence spectra (Figure 4.48).

The samples excited at 350 nm; the peak at 455 nm was reduced 23 units in fluorescence intensity at the initial adsorption point (It = 0) compared to raw NHA in the emission fluorescence spectra (Figure 4.48a). ΔFI was found 96 between the peaks of raw NHA and the sample treated for 60 minutes. Parallel relationship was noticeable when the samples were excited at 370 nm. The peak at 462 nm was reduced 20 units in fluorescence intensity at the initial adsorption point (It=0) compared to raw NHA. ΔFI was found 43 between the peaks of raw NHA and the sample treated for 60 minutes.

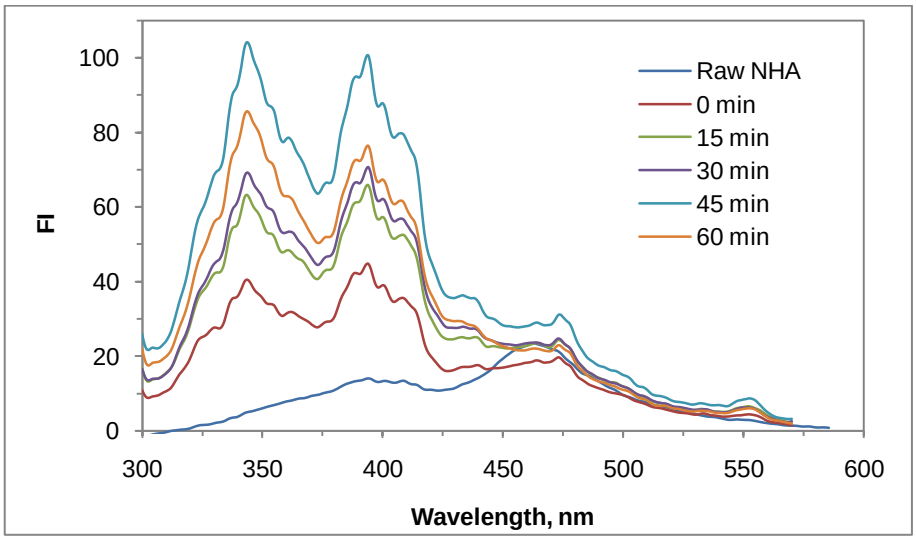

Figure 4.49. The synchronous scan fluorescence spectra of oxidized NHA (HA: 30 mg L^{-1}, TiO_2: 0.25 mg mL^{-1}; I_0=2.85x10^{16} quanta sec^{-1}, Δλ=18 nm)

The shape of synchronous fluorescence spectra of NHA (Figure 4.49) was altered by photocatalytic oxidation process. The typical humic acid peaks recorded at 460 nm

with 23 FI, and at 394 nm with 14 FI. At time zero (t=0 min), the major peak did not extinct as it did for lower concentrations, but a new peak rose in the region of 350 nm with 40 FI. Increasing the reaction time caused an increase in the fluorescence intensity of the peaks. For example, after 45 minutes of photocatalytic treatment ΔFI = 5 at 460 nm, ΔFI = 86 at 394 nm, ΔFI = 104 at 350 nm. Also, a new peak was noticed in the region of 550 nm after 45 minutes of treatment.

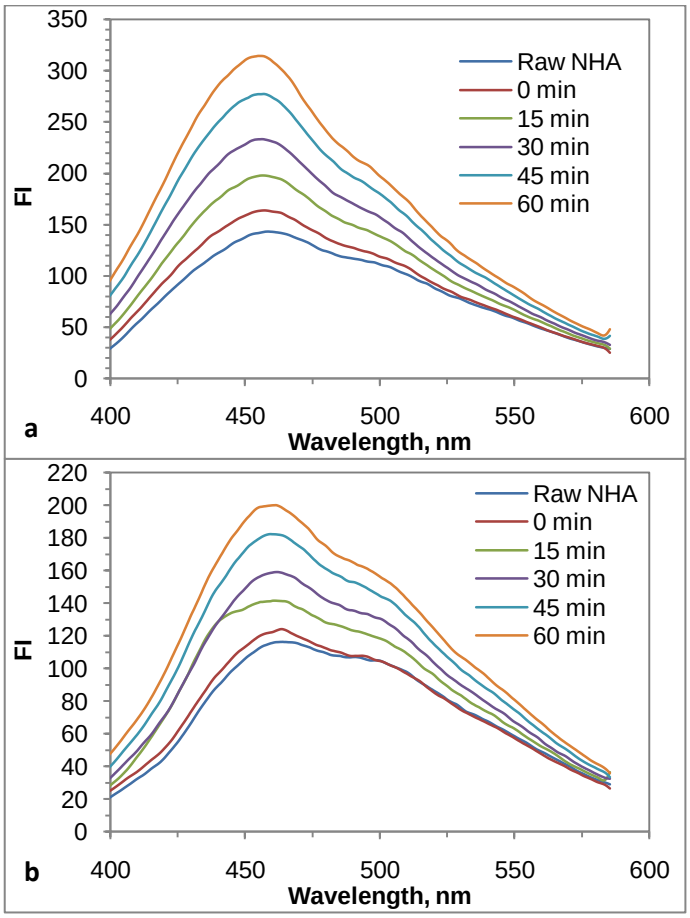

Figure 4.50. The emission fluorescence spectra at excitation wavelength (a) 350 nm and (b) 370 nm of oxidized NHA (HA: 50 mg L^{-1}, TiO_2: 0.25 mg mL^{-1}; I_0=2.85x10^{16} quanta sec^{-1})

The highest initial NHA concentration studied was 50 mgL^{-1}, and the fluorescence emission spectra were evaluated together with the synchronous fluorescence spectra as it was done for lower NHA dilutions (Figure 4.50a, Figure 4.50b and Figure 4.51).

The peaks observed in the emission fluorescence spectra were monotonously increasing with increasing reaction time (Figure 4.50a and Figure 4.50b). When the samples were excited at 350 nm, the peaks mounted at 460 nm and ΔFI = 168 between the highest (60 min) and the lowest (Raw NHA). However when 15 minutes of time intervals considered, ΔFI were 19, 34, 35, 44, 36 from time zero to 60 min. Maximum difference was between the samples irradiated for 30 – 45 minutes, while the minimum difference was detected between raw NHA and time zero. Similar peak formation observed when the samples excited at 370 nm. The peaks mounted at 465 nm with fluorescence intensities of: 116, 123, 141, 157, 180 and 197 respectively (Figure 4.50b). However when we consider 15 minutes of time intervals, ΔFI was calculated 7, 18, 16, 23 and 17 from time zero to 60 minutes correspondingly.

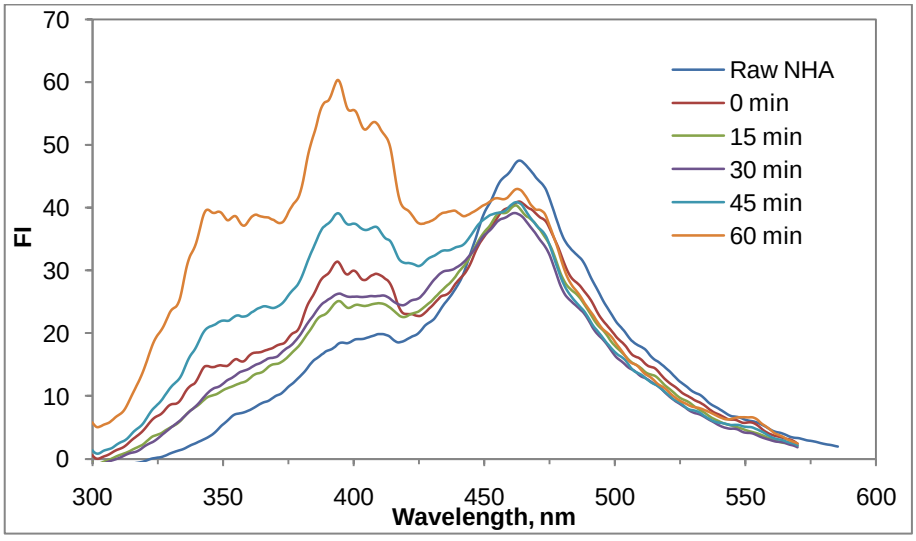

Figure 4.51. The synchronous scan fluorescence spectra of oxidized NHA (HA: 50 mg L^{-1}, TiO_2: 0.25 mg mL^{-1}; I_0=2.85x10^{16} quanta sec^{-1}, Δλ=18 nm)

Synchronous scan fluorescence spectra of oxidized 50 mg L^{-1} NHA was shown in Figure 4.51. The major peak was mounted at 460 nm with nearly 47 FI, and the moderate peak recorded at 410 nm which had 20 FI as expected. Different from lower concentrations of NHA, although the shape of the spectra were not altered by 15 and 30 minutes of photocatalytic oxidation process a new peak at 350 nm was formed by extended reaction periods e.g. 60 minutes. The major peak reduced to 39 FI after 30 minutes, but 43 FI was detected after 60 minutes of photocatalytic oxidation. On the other hand, the moderate peak at 410 nm was in increasing trend with increasing reaction time periods. After 60 minutes of irradiation a dramatic raise was observed, 52 FI was measured. Also a new peak mounted after 60 minutes of reaction period with 39 FI.

With reference to the observed changes in fluorescence spectra of treated NHA, the efficiency of photocatalytic oxidation to remove organic carbon content was found to be depending on the initial concentration of the humic acid. The reason could be better visualized when UV_{254} and DOC removals were also considered as effective parameters under the specified experimental conditions.

Upon 60 minutes of irradiation period during photocatalytic oxidation 83 %, 51 %, 45 % and 40 % DOC removals were attained with respect to initial NHA concentrations of 10 mg L^{-1}, 20 mg L^{-1}, 30 mg L^{-1} and 50 mg L^{-1}. While UV_{254} removal efficiency of photocatalytic degradation displayed a decreasing trend with increasing concentrations of NHA, it could be accepted as effective since 95 %, 75 %, 48 %, and 26 % removal were attained for the initial NHA concentrations of 10 mg L^{-1}, 20 mg L^{-1}, 30 mg L^{-1} and 50 mg L^{-1} respectively.

4.2.4. Photocatalyst Dosage Effect

Generally, due to the higher surface area of the photocatalyst that is available for adsorption and degradation an increase is expected in removal rate with raising catalyst dosage. The geometry, the working conditions of the photoreactor and the type of UV-lamp are playing important role on the determination of fundamental concentration.

An optimum photocatalyst loading was reported by Bekbölet and co-workers, for 50 mg L^{-1} of humic acid the increase of TiO_2 loading from 0.1 to 1.0 mg L^{-1} revealed an increase in the degradation percentage from 37.5 to 88.4 in terms of DOC after 2 hours of irradiation (Bekbölet, 1996). On the other hand above a certain concentration, the catalyst particles causing light scattering in the solution (solution becomes more opaque). Therefore light penetration is reduced in the slurry; a consequent rate decrease was practiced. Moreover it was also stated by Bekbölet and Ozkosemen, 1996, that further increase of photocatalyst loading to 2.0 mg mL^{-1} and 5.0 mg mL^{-1} did not expose an improved photocatalytic degradation rate. Chen and Chou, 1993 explained this phenomenon in terms of hindered light intensity due to the increased opacity of the solutions and deactivation of the activated catalyst molecules by collision with ground state particles.

With reference to the light absorption characteristics and opacity condition of the slurries, the effect of the change in the loading of the photocatalyst was examined in the range of 0.1 mg mL^{-1} to 1.0 mg mL^{-1} TiO_2, while HA concentration kept constant 20 mg L^{-1}. Considering that 46 % DOC and 55 % UV_{254} and 74 %$Color_{436}$ removals were attained for the photocatalytic degradation of 20 mg L^{-1} FHA in the presence of 0.25 mg mL^{-1} TiO_2, for comparison purposes, all samples were subjected to photocatalytic oxidation for an irradiation period of 30 minutes under all conditions.

4.2.4.1. TiO_2 Loading Effect on the Photocatalytic Oxidation of FHA. TiO_2 loading effect on the photocatalytic oxidation of FHA was also studied and represented in Figure 4.52a and Figure 4.52b. In a comparative manner, UV-vis spectra of the treated humic acid solutions displayed the same decreasing trend in absorbance values with respect to in increasing wavelength**.** The initial condition (t=0) at which the role of pre-adsorption could be visualized were also displayed in Figure 4.50a with reference to the raw FHA. Following an irradiation period of 30 minutes, the UV-vis spectral evaluation of the samples showed the same logarithmic decay profiles as well.

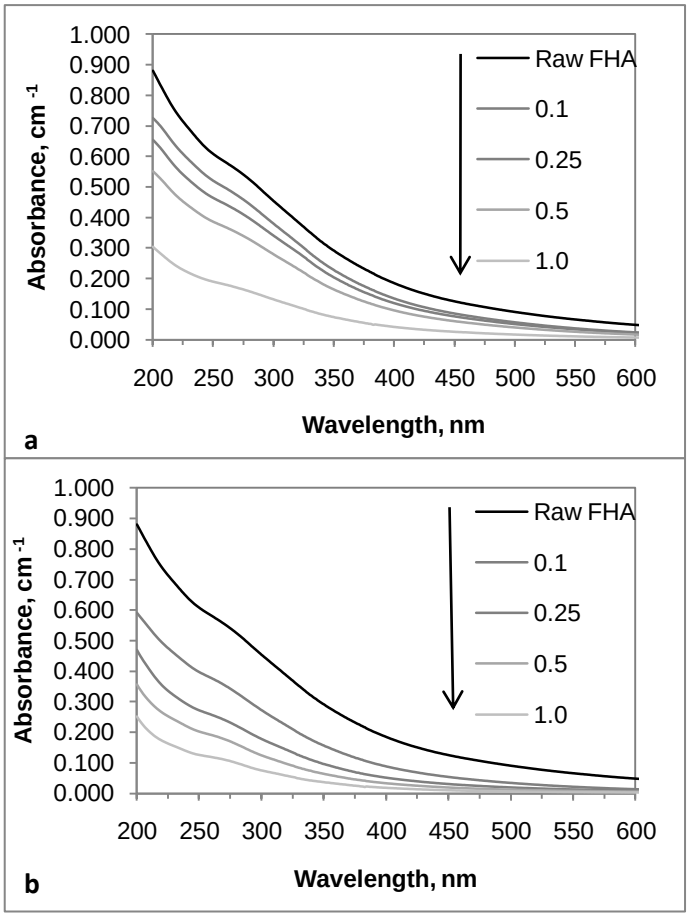

Figure 4.52. Effect of TiO_2 loading on the UV-vis spectra of FHA (a) at time zero and (b) upon irradiation period (It) of 30 min (HA: 20 mg L^{-1}, TiO_2: 0.25 mg mL^{-1}; I_0=2.85x10^{16} quanta sec^{-1})

Removal percents of $Color_{436}$ and UV_{254} with respect to TiO_2 loading were shown in Figure 4.53 for FHA. After 30 minutes of irradiation, both $Color_{436}$ and UV_{254} parameters showed declining trend with increasing TiO_2 dosage. UV_{254} and $Color_{436}$ parameters of FHA did not change more than 30 % at time zero for the minimum TiO_2 concentration. Nevertheless, 79 % of UV_{254} and 69 % of $Color_{436}$ elimination were achieved for the greatest TiO_2 dose.

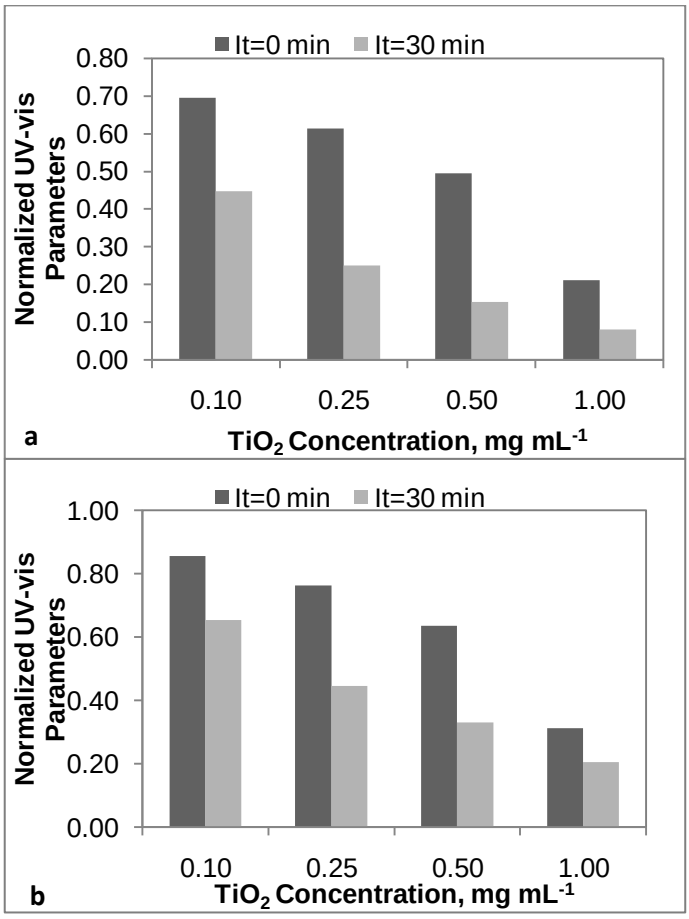

Figure 4.53. Effect of TiO_2 loading on removal efficiency of FHA in terms of (a) $Color_{436}$ and (b) UV_{254} upon irradiation period (It) of 30 min (HA: 20 mg L^{-1}, TiO_2: 0.25 mg mL^{-1}; I_0=2.85x10^{16} quanta sec^{-1})

While 40 % of UV_{254} and 60 % of $Color_{436}$ exclusion attained for 0.1 mg mL^{-1} TiO_2 concentration, it was observed that at the maximum concentration of the photocatalyst loading only 21 % of the UV_{254} and 8 % of the $Color_{436}$ was remaining in the solution after 30 minutes of photocatalytic oxidation of 20 mg L^{-1} FHA. Besides, the photocatalytic degradation profiles were also assessed through fluorescence spectral evaluation. In a similar manner as presented for photocatalytic degradation of humic acid (20 mg L^{-1}), fluorescence spectra were recorded for 350 nm excitation wavelength in emission mode as well as synchronous mode.

By studying TiO_2 loading effect between 0.1 mg mL^{-1} to 1.0 mg mL^{-1} on fluorescence spectra of photocatalytically oxidized FHA, following results were disclosed as displayed in Figure 4.54. Emission fluorescence spectra of photocatalytically oxidized FHA (20 mg L^{-1}) excited at 350 nm were shown in Figure 4.54A and Figure 4.54B for time zero and after 30 minutes of irradiation respectively. A peak mounted in the region of 450 nm by the effect of excitation at 350 nm of the oxidized FHA samples. At time zero, the peak was reduced from 140 FI to 120 FI irrespective of TiO_2 loading dose. While increasing the TiO_2 dose from 0.1 to 0.5 mg mL^{-1} caused an increasing trend after 30 minutes of photocatalytic oxidation, further increase in the photocatalyst dose resulted in a reduction in fluorescence intensity of the peak.

Moreover, synchronous scan fluorescence spectra of photocatalytically oxidized FHA (20 mg L^{-1}) were shown in Figure 4.55A and Figure 4.55B for time zero and after 30 minutes of irradiation respectively. Two peaks were displayed by the synchronous spectra; a high peak in the region of 470 nm and a moderate peak ~400 nm. While the samples that were not irradiated did not cause a new peak appearance, after 30 minutes of irradiation a peak ~350 nm was detected. It is obviously revealed that increasing the concentration of TiO_2 caused a reduction in the peak height both for time zero and after 30 minutes of treatment. Maximum reduction was achieved due to

the maximum TiO_2 loading dose; $\Delta FI \cong 20$ for time zero, $\Delta FI > 30$ after 30 minutes of irradiation.

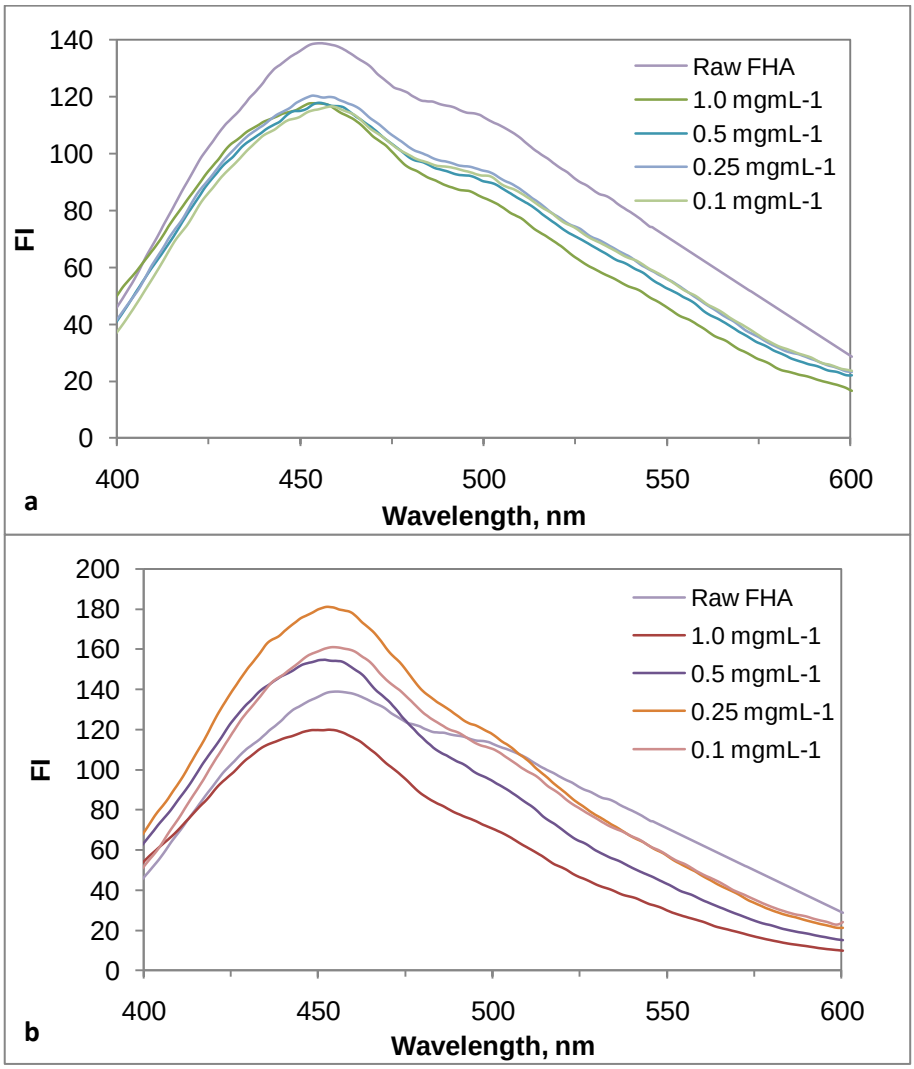

Figure 4.54. Emission fluorescence spectra of photocatalytically oxidized FHA (a) at time zero and (b) upon irradiation period (It) of 30 min (HA: 20 mg L^{-1}, TiO_2: 0.25 mg mL^{-1}; I_0=2.85x10^{16} quanta sec^{-1}, Excitation wavelength: 350 nm)

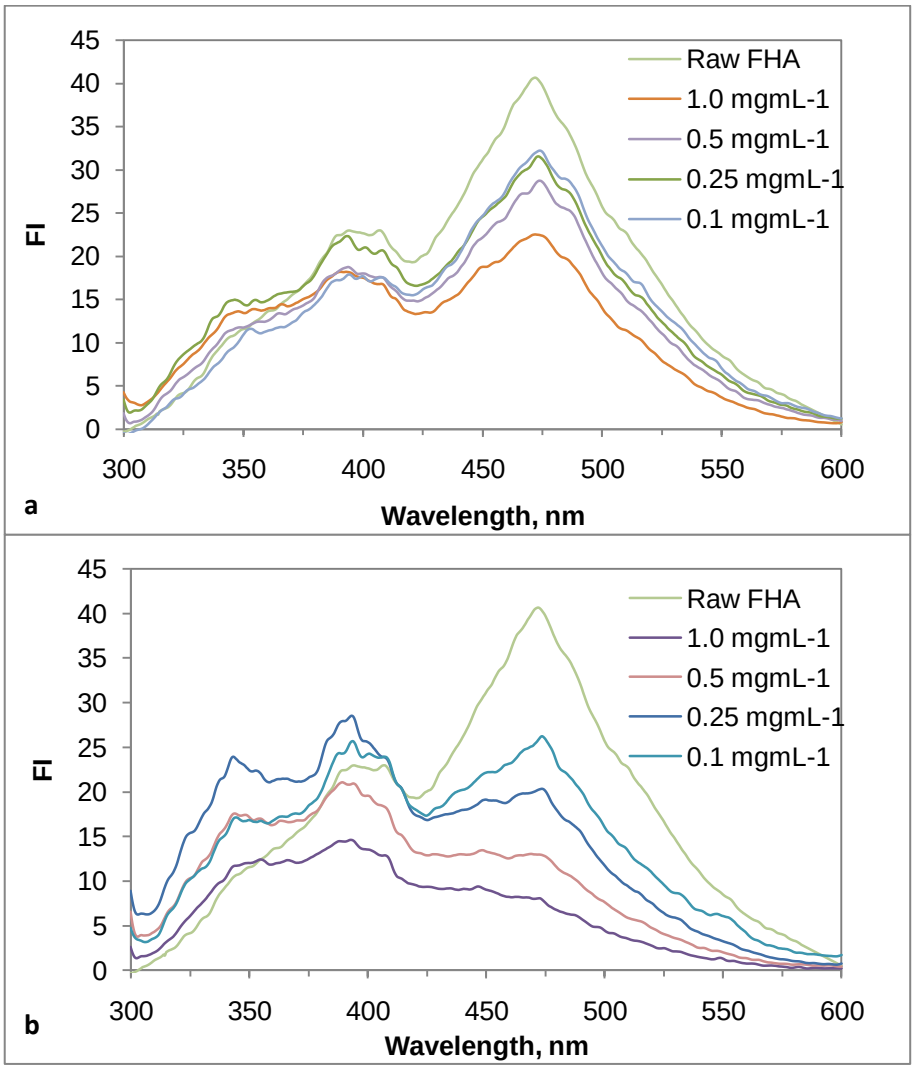

Figure 4.55. Synchronous scan fluorescence spectra of photocatalytically oxidized FHA (a) at time zero and (b) upon irradiation period (It) of 30 min (HA: 20 mg L^{-1}, TiO_2: 0.25 mg mL^{-1}; I_0=2.85x10^{16} quanta sec^{-1}, $\Delta\lambda$=18 nm)

4.2.4.2. TiO_2 Loading Effect on the Photocatalytic Oxidation of NHA. Figure 4.56a and Figure 4.56b demonstrated the TiO_2 loading effect on the photocatalytic oxidation of NHA. Comparatively; UV-vis spectra of the treated NHA solutions exhibited the same decreasing trend in absorbance values with respect to in increasing wavelength**.** The initial condition (t=0) at which the role of pre-adsorption could be visualized were also displayed in Figure 4.56a with reference to the raw NHA.

Subsequently after an irradiation period of 30 minutes, the UV-vis spectra of the samples were assessed and illustrated the same logarithmic decay profiles also. Moreover, selected UV-vis parameters ($Color_{436}$ and UV_{254}) were also evaluated as well as the UV-vis spectra as shown in Figure 4.57. $Color_{436}$ and UV_{254} parameters were decreasing with respect to increasing TiO_2 loading, and the related results obtained through photocatalytic oxidation were discussed below.

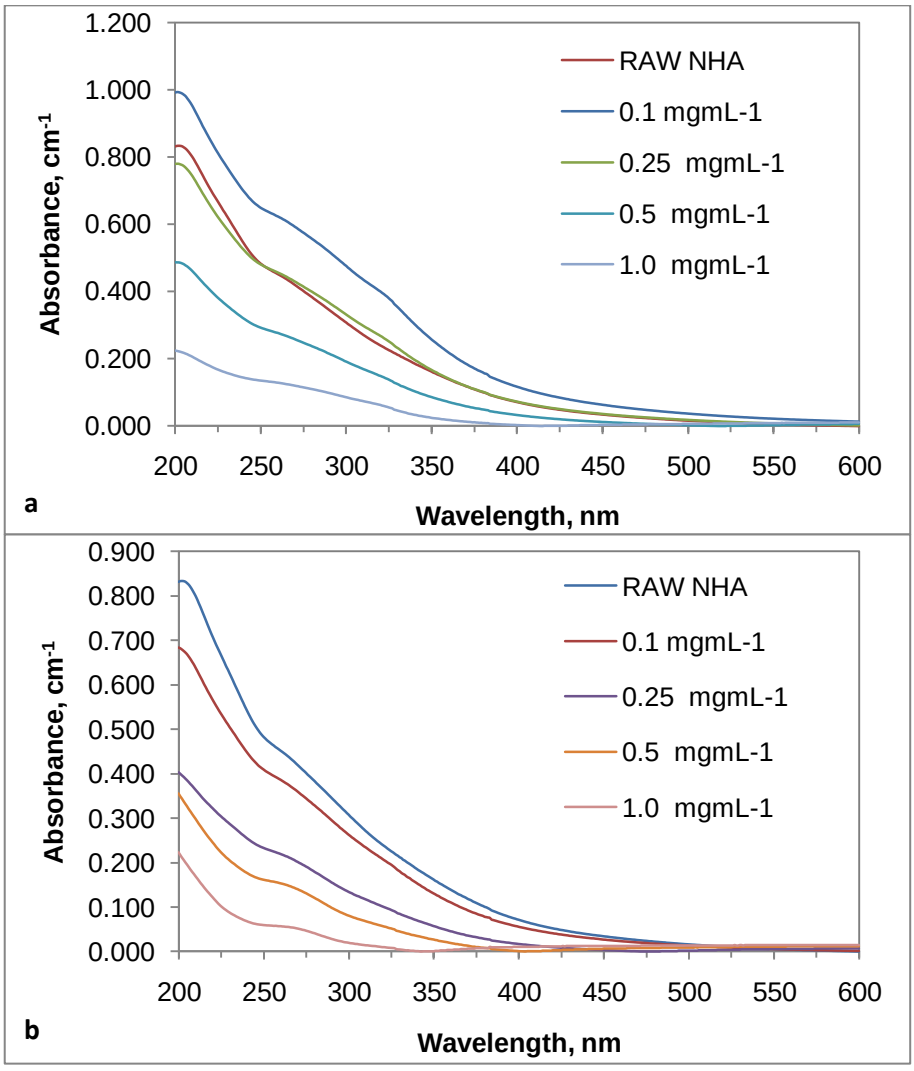

Figure 4.56. Effect of TiO_2 loading on the UV-vis spectra of NHA (a) at time zero and (b) upon irradiation period (It) of 30 min

At time zero; normalized UV_{254} and $Color_{436}$ parameters of NHA did not change more than 4 % for the minimum TiO_2 loading. However, 72 % of UV_{254} and 95 % of $Color_{436}$ elimination were achieved for the maximum TiO_2 loading following 30 minutes of photocatalytic oxidation. While 61 % of $Color_{436}$ and 39 % of UV_{254} were removed in the presence of 0.5 mg mL^{-1} TiO_2, 13 % of $Color_{436}$ and 10 % of UV_{254} were removed in the presence of 0.25 mg mL^{-1} TiO_2 loading. Accordingly, color forming moieties represented by $Color_{436}$ were more selectively eliminated than the organic core represented by UV_{254} of NHA by the photocatalytic oxidation.

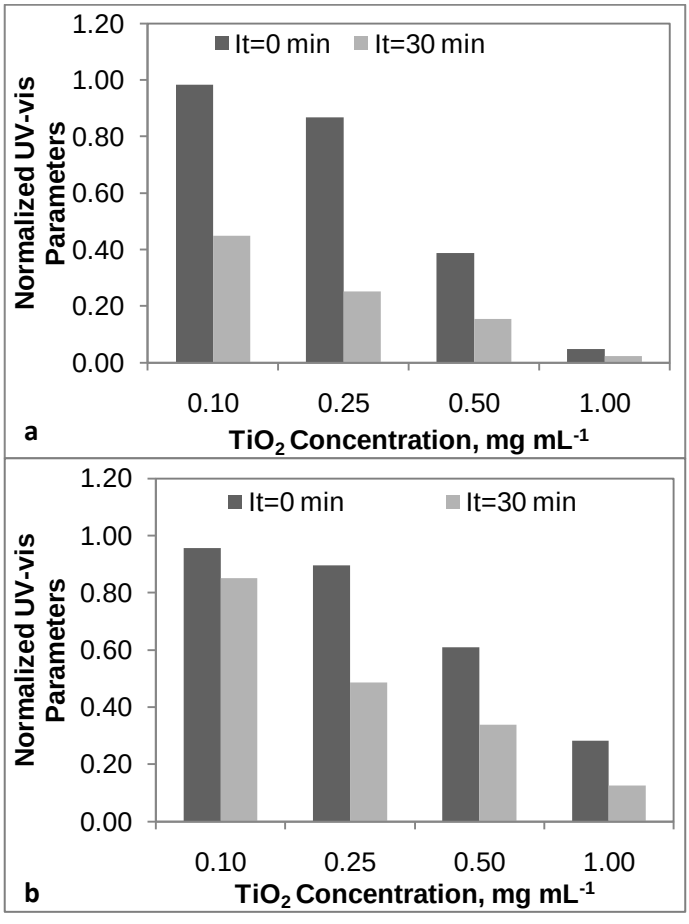

Figure 4.57. Effect of TiO_2 loading on removal efficiency of NHA in terms of (a) $Color_{436}$ and (b) UV_{254} upon irradiation period (It) of 30 min (HA: 20 mg L^{-1}, TiO_2: 0.25 mg mL^{-1}; I_0=2.85x10^{16} quanta sec^{-1})

30 minutes of illumination resulted in 15 % of UV_{254} and 55 % of $Color_{436}$ exclusion for 0.1 mg mL^{-1} TiO_2 concentration. Yet, at the highest concentration of the photocatalyst loading only 13 % of the UV_{254} and 2 % of the $Color_{436}$ was remaining in the solution after 30 minutes of irradiation of 20 mg L^{-1} NHA.

Furthermore the photocatalytic degradation profiles of humic acid were also evaluated through fluorescence spectral assessment. In a similar approach as presented for photocatalytic degradation of humic acid (20 mgL^{-1}), fluorescence spectra were recorded for 350 nm excitation wavelengths in emission mode in addition to synchronous mode. Following results were disclosed as displayed in Figure 4.58 and Figure 4.59 through the investigation of the TiO_2 loading effect starting from 0.1 mg mL^{-1} to 1.0 mg mL^{-1} on fluorescence spectra of photocatalytically oxidized NHA.

Emission fluorescence spectra of photocatalytically oxidized NHA (20 mg L^{-1}) excited at 350 nm were shown in Figure 4.58A and Figure 4.58B for time zero and after 30 minutes of irradiation, respectively. A peak observed approximately 450 nm by the effect of excitation at 350 nm of the oxidized NHA samples, similar to oxidized FHA. At time zero, the peak was increased in fluorescence intensity from 90 FI to 165 FI in the presence of 0.1 $mgmL^{-1}$ TiO_2 loading dose compared to raw NHA.

However, the peak height was reduced when TiO_2 loading was 1.0 mg mL^{-1} to 70 FI. Increasing the TiO_2 dose from 0.1 mg mL^{-1} to 0.5 mg mL^{-1} caused an increasing trend after 30 minutes of photocatalytic oxidation with approximately $\Delta FI = 45$, further increase in the photocatalyst dose resulted in a reduction in fluorescence intensity of the peak with $\Delta FI = 45$.

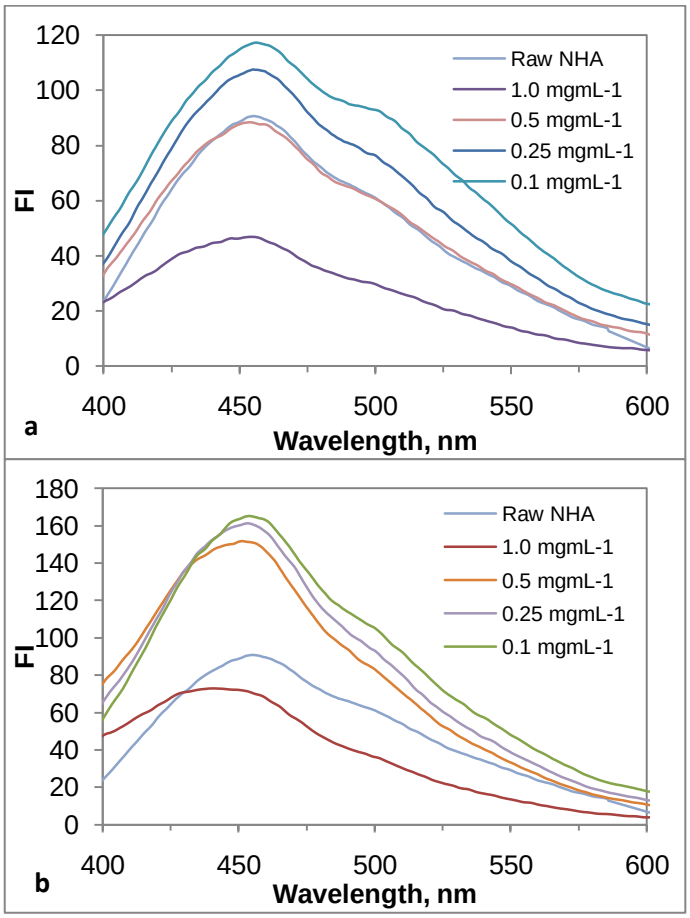

Figure 4.58. Emission fluorescence spectra of photocatalytically oxidized NHA (a) at time zero and (b) upon irradiation period (It) of 30 min (HA: 20 mg L^{-1}, TiO_2: 0.25 mg mL^{-1}; I_0=2.85x10^{16} quanta sec^{-1}, Excitation wavelength: 350 nm)

Addition to the emission spectra, synchronous scan fluorescence spectra of photocatalytically oxidized NHA (20 mg L^{-1}) were shown in Figure 4.59A and Figure 4.59B for time zero and after 30 minutes of irradiation, respectively. Two peaks were displayed by the synchronous spectra; a high peak in the region of 460 nm and a moderate peak ~400 nm. In consideration data shown in Figure 4.59A, 0.1 mg mL^{-1} of TiO_2 loading resulted in a new peak occurrence around 350 nm with nearly 165 FI, although the major peak at 470 nm was diminished. Experiments carried out with higher TiO_2 loadings i.e. 0.25, 0.5 and 1.0 mg mL^{-1} produced considerably lower peak

heights at ~350 nm and ~400 nm than 0.1 mg mL^{-1} TiO_2. The NHA samples which were exposed to photocatalytic oxidation for 30 minutes caused elimination of the major peak at 470 nm as well (Figure 4.59B).

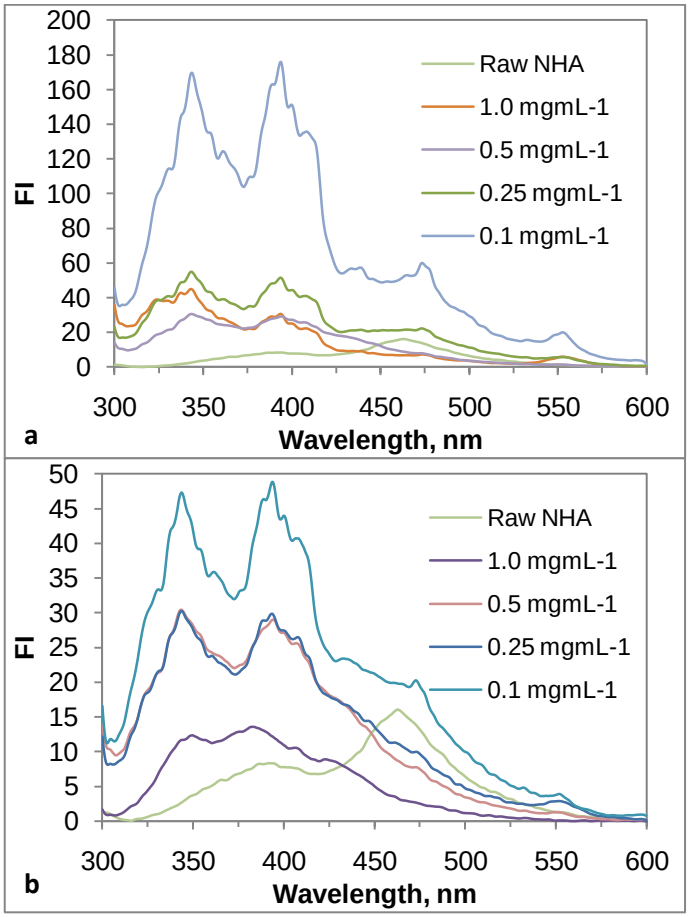

Figure 4.59. Synchronous scan fluorescence spectra of photocatalytically oxidized NHA (a) at time zero and (b) upon irradiation period (It) of 30 min (HA: 20 mg L^{-1}, TiO_2: 0.25 mg mL^{-1}; I_0=2.85x10^{16} quanta sec^{-1}, Δλ=18 nm)

It was noticeable that, when TiO_2 added slurries were irradiated for 30 minutes the peaks exhibited lower fluorescence intensities different from the synchronous fluorescence spectra of time zero samples, but still surpassed the raw NHA's

fluorescence intensity. When Figure 4.59A and Figure 4.59B were compared, $\Delta FI \cong 150$ for 0.1 mg mL^{-1} TiO_2, but 1.0 mg mL^{-1} TiO_2 loading resulted in approximately 10 FI after 30 minutes of treatment.

4.2.5. Kinetic Model Evaluation

Additionally to the UV-vis and fluorescence spectroscopic characterization of FHA and NHA, photocatalytic oxidation of model humic acids was also accomplished using TiO_2 Degussa P-25 as the photocatalyst. Irradiation time dependent degradation data were processed based on pseudo first order and Langmuir Hinshelwood kinetic models. The kinetic model parameters were evaluated and discussed intra system iei. FHA vs NHA and inter system i.e. AHA, RHA, IHSS soil HA , IHSS HA and IHSS FA.

4.2.5.1. Pseudo First Order Kinetic Model. The organic compounds (e.g. humic acid, HA) present in the illuminated titania slurry undergo many chain and consecutive reactions. In an ideal case, all intermediate compounds are fully mineralized to carbon dioxide and water. However under the specified experimental conditions the resultant solutions contained a measurable amount of organic contents either expressed by UV-vis parameters or DOC. Humic substances is known to obey pseudo first order kinetic model as expressed by the equation (15) (Bekbölet et al., 1998; Bekbölet et al., 2002).

$$R = - dA/dt = - k A \qquad (15)$$

The terms represent the following meanings; R: Pseudo first order rate in terms of the specified UV-vis parameters (m^{-1} min^{-1}) or in terms of DOC (mg L^{-1} min^{-1}); A: Specified UV-vis parameters (m^{-1}) or DOC content of humic substances (mg L^{-1}); t: Irradiation time (min) and k: Pseudo first order reaction rate constant (min^{-1}).

The kinetic evaluation of the experimental data for the photocatalytic removal of FHA and NHA (20 mg L^{-1}) in the presence of 0.25 mg mL^{-1} Degussa P-25 TiO_2 revealed the following model parameters for $Color_{436}$, UV_{365}, UV_{300}, UV_{280}, UV_{254} and DOC as presented in Table 4. Half life, rate and rate constants were calculated. The related half life values could also be assessed by the equation $t_{1/2}$=0.693/k.

Table 4.4. Pseudo first order kinetic model parameters of different humic acids (HA: 20 mgL^{-1}, TiO_2: 0.25 mg mL^{-1}, $I_0=2.85x10^{16}$ quanta sec^{-1})

	$Color_{436}$	**UV_{365}**	**UV_{280}**	**UV_{254}**	**DOC**
FHA					
k, min^{-1}	$3.28x10^{-2}$	$2.85x10^{-2}$	$2.08\ x10^{-2}$	$1.93x10^{-2}$	$1.55x10^{-2}$
R, m^{-1} min^{-1} / mg L^{-1} min^{-1}	0.352	0.609	0.958	1.021	0.123
$t_{1/2,}$ min	21	24	33	36	45
NHA					
k, min^{-1}	$5.8x10^{-2}$	$3.46x10^{-2}$	$2.32x10^{-2}$	$2.15x10^{-2}$	$1.10x10^{-2}$
R, m^{-1} min^{-1} / mg L^{-1} min^{-1}	0.244	0.445	0.889	1.008	0.106
$t_{1/2,}$ min	12	20	30	32	63

Pseudo First Order Kinetic Model Parameters of FHA: Pseudo first order reaction rate constants (k, min^{-1}) presented in Table 4.4 indicated that color forming moieties (followed by $Color_{436}$) were degraded more selectively than the organic skeleton (followed by UV_{365}, UV_{280} and UV_{254}) in the structure of FHA (20 mg L^{-1}). Although the rate constants calculated for $Color_{436}$, UV_{365}, UV_{280}, UV_{254} and DOC were in the same order of magnitude $k_{Color436}$ was 1.7 times greater than k_{UV254}. However, k_{DOC} and k_{UV254} were found to be quiet closer to each other as $1.55x10^{-2}$ and $1.93x10^{-2}$ respectively. On the other hand, half-lives ($t_{1/2,}$ min) corresponding to $Color_{436}$, UV_{365}, UV_{280} and UV_{254} were increasing with decreasing wavelength. The greatest half life of 45 minutes was calculated for the removal of DOC content that could be ascertained

to the removal of UV_{254} with 36 minutes which was generally accepted as the indicator of DOC content in HA.

Table 4.5. Pseudo first order kinetic model parameters of FHA (HA: 10, 20, 30, 40 and 50 mg L^{-1}, TiO_2: 0.25 mg mL^{-1}, I_0=2.85x10^{16} quanta sec^{-1})

HA concentration	**10 mgL^{-1}**	**20 mgL^{-1}**	**30 mgL^{-1}**	**40 mgL^{-1}**	**50 mgL^{-1}**
Color$_{436}$					
k, min^{-1}	0.046	0.033	0.019	0.014	0.010
R, m^{-1} min^{-1}	0.269	0.352	0.577	0.566	0.499
$t_{1/2,}$ min	15	21	37	50	68
UV$_{365}$					
k, min^{-1}	0.052	0.029	0.016	0.012	0.009
R, m^{-1} min^{-1}	0.504	0.609	0.497	0.502	0.470
$t_{1/2,}$ min	13	24	43	57	76
UV$_{280}$					
k, min^{-1}	0.051	0.021	0.011	0.008	0.007
R, m^{-1} min^{-1}	1.138	0.958	0.741	0.747	0.737
$t_{1/2,}$ min	14	33	63	83	105
UV$_{254}$					
k, min^{-1}	0.048	0.019	0.012	0.008	0.006
R, m^{-1} min^{-1}	0.248	1.021	0.619	0.469	0.399
$t_{1/2,}$ min	14	36	59	91	114
DOC					
k, min^{-1}	0.013	0.016	0.005	0.006	0.0015
R, mg L^{-1} min^{-1}	0.049	0.123	0.056	0.093	0.030
$t_{1/2,}$ min	53	45	139	116	462

Furthermore, different concentrations of FHA (10 to 50 mg L^{-1}) were also treated to obtain pseudo first order kinetic parameters with a manner of comparison. These

parameters were calculated for $Color_{436}$, UV_{365}, UV_{280} and UV_{254} and were demonstrated in Table 4.5. From a general point of view, pseudo first order rate constant (k, min^{-1}) of $Color_{436}$ was found to be higher than the other parameters provided that the initial humic acid concentration should be greater than 10 mg L^{-1} (Table 4.5), as a result of the measured absorbance was decreasing with increasing wavelength. Increasing the initial concentration of FHA reaction rate constants of $k_{Color436}$, k_{UV365}, k_{UV280} and k_{UV254} followed a decreasing trend as well as the reaction rates of $R_{Color436}$, R_{UV365}, R_{UV280} and R_{UV254}. On the contrary half lives corresponding to $Color_{436}$, UV_{365}, UV_{280} and UV_{254} were increasing with increasing FHA concentration. While $k_{Color436}$ was found to be 5 times lower for 50 mg L^{-1} compared to 10 mg L^{-1}, the half life was extended beyond 1 hour from 15 minutes. Additionally k_{UV254} was found to be 8 times greater for 10 mg L^{-1} compared to 50 mg L^{-1}, while the half life was extended nearly to two hours. All of the parameters exhibited considerably similar pseudo first order kinetic model parameters (k, min^{-1}; t, min; and R, $m^{-1}min^{-1}$) for 10 mg L^{-1} humic acid concentration whereas increasing initial concentration the kinetic model parameters displayed significant differences.

Pseudo First Order Kinetic Model Parameters of NHA: Pseudo first order reaction rate constants (k, min^{-1}) presented in Table 4.4 pointed out that color forming moieties (followed by $Color_{436}$) were more selectively oxidized than the organic compounds (followed by UV_{365}, UV_{280} and UV_{254}) in the structure of NHA as well as FHA. As it was reported for FHA (20 mg L^{-1}), the rate constants calculated for $Color_{436}$, UV_{365}, UV_{280}, UV_{254} and DOC were in the same order of magnitude for NHA (20 mg L^{-1}) too. Furthermore the relationship between the rate constants were investigated, $k_{Color436}$ was 2.7 times greater than k_{UV254} while k_{DOC} was nearly the half of the k_{UV254}. On the other hand, half-lives ($t_{1/2,}$ min) corresponding to $Color_{436}$, UV_{365}, UV_{280} and UV_{254} were increasing with decreasing wavelength. The greatest half life of 63 minutes was calculated for the removal of DOC content that could be ascertained to the removal of UV_{254} with 32 minutes which was generally accepted as the indicator of DOC content in HA.

Table 4.6. Pseudo first order kinetic model parameters of NHA (HA: 10 mg L^{-1}, 20 mg L^{-1}, 30 mg $L^{-1}$and 50 mg L^{-1}; TiO_2: 0.25 mg mL^{-1}, I_0=2.85x10^{16} quanta sec^{-1}

HA concentration	**10 mgL^{-1}**	**20 mgL^{-1}**	**30 mgL^{-1}**	**50 mgL^{-1}**
Color$_{436}$				
k, min^{-1}	0.038	0.058	0.0145	0.0085
R, m^{-1} min^{-1}	0.120	0.244	0.101	0.097
$t_{1/2,}$ min	18	20	48	82
UV$_{365}$				
k, min^{-1}	0.048	0.0346	0.0128	0.0072
R, m^{-1} min^{-1}	0.394	0.445	0.265	0.245
$t_{1/2,}$ min	14	20	54	96
UV$_{280}$				
k, min^{-1}	0.049	0.0232	0.0102	0.0052
R, m^{-1} min^{-1}	1.120	0.889	0.619	0.522
$t_{1/2,}$ min	14	30	68	133
UV$_{254}$				
k, min^{-1}	0.049	0.0215	0.0098	0.0048
R, m^{-1} min^{-1}	1.368	1.008	0.729	0.590
$t_{1/2,}$ min	14	32	71	145
DOC				
k, min^{-1}	0.028	0.012	0.0114	0.0079
R, mg L^{-1} min^{-1}	0.328	0.116	0.263	0.213
$t_{1/2,}$ min	25	58	60	88

Moreover, the initial humic acid, NHA concentration was varied in between 10 mg L^{-1} and 50 mg L^{-1} and subjected to photocatalytic oxidation. The degradation data were evaluated by using pseudo first order kinetic model. Pseudo first order kinetic parameters were calculated for UV-vis parameters as $Color_{436}$, UV_{365}, UV_{280} and UV_{254} and illustrated in Table 4.6. Increasing the initial concentration of NHA, photocatalytic degradation rate constants of $k_{Color436}$, k_{UV365}, k_{UV280} and k_{UV254} followed

a decreasing trend as well as the reaction rates as expressed for $R_{Color436}$, R_{UV365}, R_{UV280} and R_{UV254}. As it can be recognized from Table 4.6 photocatalytic degradation rate constants of $k_{Color436}$, k_{UV365}, k_{UV280} and k_{UV254} were increasing as the wavelength was decreasing for all NHA concentrations, as a result the measured absorbance was decreasing with increasing wavelength. In contrast, half lives related to $Color_{436}$, UV_{365}, UV_{280} and UV_{254} were increasing with increasing NHA concentration. While $k_{Color436}$ was found to be 4.5 times higher for 10 mg L^{-1} compared to 50 mg L^{-1}, the half life was extended beyond 82 minutes from 18 minutes. In addition, k_{UV254} was found to be ten times greater for 10 mg L^{-1} compared to 50 mg L^{-1}, while the half life was extended from 14 minutes to nearly 2.5 hours.

Comparative evaluation of the experimental data as expressed in the form of kinetic model parameters were assessed for FHA and NHA. (Tables 4.4, Table 4.5 and Table 4.6). Considering that UV_{254} was generally used as a surrogate parameter for DOC, the rate constants calculated for DOC removal were expected to follow the same trend observed for UV_{254}. However the DOC removal rate constant for NHA was found to be lower than that calculated for FHA. DOC rate constants for FHA and NHA were relatively lower compared to the UV_{254} rate constants. Additionally, in accordance with the low photocatalytic degradation rate constants of DOC, quite higher half-life values for all of the parameters were obtained as presented in Table 4.4. While the half-life of FHA and NHA in means of UV_{254} parameter was 36 minutes and 32 minutes, DOC degradation revealed higher half-life with 45 minutes and 63 minutes respectively. Although UV-vis spectroscopic parameter rate constants were found to be in the same order of magnitude, removal rate constants were determined to reflect higher degradation rates for NHA with respect to FHA. The removal of color forming moieties was comparatively faster than the removal of UV absorbing centers for both of the humic models.. On the other hand, UV_{365} removal rates were found to be relatively lower than $Color_{436}$ but exhibit higher removal rates than UV_{280} and higher for NHA than FHA.

For comparison purposes and to provide an overview of photocatalytic degradation of the model humic substances studied so far a table is prepared to display the pseudo first order kinetic model parameters (Table 4.7). Pseudo first order kinetic parameters for fulvic acid were also presented in Table 4.7 to express the different structural and conformational properties of fulvic acids in relation to humic acids. Moreover DOC removal parameters were excluded due to insufficient reported data presented (Uyguner and Bekbölet, 2005a). The selection of initial concentration of humic acid as 50 mg L^{-1} exhibited a wide range of initial UV_{254} parameter (91.1 m^{-1} – 186.3 m^{-1}). In a similar manner $Color_{436}$ parameter also displayed a variation in the range of 5.1 m^{-1} - 38 m^{-1} irrespective of the humic substance structure. Due to the presence of significant variations in the initial UV_{254} contents of the substrates the comparative evaluation of the humic substances were directed to the removal rates rather than removal rate constants ($Rate_{254}$, m^{-1} min^{-1} = k, min^{-1} x UV_{254}, m^{-1}). Bearing in mind the above given information UV_{254} removal rates were attained in the following order: IHSSsoilHA > AHA > FHA > IHSSHA > NHA > RHA > IHSSFA. This sequence of removal rates could not be attributable to the source characteristics of humic substances. Probably, the reason could be explained by differing adsorption properties of the untreated and treated humic moieties onto titanium dioxide surface during irradiation periods. Following the same approach, the removal rates of the other UV-vis parameters were also in a decreasing manner in comparison to UV_{254}.

$Color_{436}$; IHSSsoilHA>AHA>FHA>IHSSHA> RHA >NHA> IHSSFA

UV_{365}; IHSSsoilHA>AHA>FHA>IHSSHA>NHA>RHA>IHSSFA

UV_{280}; IHSSsoilHA>AHA>FHA>IHSSHA>NHA>RHA>IHSSFA

UV_{254}; IHSSsoilHA > AHA > FHA > IHSSHA > NHA > RHA > IHSSFA

IHSS FA was found to be considerably lower in UV-vis parameter removal efficiencies irrespective of the parameter as well as the source of the humic substances. On the other hand, the removal rates of almost all of the UV-vis parameters followed the same trend except for NHA and RHA color forming moieties.

Table 4.7. Pseudo first order kinetic parameters of model compounds (HA: 50 mgL^{-1}, TiO_2: 0.25 mg mL^{-1}, $I_0=2.85x10^{16}$ quanta sec^{-1})

$Color_{436}$	**A_0, m^{-1}**	**k, min^{-1}**	**$t_{1/2}$, min**	**R, m^{-1} min^{-1}**
FHA	25.4	$1.03x10^{-2}$	67	0.262
NHA	11.4	$8.5x10^{-3}$	82	0.097
AHA*	18.8	$1.60x10^{-2}$	43	0.301
IHSS FA*	5.1	$7.22x10^{-3}$	96	0.0368
IHSS HA*	15.9	$8.3x10^{-3}$	84	0.132
IHSS Soil HA*	28.1	$1.35x10^{-2}$	51	0.379
RHA*	38	$3.04x10^{-3}$	228	0.115
UV_{365}				
FHA	51.6	$9.1x10^{-3}$	76	0.470
NHA	34.0	$7.2x10^{-3}$	96	0.245
AHA*	39.2	$1.49x10^{-2}$	47	0.584
IHSS FA*	19.4	$6.46x10^{-3}$	107	0.125
IHSS HA*	44.3	$7.03x10^{-3}$	99	0.311
IHSS Soil HA*	48.4	$1.24x10^{-2}$	56	0.600
RHA*	72.9	$2.69x10^{-3}$	258	0.196
UV_{280}				
FHA	111.7	$6.6\ x10^{-3}$	105	0.737
NHA	100.4	$5.2x10^{-3}$	133	0.522
AHA*	92.1	$1.09x10^{-2}$	64	1.004
IHSS FA*	68.4	$4.02x10^{-3}$	172	0.275
IHSS HA*	120.2	$5.45x10^{-3}$	127	0.655
IHSS Soil HA*	99.3	$1.10x10^{-2}$	63	1.092
RHA*	159.4	$2.13x10^{-3}$	325	0.339
UV_{254}				
FHA	129.2	$6.1x10^{-3}$	114	0.788
NHA	122.9	$4.8x10^{-3}$	144	0.590
AHA*	108.1	$1.03x10^{-2}$	67	1.113
IHSS FA*	91.1	$3.76x10^{-3}$	184	0.342
IHSS HA*	148.1	$4.90x10^{-3}$	141	0.726
IHSS Soil HA*	114.9	$1.07x10^{-2}$	65	1.229
RHA*	186.3	$2.01x10^{-3}$	345	0.374

* Data collected from Uyguner and Bekbölet, 2005a, where, AHA denotes humic acid supplied from Aldrich, RHA denotes humic acid from Roth and IHSS denotes IHSS, Internatonal Humic Substances Society.

4.2.5.2. Langmuir Hinshelwood Kinetic Model. The photo-degradation kinetics of many organic compounds in TiO_2 suspensions under UV irradiation has often been modeled to the Langmuir-Hinshelwood (L-H) equation (Eq. (16)) which also covers the adsorption properties of the substrate on the photocatalyst surface (Turchi and Ollis, 1989). With regards to that photocatalysis takes place at the surface, the concentration of substrate adsorbed to the surface directly influences the overall rate of adsorption.

The rate of degradation of humic acid in terms of $Color_{436}$, UV_{254} and other UV-vis parameters was expressed in the following empirical type Langmuir-Hinshelwood relationship:

$$R_{LH} = dA / dt = k_{LH} K_{LH} A_0 / (1+K_{LH} A_0) \quad (16)$$

where the model terms represent the following meanings; R_{LH}: Rate of the reaction (m^{-1} min^{-1}), k_{LH}: Reaction rate constant (m^{-1} min^{-1}), K_{LH}: Adsorption coefficient of substrate onto photocatalyst TiO_2 under irradiation conditions (m), A_0:Initial value of the specified UV-vis parameters of humic substances (m^{-1}).

Moreover, the above given rate parameters could be calculated by the following equation (Eq. (17)):

$$t_{1/2} = \left(\frac{0.693}{k_{LH} K_{LH}}\right) + \left(\frac{0.5}{k_{LH}}\right) * C_0 \quad (17)$$

Using 20 mg L^{-1} FHA and NHA in the presence of 0.25 mg mL^{-1} TiO_2 Degussa P-25 as presented in Table 4.8, a new sequence of photocatalytic experiments were

studied to assess the Langmuir-Hinshelwood kinetics. Representative Langmuir-Hinshelwood kinetic model rate was calculated for 20 mgL^{-1} humic acid concentration.

Table 4.8. L-H kinetic model parameters of FHA and NHA (HA: 20 mg L^{-1}, TiO_2: 0.25 mg mL^{-1}, $I_0=2.85x10^{16}$ quanta sec^{-1})

	$Color_{436}$	**UV_{365}**	**UV_{280}**	**UV_{254}**	**DOC**
FHA					
k_{LH}, min^{-1}	0.215	0.328	0.480	0.505	0.031
K_{LH}, m / mg L^{-1}	0.595	0.450	0.135	0.095	0.413
$t_{1/2}$, min	30	37	59	67	185
R_{LH}, m^{-1} min^{-1}/ mg L^{-1} min^{-1}	0.186	0.200	0.411	0.421	0.023
NHA					
k_{LH}, min^{-1}	0.058	0.151	0.319	0.359	0.210
K_{LH}, m / mg L^{-1}	0.787	0.272	0.084	0.065	0.110
$t_{1/2}$, min	51	60	86	95	56
R_{LH}, m^{-1} min^{-1}/ mg L^{-1} min^{-1}	0.045	0.117	0.243	0.271	0.115

The L-H removal rates constants of UV-vis parameters were found to be in the order of $UV_{254}>UV_{280}>UV_{365}>Color_{436}$. The effect of the adsorption coefficient could be assessed by the order of $Color_{436}>UV_{365}>UV_{280}>UV_{254}$. The half-life values significantly expressed the considerably faster removal of color forming moieties with respect to UV absorbing aromatic core. The given explanatory information was found to be valid for both of the studied humic acids as FHA and NHA. When the two kinetic models were compared; the increasing trend of the L-H rates was similar to that of first order rates for selected UV-vis parameters. However, the calculated L-H rates for FHA were approximately half the value of the pseudo first order rates of $Color_{436}$, UV_{365}, UV_{280} and UV_{254}. Parallel correlation was noticed for NHA too; pseudo first order rates of $Color_{436}$, UV_{365}, UV_{280} and UV_{254} were approximately five times greater

than the L-H rate. In addition, similar correlation between R and R_{LH} were observed for NHA. Further evaluation of the L-H kinetic model parameters calculated for FHA and NHA (Table 4.8) was presented in Table 4.9 in comparison to the previously published data (Uyguner and Bekbölet, 2005a). Additional comparison between DOC removal rate constants, half life values and rates would also be informative. It was noticed thah k_{LH} (FHA) < k_{LH} (NHA), while K_{LH} (FHA) > K_{LH} (NHA). FHA was found to have more than three times of longer half life than NHA. R_{LH} for NHA was found to be five times higher than for FHA (Table 4.8).

Table 4.9. L-H kinetic model parameters of IHSS HA, IHSS SHA, AHA and RHA (HA: 50 mg L^{-1}, adapted from Uyguner and Bekbölet, 2005a)

	$Color_{436}$	**UV_{365}**	**UV_{280}**	**UV_{254}**
IHSS HA				
k_{LH}, min^{-1}	0.0903	0.206	0.435	0.469
K_{LH}, m	1.47	0.337	0.134	0.0838
$t_{1/2}$, min	93	118	150	176
R_{LH}, m^{-1} min^{-1}	0.0866	0.193	0.410	0.434
IHSS Soil HA				
k_{LH}, min^{-1}	0.244	0.399	0.714	0.805
K_{LH}, m	0.398	0.345	0.120	0.105
$t_{1/2}$, min	65	66	78	80
R_{LH}, m^{-1} min^{-1}	0.224	0.376	0.659	0.743
AHA				
k_{LH}, min^{-1}	0.188	0.376	0.627	0.697
K_{LH}, m	0.584	0.360	0.122	0.109
$t_{1/2}$, min	56	57	83	87
R_{LH}, m^{-1} min^{-1}	0.172	0.351	0.576	0.642
RHA				
k_{LH}, min^{-1}	0.0698	0.115	0.195	0.214
K_{LH}, m	0.217	0.0936	0.0395	0.0332
$t_{1/2}$, min	318	381	499	533
R_{LH}, m^{-1} min^{-1}	0.0623	0.100	0.168	0.184

For clarity purposes the information given in Tables 4.8 and 4.9 were complied in a simple manner to express the relationship between L-H kinetic model parameters and the specified UV-vis parameters of the humic acid samples.

The L-H kinetic model rate constants were found to be in an irregular order and could be presented in the following order for the specified UV-vis parameters;

$Color_{436}$; IHSSsoilHA>AHA>FHA>IHSSHA> RHA >NHA

UV_{365}; IHSSsoilHA>AHA>FHA>IHSSHA>NHA>RHA

UV_{280}; IHSSsoilHA>AHA> FHA>IHSSHA > NHA>RHA

UV_{254}; IHSSsoilHA>AHA>FHA>IHSSHA>NHA>RHA

The L-H kinetic model adsorption coefficients were found to be in an irregular order and could be presented in the following order for the UV-vis parameters;

$Color_{436}$; IHSSHA>NHA >FHA >AHA> IHSSsoilHA> RHA

UV_{365}; FHA >AHA ~ IHSSsoilHA ~ IHSSHA>NHA>RHA

UV_{280}; FHA ~IHSSHA> AHA ~ IHSSsoilHA> NHA>RHA

UV_{254}; AHA~ IHSSsoilHA>FHA>IHSSHA>NHA>RHA

The L-H kinetic model half-life values could be presented in the same order irrespective of the UV-vis parameters;

$Color_{436}$; RHA >IHSSHA >IHSSsoilHA>AHA> NHA >FHA

UV_{365}; RHA >IHSSHA >IHSSsoilHA>AHA> NHA >FHA

UV_{280}; RHA >IHSSHA >IHSSsoilHA>AHA> NHA >FHA

UV_{254}; RHA >IHSSHA >IHSSsoilHA>AHA> NHA >FHA

The L-H kinetic model rates were found to be in an irregular order and could be presented in the following order for the UV-vis parameters;

$Color_{436}$; IHSSsoilHA>FHA >AHA >IHSSHA> RHA >NHA

UV_{365}; IHSSsoilHA>AHA>FHA>IHSSHA>NHA>RHA

UV_{280}; IHSSsoilHA> AHA> FHA ~IHSSHA>NHA>RHA

UV_{254}; IHSSsoilHA>AHA> IHSSHA >FHA >NHA>RHA

As could be seen from the above given irregular sequence of UV-vis parameters, no significant correlation could be deduced for any kinetic model parameter. Further insight could be directed to the elucidation of the fluorescence parameters for the understanding of the mechanism of the photocatalytic degradation occurring via oxidation pathways.

When the two kinetic models were compared main discrepancy was because of the different rate equations. While R_{L-H} (Eq 16) includes a separate adsorption coefficient, pseudo first order rate constant (k) covers both oxidation and adsorption effect in Eq 15. However, the increasing trend of the L-H rates was similar to that of pseudo first order rates. Additionally, the calculated L-H rates for the FHA were roughly half the value of the pseudo first order rates of selected UV-vis parameters $Color_{436}$, UV_{365}, UV_{280} and UV_{254}. Parallel correlation between R and R_{LH} were observed for NHA too.

5. CONCLUSIONS

This study represents a significant content for the evaluation of aquatic and terrestrial origin humic acids as FHA and NHA, with respect to their UV-vis and fluorescence properties as representatives to natural organic matter in drinking water supplies with reference to the previously studied model humic substances, humic and fulvic acids *i.e.* AHA, RHA, IHSS HA, IHSS SHA and IHSS FA.

Information about origin characteristics were revealed as follows: FHA, which is a terrestrial origin humic acid, exhibited 25.4 m^{-1} of $Color_{436}$, whereas NHA illustrated less than half of the value of color forming moieties than FHA as can be seen from Figure 4.1. FHA and NHA had considerably similar UV_{280} and UV_{254} values, emphasizing strong aromatic character. With the purpose of comparison, the data obtained from experimental studies of FHA and NHA were presented in Table 4.1 with reference to the data reported by Uyguner and Bekbolet, 2005a. All humic acids could be expressed by the following decreasing trend in $Color_{436}$ parameter as; RHA > IHSS SHA > FHA > AHA > IHSS HA > NHA. Since both humic acids IHSS HA and NHA were aquatic origin, the lowest $Color_{436}$ values were obtained as expected. Terrestrial humic acids had remarkably higher $Color_{436}$ values than aquatic humic acids. Furthermore, RHA was reported to have appreciably high UV_{280} and UV_{254} values as regards the other humic acids emphasizing strong aromatic character. The order of UV_{280} and UV_{254} absorbing moieties of the samples follows a decreasing trend as; RHA > IHSS HA > FHA > NHA > IHSS SHA > AHA, reflecting non-source dependency. Bearing in mind that DOC content of humic acids were presented for 50 mg L^{-1} humic acid concentration in Table 4.1; NHA = 29.01, FHA = 19.78, RHA = 19.53, IHSS HA = 16.16, AHA = 15.5 IHSS soil HA = 15.48 mg L^{-1}. The alterations observed in $SCOA_{436}$ would be restricted by the irradiation time, since relatively higher removal rate of $Color_{436}$ with reference to the removal rates of UV_{365}, UV_{280} and UV_{254} was observed. As a result, $SCOA_{436}$ parameter possibly would not exhibit a

distinctive consequence attributable to the lower $Color_{436}$ detected during extended periods of photocatalytic oxidation process. Humic acids were degraded to a smaller amount UV-vis absorbing compounds in the course of the formation of a chain of intermediates and their subsequent reactions, as could be verified by the decrease in the SCOA/SUVA values.

The synchronous scan fluorescence spectra measured proved to be useful for highlighting similarities and differences in the composition of the studied HA. The terrestrial FHA and aquatic NHA have characteristic peaks around 470 nm and 460 nm respectively. Both humic acids displayed a peak with shoulders around 400 nm as represented in Figure 4.5. Also DOC normalized synchronous scan fluorescence spectra of FHA and NHA were shown in Figure 4.9. FHA found to have more than twice the value of fluorescence intensity of NHA. Uyguner and Bekbolet, 2005c, stated consistent data with the results presented in this study: the terrestrial IHSS Soil HA, FHA and AHA had typical peaks around 470 nm with relatively higher intensities than those of Roth and IHSS HA. In addition, a minor peak around 400 nm was reported for IHSS Soil HA as found for FHA and NHA. However, the synchronous scan fluorescence spectra of Roth and IHSS HA were very similar to each other and demonstrated wide bands without any significant feature (Uyguner and Bekbolet, 2005c).

Detailed UV-vis and fluorescence explanation were provided: As already stated formerly, the UV-visible spectra of humic acids are broad, featureless and monotonously decrease with increasing wavelength. UV-visible spectra obtained from the photocatalytic oxidation of FHA and NHA also followed the same decreasing trend as presented in Figure 4.20 and Figure 4.24.

While 89 % of $Color_{436}$ removed in 60 minutes of irradiation of FHA, 98 % of $Color_{436}$ elimination achieved for NHA. Additionally, UV_{254} changes observed to be reduced 73 % following 60 minutes of irradiation for FHA, 75 % removal achieved for NHA.

DOC content was also decreased by photocatalytic oxidation, while 63% of DOC removal for FHA was attained, 51 % reduction assessed for FHA through 60 minutes of treatment.

On the other hand investigation of synchronous fluorescence spectra of photocatalytically oxidized humic acids, it was remarkable that the characteristic peak (obtained about 472 nm) of FHA was significantly reduced as could be seen via Figure 4.23 even with the sole action of TiO_2 prior to irradiation; moreover the importance of initial adsorption of the humic acid onto TiO_2 was proved. Different from FHA, besides the characteristic peak of NHA was eliminated through photocatalytic oxidation process, the emergence of two new peaks around 340 and 390 nm was recorded (Figure 4.27). Furthermore, systematically increasing in fluorescence intensity with increasing reaction time periods of those two peaks were noticeable. Furthermore, it can be concluded from Figure 4.23 and Figure 4.27, oxidation of FHA and NHA followed different patterns for both humic acids. While more fluorescent species were removed through photocatalytic oxidation of FHA, new fluorescent compounds were in increasing trend around 350 nm and 400 nm with longer oxidation periods for NHA.

Kinetic modeling provided distinctive results, removal rate of $Color_{436}$ parameter was always faster than UV_{254} removal as well as DOC. When the two kinetic models were compared; the increasing trend of the L-H rates was similar to that of first order rates. However, the calculated L-H rates for the FHA were approximately half the value of the pseudo first order rates of $Color_{436}$, UV_{365}, UV_{280} and UV_{254}. In addition, similar correlation between R and R_{LH} were observed for NHA. Since irregular sequence of UV-vis parameters were obtained, no significant correlation could be deduced for any kinetic model parameter.

Major drawbacks could be explained as follows: Comparison with previously published research studies was limited due to the lack of the research with relative operational parameters such as substrate specifications, photocatalyst type and dose, light intensity of the light source, pH of the reaction medium as well as the solution matrix. In addition including complimentary adsorption data would extend understanding of the kinetic mechanism of HA degradation by photocatalysis.

6. REFERENCES

Abbt-Braun, G., Frimmel, F. H., 2002. The Relevance of Reference Materials: Isolation and General Characterization. In Frimmel, F. H., Abbt-Braun, G., Heumann, K. G., Hock, B., Lüdemann, H.-D., Spiteller, M. (Eds.), Refractory Organic Substances (ROS) in the Environment, 1-38, Wiley VCH, Weinheim.

Abbt-Braun, G., Lankes, U., Frimmel, F.H., 2004. Structural characterization of aquatic humic substances: The need for a multiple method approach. Aquatic Science, 66, 151–170.

Bekbölet, M., 1996. Destructive removal of humic acids in aqueous media by photocatalytic oxidation with illuminated titanium dioxide. Journal of Environmental Science and Health, A (31), 845-858.

Bekbölet, M. and Balcioglu, I., 1996. Photocatalytic Degradation Kinetics of Humic Acid in Aqueous TiO_2 Dispersions: The Influence of Hydrogen Peroxide and Bicarbonate Ion. Water Science and Technology, 34, 73-80.

Bekbölet, M. and Ozkosemen, G., 1996. A preliminary investigation on the photocatalytic degradation of a model humic acid. Water Science and Technology, 33, 189-194.

Bekbölet, M., Boyacıoğlu, Z., Özkaraova, B., 1998. The influence of solution matrix on the photocatalytic removal of color from natural waters. Water Science and Technology, 38, 155-162.

Bekbölet, M., Süphandağ, A.Ş., Uyguner, C.S., 2002. An investigation of the photocatalytic efficiencies of TiO2 powders on the decolourisation of humic acids. Journal of Photochemistry and Photobiology A: Chemistry, 148, 121-128.

Bekbölet, M., Uyguner, C.S., Selcuk, H., Rizzo, L., A.D. Nikolaou, A.D., Meric, S. and Belgiorno, V., 2005. Application of oxidative removal of NOM to drinking water and formation of disinfection by-products. Desalination, 176, 155-166.

Bloom P.R. and Leenheer, J.A., 1989. Vibrational, electronic and high energy spectroscopic methods for characterizing humic substances, In Humic Substances II, Eds. M.H.B. Hayes, P. MacCarthy, R.L. Malcolm and R.S. Swifth, pp. 409-446. John Wiley and Sons, New York.

Buffle, J., Greter, F.L., Haerdi, W., 1977. Measurement of complexation properties of humic and fulvic acids in natural waters with lead and copper ion-selective electrodes. Analytical Chemistry, 49, 216- 222.

Buffle, J., Deladoey, P., Zumstein, J. and Haerdi, W., 1982. Analysis and characterization of natural organic matters in fresh waters I. Study of analytical techniques. Schweiz Z. Hydrol., 44(2), 325-362.

Chen, Y., Senesi, N. and Schnitzer, M., 1977. Information provided on humic substances by E_4/E_6 ratios. Soil Science Society American Journal, 41, 352.

Chen, L.C. and Chou, T.C., 1993. Photobleaching of methyl orange in titanium dioxide suspended in aqueous solution. Journal of Mol. Catal., 85, 201-214.

Chen, J., G., B., LeBoeuf, P., H., Dai, S., 2002. Spectroscopic characterization of the structural and functional properties of natural organic matter fractions. Chemosphere, 48, 59-68.

Chin Y.P., Aiken G. and Loughlin E.O., 1994. Molecular weight, polydispersity and spectroscopic properties of aquatic humic substances. Environmental Science and Technology, 28, 1853-1858.

Cho, Y., and Choi, W., 2002. Visible light-induced reactions of humic acids on TiO_2. Journal of Photochemistry and Photobiology A: Chemistry, 148, 129-135.

Choudhry, G.G., 1981. Humic substances: Photophysical, photochemical and free radical characteristics. Environmental Chemistry, 4, 261-295.

Davies, G., Ghabbour, E.A., 1998. Humic Substances, Structures, Properties and Uses, Royal Society of Chemistry, Cambridge, UK, 10.

De Haan, H., De Boer, T., Kramer, H.A. and Voerman, J., 1982. Applicability of light absorbance as a measure of organic carbon in humic lake water. Water Research, 16, 1047-1050.

D'Orazio, V., Loffredo, E., Brunetti, G., Senesi, N., 1999. Trillate adsorption onto humic acids of different origin and nature. Chemosphere, 39, 183-198.

Dorfman L. M. and Adams G. E., 1973. Reactivity of the Hydroxyl Radical, National Bureau of Standards, Report No. NSRDS-NBS-46.

Edzwald J.K., Becket W.C. and Wattier K.L., 1985. Surrogate parameters for monitoring organic matter and THM precursors. J. AWWA, 77(4) 122-132.

Frimmel, F.H., 1998. Characterization of natural organic matter as major constituents in aquatic systems. Journal of Contaminant Hydrology, 35, 201-216.

Frimmel, F.H., Abbt-Braun, G., Heumann, K.G., Hock, B., Lüdemann, H.D., Spiteller, M. (Eds), 2002. Refractory Organic Substances in the Environment, Wiley-VCH, Weinheim.

Gaffney, J.S., Marley, N.A., Clark, S.B., 1996. Humic and Fulvic Acids: Isolation, Structure and Environmental Role, ACS Symposium Series 651, American Chemical Society, U.S.A.

Ghosh, K., Schnitzer, M., 1980. Macromolecular structures of humic substance. Soil Science, 129, 266–276.

Goslan, E.H., Voros, S., Banks, J., Wilson, D., Hillisd, P., Campbell, A.T., Parsons, S.A., 2004. A model for predicting dissolved organic carbon distribution in a reservoir water using fluorescence spectroscopy. Water Research, 38, 783–791.

Gönenç, D., Bekbölet, M., 2001. Interactions of hypochlorite ion and humic acid: Photolytic and photocatalytic pathways. Water Science and Technology, 44, 205-210.

Hatchard, C.G., Parker, C. A., 1956. A new sensitive chemical actinometer II. Potassium ferrioxalate as a standard chemical actinometer. Proceedings of Royal Society London Series A, 235, 518-536.

Hautala, K., Peravuori, J., Pihlaja, K., 2000. Measurement of aquatic humus content by spectroscopic analysis. Water Research, 34, 246-258.

Hayes, M. H. B., MacCarthy, P., Malcolm, R. L., Swift, R.S., (Eds), 1989. Humic Substances II: In Search of Structure, John Wiley and Sons, Inc., New York, USA, 257-446.

Hofrichter, M. and Steinbüchel A. (Eds.), 2001. Biopolymers, Lignin, Humic Substances and Coal, Wiley-VCH.

Kalbitz, K., Geyer, S., Geyer, W., 2000. A comparative characterization of dissolved organic matter by means of original aqueous samples and isolated humic substances. Chemosphere, 40, 1305-1312.

Kerç, A., Bekbölet, M., Saatçi A.M., 2003. Sequential oxidation of humic acids by ozonation and photocatalysis. Ozone Science and Engineering, 25, 497-504.

Langhals, H., Abbt-Braun, G., Frimmel, F., H., 2000. Association of humic substances: Verification of Lambert-Beer's law. Acta Hydrochimica et Hydrobiologica, 28, 329–332.

Leenheer, J.A., 1981. Comprehensive approach to preparative isolation and fractionation of dissolved organic carbon from natural waters and waste waters. Environmental Science and Technology, 15, 578–587.

Li, C.W., Korshin, G.V., Benjamin, M.M., 1998. Monitoring DBP formation with differential UV spectroscopy. Journal of American Water Works Association, 90, 88-100.

Li, X.Z., Fan, C.M. and Sun, Y.T., 2002. Enhancement of photocatalytic oxidation of humic acid in TiO_2 suspensions by increasing cation strength. Chemosphere, 48, 453-460.

Matthews, R.W., 1991. Enviroment: Photochemical and Photocatalytic Processes. Degradation of Organic Compounds. In Pelizetti, E., Schiavello, M.(Eds.), Photochemical Conversion and Storage of Solar Energy, 427-449, Kluwer academic Publishers, The Netherlands.

Maurice P. A., Pullin M. J., Cabaniss S. E., Zhou Q., Dejanovic K. N., Aiken G. R., 2002. A comparison of surface water natural organic matter in raw filteredwater samples, XAD, andreverse osmosis isolates. Water Research 36, 2357–2371.

McKnight D.M., Bencala K.E., Zellweger G.W., Aiken G.R., Feder G.L., Thorn K.A., 1992. Sorption of dissolved organic carbon by hydrous aluminum and iron oxides occurring at the confluence of Deer Creek with the Snake River Summit County, Colorado. Environmental Science Technology 26:1388–96.

Mobed, J.J., Hemmingsen, S.L., Autry, J.L., McGown, L.B., 1996. Fluorescence characterization of IHSS humic substances: Total luminescence spectra with absorbance correction. Environmental Science and Technology, 30, 3061-3065.

Mrkva, M., 1983. Evaluation of correlations between absorbance at 254 nm and COD of river waters. Water Research, 17, 231-235.

Najm, I.N., Patania, N.L., Jacangelo, J.G., Krasner, S.W., 1994. Evaluating surrogates for disinfection by-products. Journal of American Water Works Association, 86, 98-106.

Namjesnik-Dejanovic K., Maurice P.A., Aiken G.R., Cabaniss S., Chin Y-P, Pullin M.J., 2000. Adsorption and fractionation of a muck fulvic acidon kaolinite andgoethite at pH 3.7, 6 and 8. Soil Science;165:545–59.

Peuravuori, J., Pihlaja, K., 1997. Molecular size distribution and spectroscopic properties of aquatic humic substances. Analytica Chimica Acta, 337, 133-149.

Peuravuori, J., Koivikko, R., Pihlaja, K., 2002. Characterization, differentiation and classification of aquatic humic matter separated with different sorbents: Synchronous scanning fluorescence spectroscopy. Water Research, 36, 4552-4562.

Reckow, D. A., Singer, P. C., Malcolm, R. L., 1990. Chlorination of humic materials: By-product formation and chemical interpretations. Environmental Science and Technology, 24, 1655.

Reynolds, D.M., Ahmad, S.R., 1997. Rapid and direct determination of wastewater BOD values using a fluorescence technique. Water Research, 31, 2012-2018.

Rivero, C., Senesi, N., Paolini, J., D'Orazio, V., 1998. Characteristics of humic acids of some Venezuelan soils. Geoderma, 81, 227-239.

Rook, J.J., 1977. Chlorination reactions of fulvic acids in natural waters. Environmental Science and Technology, 11, 478-482.

Schnitzer, M., Khan, S.U., 1972. Humic Substances in the Environment. Marcel Dekker, New York, U.S.A.

Schulten, H.R., Gleixner, G., 1999. Analytical pyrolysis of humic substances and dissolved organic matter in aquatic systems: structure and origin. Water Research, 33, 2489-2498.

Scully, N.M., Lean, D.R.S., 1994. The attenuation of ultraviolet light in temperate lakes. Archieves of Hydrobiology, 43, 135-144.

Seitz, W.R., 1981. Luminescence spectrometry (flourimetry and phosphorimetry). In Elving P.J., Kolthoff I.M., Meehan E.J. (Eds.), Treatise on Analytical Chemistry, 1. Theory and Practice, 159-248, Volume 7, Second Ed., John Wiley & Sons, New York.

Senesi, N., 1990. Molecular and quantitative aspects of the chemistry of fulvic acid and its interactions with metal ions and organic chemicals Part II: The fluorescence spectroscopy approach. Analytica Chimica Acta, 232, 77-106.

Senesi, N., Miano, T.M., Provenzano, M.R., Brunetti, G., 1991. Characterization, differentiation, and classification of humic substances by fluorescence spectroscopy. Soil Science, 152, 259-271.

Shin, H.S., Monsallier, J.M., Choppin, G.R., 1999. Spectroscopic and chemical characterizations of molecular size fractioned humic acid. Talanta, 50, 641-647.

Skoog, D.A., Leary, J.J., 1992. Principles of Instrumental Analysis, 4th Edition, Saunders College Publishing, U.S.A.

Standard Methods for the Examination of Water and Wastewater, 1999. APHA, AWWA, WPCF, 20th Edition, American Water Works Association, USA.

Stevenson, J. (Eds.), 1982. Humus Chemistry: Genesis, composition, reactions. John Wiley and Sons, New York, Inc., U.S.A.

Suffet I.H. and MacCarthy P. (Eds.), 1989. Aquatic Humic Substances, Influence of Fate and Treatment of Pollutants, Advances in Chemistry Series, American Chemical Society, Washington DC.

Thurman, E.M., and Malcolm, R.L., 1981. Preparative isolation of aquatic humic substances. Environ. Sci. Technol., 15, 463-466.

Thurman, E. M., 1985. Organic geochemistry of natural waters. Kluwer Academic, 497pp, Boston, MA, USA.

Traina, S.J., Novak, J., Smeck, N.E., 1990. An ultraviolet absorbance method of estimating the percent aromatic carbon content of humic acids. Journal of Environmental Quality, 19, 151-153.

Turchi, C.S., Ollis, D.F., 1989. Mixed reactant photocatalysis: Intermediates and mutual rate inhibition. Journal of Catalysis, 119, 483-496.

Urano, K., Wada, H., Takemasa T., 1983. Empirical rate equation for trihalomethane formation with chlorination of humic substances in water. Water Research, 17, 1797-1802.

Uyguner, C.S., Bekbölet, M., 2004a. Photocatalytic degradation of natural organic matter: Kinetic considerations and light intensity dependence. International Journal of Photoenergy, 6, 73-80.

Uyguner C.S., 2005. Elucidation of the Photocatalytic Removal Pathways of Humic Substances: Progress towards Mechanistic Explanations. Bogazici University.

Uyguner, C.S. and Bekbölet, M., 2005a. A comparative study on the photocatalytic degradation of humic substances of various origins. Desalination, 176, 167-176.

Uyguner C.S., Bekbölet M., 2005b. Evaluation of humic acid photocatalytic degradation by UV-vis and fluorescence spectroscopy. Catalysis Today, 101, 267-274.

Uyguner, C.S. and Bekbölet, M., 2005c. Implementation of spectroscopic parameters for practical monitoring of natural organic matter. Desalination, 176, 47-55.

Uyguner C.S. and Bekbölet M., 2006. Control of Disinfection By-Products in Drinking Water Systems, A Review on the Photocatalytic Degradationof Humic Substances Nikolau A., Rizzo L. and Selcuk H. (Eds.), pp. 419-446, Nova Science Publishers.

Wang, G.S., Hsieh, S.T., Hong, C.S., 2000. Destruction of humic acid in water by UV light-catalyzed oxidation with hydrogen peroxide. Water Research, 34, 3882- 3887.

Westerhoff, P., Aiken, G., Amy, G., Debroux J., 1999. Relationships between the structure of natural organic matter and its reactivity towards molecular ozone and hydroxyl radicals. Water Research, 33, 2265-2276.

Wiszniowski, J., Robert, D., Surmacz-Gorska, J., Miksch, K., Weber, J.V. 2003. Photocatalytic mineralization of humic acids with TiO2: Effect of pH, sulfate and chloride anions. International Journal of Photoenergy, 5, 69-74.

Zhou Q., Maurice P.A.., Cabaniss S.E., 2001. Size fractionation upon adsorption of fulvic acid on goethite: equilibrium andkinetic studies. Geochim Cosmochim Acta;65 : 803–12.